On the putative role of Pelota in stem cell differentiation

vorgelegt von
Aleksandra Kata
aus Łódź, Polen

Göttingen 2009

D 7

Referent: Prof. Dr. med Dr. h.c. W. Engel

Korreferentin: Prof. Dr. S. Hoyer-Fender

Tag der mündlichen Prüfung:

TABLE OF CONTENTS

TABLE OF CONTENTS

TABLE OF CONTENTS

TABLE OF CONTENTS

TABLE OF CONTENTS

ABBREVIATIONS

Abbreviations:

129/Sv	129/Sv/Ola mouse strain
AP	Alkaline Phosphatase
ATP	Adenosinetriphosphate
bp	base pair
BLAST	Basic Local Alignment Search Tool
BSA	Bovine Serum Albumin
°C	Celsius Degree
C57BL	C57BL/6J mouse strain
cDNA	complementary DNA
cKO	conditional knockout
d	day/s
dATP	desoxyriboadenosintriphosphate
dH_2O	destilled water
DAPI	Diamidino-2-phenylindole dihydrochloride
dCTP	Desoxyribocytosinetriphosphate
DMEM	Dulbecco's Modified Eagle Medium
DEPC	Diethylpyrocarbonate
DNA	Deoxyribonucleic acid
DNAse	Deoxyribonuclease
dNTP	deoxynucleotidetriphosphate
dT	deoxythymidinate
DTT	Dithiothreitol
EDTA	Ethylene Diamine Tetraacetic Acid
ES	Embryonic Stem
et al.	et alii (and others)
EtBr	Ethidium Bromide
Fig.	Figure
FCS	Fetal Calf Serum
FVB	FVB/N mouse strain
g	gravity
HPRT	hypoxanthin-phosphoribosyl-transferase
ICM	Inner Cell Mass
IPTG	Isopropyl-ß-thiogalactopyranoside
kb	kilobase
kDa	kiloDalton
mg	milligram
ml	milliliter
µl	microliter
µm	micrometer
min	minute
mM	millimolar
mRNA	Messenger-RNA
NaAc	Sodium Acetate
NCBI	National Center for Biotechnology
Neo	Neomycin
ng	nanogram
nm	nanometer
nt	nucleotide

ABBREVIATIONS

OD	Optical Density
ORF	Open Reading Frame
PBS	Phosphate Buffered Saline
PCR	Polymerase Chain Reaction
PFA	Paraformaldehyde
PMSF	Phenylmethanesulfonilfluoride
RNA	Ribonucleic Acid
RNase	Ribonuclease
RT-PCR	Reverse-Transcription-PCR
RT	Room Temperature
Sdha	Succinate dehydrogenase
SDS	Sodium Dodecyl Sulfate
Tris	Tris(hydroxymethyl)-aminomethane
U	Unit
UTR	untranslated region
Vol.	Volume
WT	Wild Type
X-Gal	5-brom-4-chlor-3-indolyl-ß-Dgalactopyranoside

Symbols of nucleic acids

A	Adenosine
C	Cytidine
G	Guanosine
T	Thymidine
U	Uridine

Symbols of amino acids

A	Ala	Alanine
B	Asx	Asparagine or Aspartic acid
C	Cys	Cysteine
D	Asp	Aspartic acid
E	Glu	Glutamic acid
F	Phe	Phenylalanine
G	Gly	Glycine
H	His	Histidine
I	Ile	Isoleucine
K	Lys	Lysine
L	Leu	Leucine
M	Met	Methionine
N	Asn	Asparagine
P	Pro	Proline
Q	Gln	Glutamine
R	Arg	Arginine
S	Ser	Serine
T	Thr	Threonine
V	Val	Valine
W	Trp	Tryptophan
Y	Tyr	Tyrosine
Z	Glx	Glutamine or Glutamic acid

INTRODUCTION

1. INTRODUCTION

1.1. The pelota gene

The murine pelota (Pelo) gene is located on chromosome 13. It consists of three exons (300, 729 and 598 bp long), but protein coding sequences are found only in two of them - start codon (ATG) and termination codon (TGA) are situated in second and third exon, respectively. Murine Pelo cDNA in comparison to that of *Drosophila,* has a 394 bp shorter 3'UTR (u̱ṉtranslated ṟegion), supposedly due to deletion in mammalian cDNA or insertion in fruit fly cDNA. This fact can be of great importance for gene functionality in mammals (Shamsadin et al., 2002). The amino acid sequence (385 residues) shares 70% homology with *Drosophila* Pelo and 36% with yeast Dom34 (Shamsadin et al., 2002).

Pelo gene has been identified in *Drosophila melanogaster* (Castrillon et al., 1993) and successive studies have revealed its broad expression in diverse species from archaebacteria to human (Lalo et al., 1994; Bult et al., 1996; Ragan et al., 1996; Shamsadin et al., 2000, 2002). Similarity in protein structure between various organisms indicates that it is highly conserved during evolution (*Fig.1*). The fact that the phenotype of a null dom34 (pelota homologue) mutant in yeast has been rescued by expression of *Drosophila* pelota (Davis and Engebrecht, 1998) is additional evidence for evolutionary conservation of the gene.

Structural analysis of pelota protein has revealed, that it consists of three conserved domains (*Fig.1B, Fig. 2*). Two of them (central and C-terminal ones) are related to domains composing eRF1 (an eukaryotic release factor 1), which is involved in termination step of protein synthesis (Frolova et al., 1994; Eurwilaichitr et al., 1999). Therefore, pelota was originally classified to eRF family, but in the course of time certain differences between Pelo and eRF proteins were brought to light. In contrary to central domain of eRF1, Pelo lacks universal GGQ (glycine-glycine-glutamine) sequence motif (Lee et al., 2007) enabling recognition of a stop codon at the A site of the ribosome and stimulation of peptidyl-tRNA bond hydrolysis (Song et al., 2000). Instead, the central domain of Pelo contains a strictly conserved tripeptide PGF (proline-glycine-phenylalanine) which strongly influences endoribonuclease function (Passos et al., 2009) and may be responsible for interaction with ribosomes (Lee et al., 2007). This sequence discrepancy suggests some functional differences between Pelo and eRF1.

INTRODUCTION
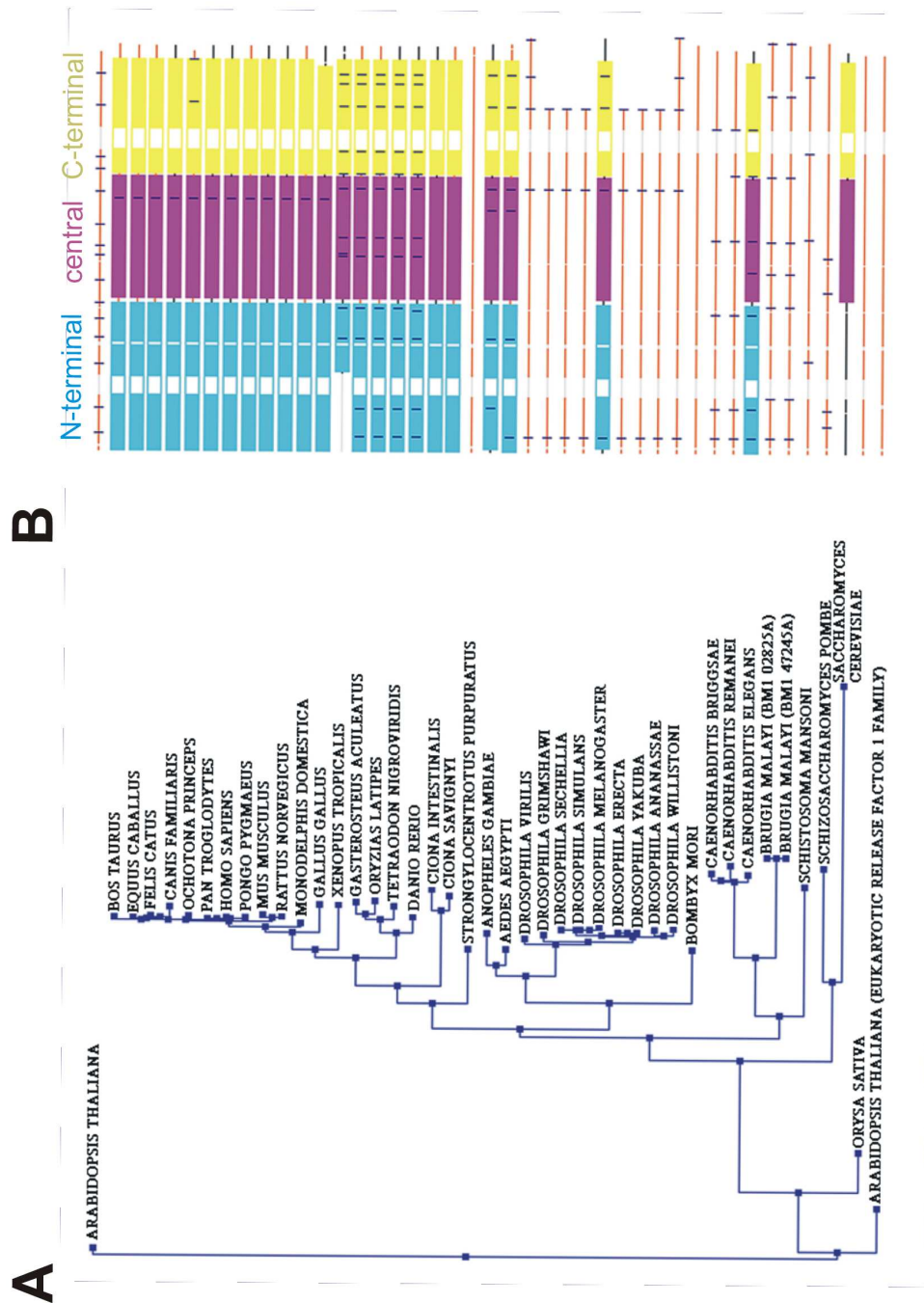
Figure 1. A phylogenetic tree of Pelota amino acid sequences (A) and alignment of domain structures (B) of various species.

The tree (A) originates from the TreeFam database. Blue, pink and yellow boxes in panel B represent Pfam domains (N-terminal, central and C-terminal, respectively); lines stand for regions not belonging to domains. Light-coloured lines are equivalents of mismatched fragments. Short vertical lines show splicing sides.

INTRODUCTION

Moreover, Pelo N-terminal domain markedly differs from eRF1 (Song et al., 2000; Lee et al., 2007; Graille et al., 2008). It contains Sm-fold structure which serves either to recognize mRNA stem loops or to recruit mRNA decay machinery (Wilusz & Wilusz, 2005; Tritschler et al., 2007). Nonetheless, the way of RNA recognition probably differs from one used by Sm-fold-containing proteins, because the Sm structure of Dom34 lacks two motifs involved in RNA binding (Graille et al. 2008). It has been found in yeast and *Thermoplasma acidophilum* that Pelo N-terminal domain exhibits endonuclease activity dependent on divalent metal ion what has unvailed a first known Sm-containing domain with catalytic features (Lee et al., 2007). Furthermore, there is a putative leucine zipper motif in C-terminal domain that participates in interactions with other proteins (Busch and Sassone-Corsi, 1990). Shamsadin et al. (2002) have disclosed putative phosphorylation sites along the whole sequence by screening of the PROSITE protein motif library, such as motifs for protein kinase C, casein kinase II and tyrosine kinase. Besides, they have detected two N-glycosylation and three N-myristoylation sites. It is unknown till now which of the sites play a role in protein functionality (*Fig.2*).

However, Pelo and eRF1 share some similarities. Graille et al. (2008) have compared eRF1 and *S. cerevisiae* Dom34 C-terminal domains which are suggested to interact with eRF3 (an eukaryotic release factor 3) and Hbs1 (Hsp70 subfamily B supresor 1, yeast eRF3 homologue), respectively. Both interaction partners belong to the GTPase family and are responsible for recognition of stop codon and enhancing of polypeptide chain release (Salas-Marco and Bedwell, 2004). Their study has revealed striking similarities of protein structural motifs being crucial for the interaction. Moreover, they have demonstrated that Dom34 enhances GTP binding to Hbs1, what is neccessary for peptidyl-tRNA hydrolysis upon GTP hydrolysis. The feature is convergent to eRF1 impact (Graille et al., 2008).

Pelota protein is localised in the cytoplasm, but it has been found to contain also a putative nuclear localization signal (NLS) at the N-terminus which is conserved from *Drosophila* to human (Eberhart and Wasserman, 1995; Davis and Engebrecht, 1998; Shamsadin et al., 2000; 2002). Nevertheless, generation of pelota mutant version in *Drosophila*, where NLS was disrupted, did not lead to loss of Pelo function. Cytoplasmatic distribution of the protein was observed as it was shown in controls. The finding indicates that Pelo is located in the cytoplasm and the putative nuclear motif is meaningless for Pelota functionality (Xi et al., 2005).

INTRODUCTION
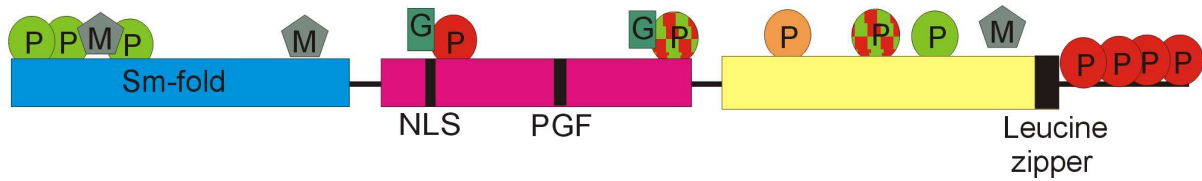
Figure 2. Scheme of PELO protein domains and putative posttranslational modifications
N-terminal domain containing amino acid range from 1 to 131 (marked in blue); a putative nuclear localization signal (NLS) was found in central domain ranging from 136 to 268 aa (marked in pink) contains a conserved PGF motif (210-212 aa); C-terminal domain from 271 to 370 aa (marked in yellow) contains leucine zipper motif at the end. P in green – protein kinase C phosphorylation sites (aa: 38-40, 43-45, 58-60,342-344); P in red – casein kinase II phosphorylation sites (aa: 176-179, 374-377, 380-383, 381-384, 382-385); P in green and red – phosphorylation sites common for protein kinase C and casein kinase II (aa: 252-255, 335-338); P in orange – tyrosine kinase phosphorylation site (276-282 aa); G in dark green – N-glycosylation sites (aa: 174-177, 236-239); M in grey – N-myristoylation sites (aa: 54-59, 97-102, 357-362).

1.2. The function of pelota gene in *Saccharomyces cerevisiae* and *Drosophila melanogaster*

Drosophila pelota null mutants exhibit spermatogenesis arrest. The initial generation of spermatogonia and four rounds of mitotic division producing spermatocytes are unaffected, but then the cells are arrested in premeiotic G2 phase and meiotic divisions never occured. In such accumulated spermatocytes some processes were observed to be disrupted, such as spindle formation and nuclear envelope breakdown (Castrillon et al., 1993). Nonetheless, germ cell development continued and resulted in 4N spermatids possessing head and tail structures. This indicates that Pelo protein does not influence spermiogenesis, but is required for G2/M transition during meiotic division. However, the role of Pelo is not restricted to meiosis – it also plays a role in fly eye development what suggests that Pelo is also functionally important in somatic growth (Ebenhart and Wasserman, 1995).

The detailed study of fruit fly ovary has shown that Pelota participates in germ stem cell (GSC) maintenance. In *Drosophila,* self-renewal of the germline is controlled by BMP (bone morphogenetic protein) signal which represses a Bam-dependent differentiation pathway. Xi et al. (2005) demonstrated that loss of Pelo leads to rapid differentiation of GSCs and loss of germline. Furthermore, they detected that BMP signal is downregulated in mutant GSCs, but it has no influence on expression of bam – the gene that is necessary and sufficient for the progression of oogenesis (Ohlstein and McKearin, 1997). To confirm the obtained results, a bam/pelota double null mutant was generated where differentiation was

INTRODUCTION

still observed. It indicates that Pelo represses a Bam-independent differentiation pathway. In accordance with these findings, overexpression of pelota did not result in downregulation of Bam and had no effect on GSC maintenance and differentiation (Xi et al., 2005).

Analysis of dom34, a pelota ortholog in *Sacharomyces cerevisiae,* revealed that its null mutant fails to segregate chromosomes properly and produces less amount of spores in comparison to wild type yeast owing to lack of efficient G1 phase progression. It was suggested that bulk protein translation is impaired, so the key proteins for the phase of cell cycle are not translated (Davis and Engebrecht, 1998). Further studies have shown that Dom34 protein indeed is involved in translation process. Namely, it recognizes stalled ribosomes and cleaves mRNA in an endonucleolytic way in conjunction with Hbs1p, a member of the GTPase family. At present it is unclear whether it is a mRNA-specific or only a structure-specific process, but it is assigned to so called No-Go decay pathway. This pathway degrades mRNA, which cannot be translated due to stalled ribosomes on it (Doma and Parker, 2006; Lee et al., 2007).

1.3. The phenotype of Pelota knockout mice

Pelota has been also characterized in human and mouse. It has been found that mouse pelota expression starts early in embryonic development and is maintained in all adult tissues including all testicular developmental stages (Shamsadin et al., 2000; 2002).

To examine the function of PELO in mammals, the gene was disrupted by homologous recombination (Adham et al., 2003). Heterozygous mice did not exhibit apparent developmental malfunctions what proves that a single allele of the gene is sufficient for normal growth. However, PELO turned out to be crucial for proper embryogenesis due to fetal lethality of Pelo$^{-/-}$ animals. To estimate the time point for their death, embryos of different age were collected and genotyped. It was found that implantation is not affected in pelota-deficient embryos – the mean number of dissected E6.5- or E7.5-deciduae from Pelo$^{+/-}$ intercrosses was similar to those received from wild-type crosses. The critical stage when embryos died was E7.5. The morphology of mutant embryos was abnormal and the embryos were reduced in size. Although all embryonic germ layers (ectoderm, mesoderm and endoderm) could be found, the extraembryonic region was substantially diminished. It was suggested that growth impairment was owing to defect in mitotic division, but not in development of germ layers. To prove this hypothesis, embryos at the stage of blastocyst

INTRODUCTION

(E3.5) were isolated and cultured *in vitro*. Pelo$^{-/-}$ blastocysts were able to attach to the dish and to hatch from zona pellucida. They began to grow, but failed to expand and died within 4 days in the culture, whereas trophoblast cells remained alive and continued growing. It was demonstrated that only the cells mitotically active (i.e. ICM) are affected, but those which do not divide - survive. This can be related to former findings in *Drosophila* and yeast that Pelo influences cell cycle regulation (Eberhart and Wasserman, 1995; Davis and Engebrecht, 1998). It was also shown in yeast that pelota deficiency leads to meiosis arrest and subsequent production of 4N spermatids, what suggests failure in chromosome segregation. An examination of cellular DNA content of murine Pelo$^{-/-}$ cells showed significant increase of aneuploid cells what indicates that PELO influences genomic stability.

INTRODUCTION

1.4. Aims of the study

Comparing up-to-date findings regarding Pelota structure and function in *Drosophila* and yeast *versus* mammals, some questions arise.

Molecular mechanism of murine PELO function has not been demonstrated yet. The best way to study it, is a system based on *in vitro* cultures, where pelota is knocked out. It would be possible to investigate the basis of a putative proliferation defect of pelota-deficient cells. It would also facilitate creating more comprehensive system to discover the pathway/mechanism, in which pelota is involved.

As it was impossible to establish an embryonic stem cell line from Pelo$^{-/-}$ blastocysts, we generated conditional knockout mouse. It enabled us to generate pelota-deficient ESC lines, where we could study whether PELO controls the maintanence of pluripotency and the differentiation processes.

Moreover, a conditional knockout mouse model can be used to study the consequences of PELO depletion in living animal. Due to the fact that spermatogenesis is a process where differentiation of pluripotent cells occurs in very apparent way during the whole life span, the conditional knockout mouse is a suitable model for studies of cell transformation from pluripotent up to differentiated state. Therefore, we generated testis-specific conditional knockout mice and analyzed available (Buyandelger, 2006) transgenic mice with testis-specific pelota overexpression.

Finally, to clearly demonstrate that the phenotype obtained in Pelo$^{-/-}$ mice specifically results from pelota deletion, we bred transgenic mice with ubiquitous overexpression of pelota gene together with classical knockout mice. The aim was to show whether exogenous PELO protein is able to rescue pelota-deficient phenotype.

MATERIALS AND METHODS

2. MATERIALS AND METHODS

2.1. MATERIALS

2.1.1. Chemicals

1 kb DNA Ladder	Invitrogen, Karlsruhe
100 bp DNA Ladder	Invitrogen, Karlsruhe
Acetic acid	Merck, Darmstadt
Agar	Difco, Detroit, USA
Agarose	Invitrogen, Karlsruhe
Ammonium acetate	Fluka, Neu Ulm
Ammonium persulfate	Sigma, Deisenhofen
Ampicillin	Sigma, Deisenhofen
Ampuwa	Fresenius, Bad Homburg
Aprotinin	Sigma, Deisenhofen
Aqua Poly/Mount	Polysciences, Inc, USA
Bacto-tryptone	Difco, Detroit, USA
Bacto-Yeast-Extract	Difco, Detroit, USA
Blocking powder	Boehringer, Mannheim
BSA	Biomol, Hamburg
Cell culture media	PAN-Systems, Nürnberg
Chemiluminescent Substrate	Pierce, Rockford, IL
Chloroform	Baker, Deventer, NL
Coomassie Blue G-250	Sigma, Deisenhofen
Diethyl pyrocarbonate (DEPC)	Sigma, Deisenhofen
Dimethyl sulfoxid (DMSO)	Merck, Darmstadt
Dithiothreitol	Sigma, Deisenhofen
dNTPs	Invitrogen, Karlsruhe
EDTA	ICN Biomedicals, Eschwege
EGTA	Applichem, Darmstadt
Ethanol	Baker, Deventer, NL
Ethidium bromide	Sigma, Deisenhofen
Eukitt-quick hardening mounting medium	Fluka, Neu Ulm

MATERIALS AND METHODS

FBS	Invitrogen, Karlsruhe
Ficoll 400	Amersham Pharmalia, Freiburg
Formaldehyde	Invitrogen, Karlsruhe
Formamide	Fluka, Neu Ulm
Glutaraldehyde	Sigma, Deisenhofen
Glycerol	Invitrogen, Karlsruhe
Glycine	Biomol, Hamburg
Goat serum	PAN-Systems, Nürnberg
HCl	Merck, Darmstadt
H_2O_2	Merck, Darmstadt
HEPES	Merck, Darmstadt
4-Hydroxytamoxifen	Sigma, Deisenhofen
Horse serum	PAN-Systems, Nürnberg
IPTG	Biomol, Hamburg
Isopropanol	Merck, Darmstadt
KCl	Merck, Darmstadt
KH_2PO_4	Merck, Darmstadt
Lambda DNA	Roche, Penzberg
Leupeptin	Sigma, Deisenhofen
Lipofectamine 2000	TM Invitrogen, Karlsruhe
Methanol	Merck, Darmstadt
2-Mercaptoethanol	Serva, Heidelberg
MgCl2	Merck, Darmstadt
Milk powder	Roth, Karlsruhe
NaCl	Merck, Darmstadt
Na_2HPO_4	Merck, Darmstadt
NaH_2PO_4	Merck, Darmstadt
$NaHCO_3$	Merck, Darmstadt
NaN_3	Merck, Darmstadt
NaOH	Merck, Darmstadt
Nonidet P40	Fluka, Neu Ulm
NuPAGE Novex Bis-Tris 4-12% Gel	Invitrogen, Karlsruhe
NuPAGE MOPS/MES SDS running buffer	Invitrogen, Karlsruhe
NuPAGE SDS sample buffer	Invitrogen, Karlsruhe

MATERIALS AND METHODS

Orange G	Sigma, Deisenhofen
OptiMEM I	Invitrogen, Karlsruhe
Paraformaldehyde	Merck, Darmstadt
PBS	PAN-Systems, Nürnberg
Penicillin/Streptomycin	PAN-Systems, Nürnberg
Peptone	Roth, Karlsruhe
Phalloidin	Sigma, Deisenhofen
Phenol	Biomol, Hamburg
Phosphoric acid	Merck, Darmstadt
Picric acid	Fulka, Neu Ulm
Proteinase K	Roche, Penzberg
Protein marker	Biorad, Sigma
$[^{32}P]$-dCTP	Amersham Pharmalia, Braunschweig
RediprimeTM II	Amersham Pharmacia, Freiburg
RNase A	Qiagen, Hilden
RNase away	Biomol, Hamburg
RNase Inhibitor	Roche, Penzberg
RNA length standard	Invitrogen, Karlsruhe
Salmon sperm DNA	Sigma, Deisenhofen
SDS	Serva, Heidelberg
SeeBlue Plus2 Pre-Stained Standard	Invitrogen, Karlsruhe
Select Peptone	Gibco/BRL, Eggenstein
S.O.C Medium	Invitrogen, Karlsruhe
Sodium acetate	Merck, Darmstadt
Sodium citrate	Merck, Darmstadt
Sun flower oil	Sigma, Deisenhofen
SuperScript II	Invitrogen, Karlsruhe
T4 DNA ligase	Promega, Mannheim
Tamoxifen	Sigma, Deisenhofen
TRI reagent	Sigma, Deisenhofen
Tris base	Sigma, Deisenhofen
Triton X-100	Serva, Heidelberg
Trypsin	PAN-Systems, Nürnberg
Tween-20	Sigma, Deisenhofen

MATERIALS AND METHODS

Vectashield (DAPI)	Vector, Burlingame
X-Gal	Biomol, Hamburg
Xylene	Merck, Darmstadt
Yeast extract	Roth, Karlsruhe

2.1.2 Solutions, buffers and media

All standard buffers and solutions were prepared according to Sambrook *et al.* (1989).

Annealing buffer (10x)	100 mM TrisHCl pH 7.5
	1 M NaCl
	10 mM EDTA
Denaturation solution	1.5 M NaCl
	0.5 M NaOH
Depurination solution	250 mM HCl
E-buffer (10x)	300 mM NaH_2PO_4
	50 mM EDTA
Bouin's solution	15 volume of Picric acid (in H_2O)
	5 volumes 37% Formaldehyde
	1 volume Acetic acid
Ligation buffer (10x)	600 mM Tris/HCl (pH 7.5)
	80 mM $MgCl_2$
	100 mM DTT
Loading buffer	15% Ficoll 400
	10 mM EDTA (pH 8)
	0,25% Orange G
	1% Glycerol

MATERIALS AND METHODS

Lysis buffer I	50 mM Tris/HCl (pH 8.0)
	100 mM EDTA
	0.5% SDS
Lysis buffer II	100 mM Tris/HCl (pH 8.0)
	5 mM EDTA
	200 mM NaCl
	0.2% SDS
	100 µg/ml Proteinase K
Lysis buffer A	50 mM Tris/HCl pH 7.0
	100 mM NaCl
	5 mM $MgCl_2$
	2% Triton X-100
	2% SDS
	1 mM PMSF
	1 mM aprotinin
	1 mM leupeptin
	1 Protease inhibitor cocktail tablet/10ml buffer
Neutralisation solution	1.5 M NaCl
	1 M Tris/HCl (pH 7.0)
SSC (20x)	3 M NaCl
	0.3 M sodium citrate (pH 7.0)
TBE buffer (5x)	450 mM Tris base
	450 mM Boric acid
	20 mM EDTA (pH 8)
TE buffer	10 mM Tris/HCl (pH 8.0)
	1 mM EDTA

MATERIALS AND METHODS

2.1.3 Laboratory materials

The laboratory materials, which are not listed here, were bought from Schütt and Krannich (Göttingen).

Cell culture flask	Greiner, Nürtingen
Culture slides	BD Falcon, Heidelberg
Disposable filter Minisart NMI	Sartorius, Göttingen
Filter paper 0858	Schleicher and Schüll, Dassel
Hybond C	Amersham, Braunschweig
Hybond N	Amersham, Braunschweig
HPTLC Aluminum folio	Merck, Darmstadt
Microcentrifuge tubes	Eppendorf, Hamburg
Petri dishes	Greiner, Nürtingen
Pipette tips	Eppendorf, Hamburg
RotiPlast paraffin	Roth, Karlsruhe
Transfection flasks	Lab-Tek/Nalge, Nunc, IL, USA
Superfrost slides	Menzel, Gläser
Whatman blotting paper	Schleicher and Schüll, Dassel
(GB 002, GB 003 and GB 004)	
X-ray films	Amersham, Braunschweig

2.1.4 Sterilisation of solutions and equipments

All solutions that are not heat sensitive were sterilised at 121°C, 105 Pa for 60 min in an autoclave (Webeco, Bad Schwartau). Heat sensitive solutions were filtered through a disposable sterile filter (0.2 to 0.45 μm pore size). Plastic wares were autoclaved as above. Glasswares were sterilised overnight in an oven at 220°C.

2.1.5 Media, antibiotics and agar-plates

2.1.5.1 Media for bacteria

LB Medium (pH 7.5)	1% Bacto-trypton

| | 0.5% Yeast extracts |
| | 1% NaCl |

LB-Agar	1% Bacto-trypton
	0.5% Yeast extracts
	1% NaCl
	1.5% Agar

The LB medium was prepared with distilled water, autoclaved and stored at 4°C.

2.1.5.2 Media for cell and embryo culture

M2 and M16 media were purchased from Sigma (Deisenhofen) and were used for washing and cultivation of mouse preimplantation embryos.

Embryonic stem (ES) cell medium:	DULBECCO´s Modified Eagles Media (DMEM)
	1 mM Non essential amino acids
	1 mM Sodium pyruvate
	10 μM ß-Mercaptoethanol
	2 mM L-Glutamine
	20% FCS
	1000 U/ml Recombinant leukaemia inhibitory factor (LIF)

Fibroblast cell medium (MEFs):	DULBECCO´s Modified Eagles Media (DMEM)
	2 mM L-Glutamine
	10% FCS
	1% penicillin/streptomycin

For long time storage of the cells in liquid nitrogen, the following freezing medium was used:

| Freezing medium: | 20% FCS |
| | 10% DMSO in DMEM |

| KO medium: | Knockout DMEM optimized for ES cells (Gibco) |
| | 20% knockout supplement |

1 mM Non essential amino acids

1 mM Sodium pyruvate

10 μM ß-Mercaptoethanol

2 mM L-Glutamine

20% FCS

1000 U/ml Recombinant leukaemia inhibitory factor (LIF)

Selective medium: Embryonic stem (ES) cell medium

400 μg/ml G418

2 μM gancyclovir

2.1.5.3 Antibiotics

Stock solutions were prepared for the antibiotics. They were filtered through sterile disposable filters and stored at –20°C. When antibiotics were needed, in each case, they were added after the autoclaved medium has cooled down to a temperature lower than 55°C.

Antibiotics	Stock solution	Working solution
Ampicillin	50 mg/ml	50 μg/ml
Kanamycin	25 mg/ml	50 μg/ml

2.1.5.4 IPTG/X-Gal plate

LB-agar with 50 μg/ml ampicillin, 100 μM IPTG and 0.4% X-Gal was poured into Petri dishes. The dishes were stored at 4°C.

2.1.6 Bacterial strains

E. coli DH5α   K-12 strain**,**F- Φ80d *lacZ*ΔM15 endA1 *rec*A1 hsdR17 (rk-, mk+) sup E44 *thi*-1 d- *gyr*A96 (lacZYA-arg) (Invitrogen, Karlsruhe)

E. coli BL21 (DE3)   B strain, F- *omp*T *hsd*SB(rB-mB-) *gal, Dcm* (Novagen, Darmstadt)

MATERIALS AND METHODS

2.1.7 Plasmids

pBluesript SK (+/-)   (Stratagene, La Jolla, USA)

pGEMTeasy   (Promega, Wisconsin, USA)

2.1.8 Synthetic oligonucleotides

The synthetic oligonucleotide primers used in this study were obtained from OPERON and dissolved in dH$_2$O (Ampuwa) to a final concentration of 100 pmol/μl.

Name	Sequence
3'regionA_F	5' CATTATCCACTGCCCACATTC 3'
3'region_R	5' TAGAACTGGCCTTCTCGCAC 3'
cKO_3'ext_F	5' GCGAATACGTCAGCAGAAG 3'
cKO_3'ext_R	5' GAGTCACAAGTGGGCAATG 3'
Cre_R	5' AGTGAAACAGCATTGCTGTCA 3'
EIIa-CreF	5' CCAGGCTAAGTGCCTTCTCTACA 3'
EIIa-CreR	5' AATGCTTCTGTCCGTTTGCCGGT 3'
EvaL1_F	5' TCTCTTGTTCTAAGATGTGCTGTG 3'
EvaL1_GenomeWalk_F2	5' ACCCTGGCGTTACCCAACTTAATCGC 3'
EvaL1_R	5' AAAGGGGCTCGATTAGATGAACT 3'
m18S_F	5' CGCAAATTACCCACTCCCG 3'
m18S_R	5' TTCCAATTACAGGGCCTCGAA 3'
mc-Kit_F	5' GCCACGTCTCAGCCATCTG 3'
mc-Kit_R	5' GTCGGGATCAATGCACGTCA 3'
mDAZL_F	5' CTCCACCTTCGAGGTTTTACC 3'
mDAZL_R	5' GTGATTTCGGTTTCATCCATC 3'
mPelo.RT-PCR-F2	5' ATCCAGCGCCACATAAACTT 3'
mPelo.RT-PCR-R2	5' CTCTCCACCTGCTTGAGTCC 3'
mPlzf_F	5' CTCCGTAAGCGTCCCCTCTGC 3'
mPlzf_R	5' GGTGCAGGCTAGCACCGTCC 3'
mSDHA_F	5' GCTTGCGAGCTGCATTTGG 3'
mSDHA_R	5' CATCTCCAGTTGTTCTCTTCCA 3'
mSox3_F	5'CACATGAAGGAGTAGTACCCGGACTA 3'
mSox_R	5' TGAGCAGCGTCTTGGTCTTG 3'

mStra8_F	5' CTGTTGCCGGACCTCATG 3'
mStra8_R	5' TCACTTCATGTGCAGAGATGATG 3'
mVASA_F	5' GAGAAGTGGGTTTCCTTCTGG 3'
mVASA_R	5' GAAAACCCTCTGCTTCGAGTC 3'
Pelo_F11	5' TGAGCCCAGACTGTACGTGAC 3'
Pelo_R14	5' AACGTCAAAGGAGGCGGTCAG 3'
Pelota3'F2	5' GGTATCATGGCCTCTATTCAG 3'
Pelota3'R2	5' GCACAGACATGACCAATACG 3'
PGK_cKO_R1	5' CCACTTGTGTAGCGCCAAGTG 3'
RosaCreER-F	5' ACCAGCCAGCTATCAACTC 3'
RosaCreER-R	5'TATACGCGTGCTAGCGAAGATCTCCATCTTCCAGCAG 3'
Stra8_F	5' GCGCTCCTAGTGTGCCAGTTTGAT 3'
Trans.pEF-F	5' CATTCTCAAGCCTCAGACAGTG 3'
Trans.pUB-F	5' TCAGTGTTAGACTAGTAAATTG 3'
Trans.hPelo-R1	5' GAGGACTCTGTCTGTACCTTG 3'

2.1.9 Mouse strains

Strains C57BL/6J, 129/Sv, CD-1 and NMRI were initially ordered from Charles River Laboratories, Wilmington, USA, and kept in Animal Facility of Institute of Human Genetics, Göttingen. ROSA26CreERT (Berns A, Netherlands) and EIIaCre (Lakso *et al.,* 1996) mice were kindly provided by Prof. Dr. med. H. Hahn, Institute of Human Genetics, Göttingen.

2.1.10 Antibodies

Goat anti-mouse IgG alkaline phosphatase conjugate	Sigma, Deisenhofen
Goat anti-rabbit IgG alkaline phosphatase conjugate	Sigma, Deisenhofen
Goat anti-rabbit GFP antiserum	Sigma, Deisenhofen
Rabbit anti-mouse IgG Cy3 conjugate	Sigma, Deisenhofen
Goat anti-rabbit IgG FITC conjugate	Sigma, Deisenhofen
Rabbit anti-mouse IgG FITC conjugate	Sigma, Deisenhofen
Mouse monoclonal anti β-tubulin	Sigma, Deisenhofen
Goat anti-rabbit IgG horse radish preoxidase conjugate	Sigma, Deisenhofen

MATERIALS AND METHODS

Rabbit anti-mouse IgG horse radish preoxidase conjugate   Sigma, Deisenhofen

Rabbit anti Pelota polyclonal antibody   Institute of Human Genetics

mouse anti GCNA1 monoclonal antibody   G. Enders, University of Kansas, USA

Rabbit anti HSP110 polyclonal antibody   Sigma, Steinheim

Rabbit anti Apg1 polyclonal antibody   Santa Cruz Biotechnology, Heidelberg

Rabbit anti Apg2 polyclonal antibody   Santa Cruz Biotechnology, Heidelberg

Rabbit anti CyclinA1 polyclonal antibody   Santa Cruz Biotechnology, Heidelberg

2.1.11 Enzymes

Antarctic Phosphatase	(BioLabs, Frankfurt am Mein)
FideliTag DNA Polymerase	(USB, Staufen)
Immolase DNA Polymerase	(Bioline, Luckenwalde)
Klenow Fragment	(Invitrogen, Karlsruhe)
Proteinase K	(Sigma, Deisenhofen)
Platinum Taq polymerase	(Invitrogen, Karlsruhe)
Restriction enzymes (with supplied buffers)	(Invitrogen, Karlsruhe)
RNase A	(Qiagen, Hilden)
RNase H	(Invitrogen, Karlsruhe)
RNase inhibitor	(Invitrogen, Karlsruhe)
Superscript-II	(Invitrogen, Karlsruhe)
Taq polymerase	(Invitrogen, Karlsruhe)
T4 DNA ligase	(Promega, Mannheim)
Trypsin	(Invitrogen, Karlsruhe)

2.1.12 Radioactive substances

α-32P-dCTP   (Amersham, Braunschweig)

2.1.13 Kits

AP Kit (86C-1 KT)	(Sigma, Deisenhofen)
Endo Free Plasmid Maxi Kit	(Qiagen, Hilden)
GenomeWalker Universal Kit	(Clontech)

MATERIALS AND METHODS

Labelling System	(Qiagen, Hilden)
Megaprime DNA Labeling Kit	(Amersham Pharmacia, Freiburg)
Midi Plasmid Kit	(Invitrogen, Karlsruhe)
Mini Plasmid Kit	(Qiagen, Hilden)
PCR Purification Kit	(Qiagen, Hilden)
QIAquick Gel Extraction Kit	(Qiagen, Hilden)
RNAeasy Kit	(Qiagen, Hilden)
RediprimeTM II Random Prime	(Amersham Pharmacia, Freiburg)

2.1.14 Equipment

Autoclave	(Webeco, Bad Schwartau)
Centrifuge 5415D	(Eppendorf, Hamburg)
Centrifuge 5417R	(Eppendorf, Hamburg)
Biophotometer	(Eppendorf, Hamburg)
DNA Sequencer Modell Megabace 1000	(Amersham, Freiburg)
Microscope BX60	(Olympus, München)
GeneAmp PCR System 9600	(Perkin Elmer, Berlin)
Histocentre 2 embedding machine	(Shandon, Frankfurt aM.)
Microtiterplate-Photometer	(BioRad laboratories, München)
Molecular Imager FX	(BioRad laboratories, München)
Phosphoimager Screen	(BioRad laboratories, München)
Semi-Dry-Blot Fast Blot	(Biometra, Göttingen)
Spectrophotometer Ultraspec 3000	(Amersham, Freiburg)
SpeedVac concentrator SVC 100H	(Schütt, Göttingen)
Thermomixer 5436	(Eppendorf, Hamburg)
TurboblotterTM	(Schleicher & Schüll, Dassel)
UV StratalinkerTM1800	(Leica, Nußloch)

MATERIALS AND METHODS

2.2 METHODS

2.2.1 Isolation of nucleic acids

2.2.1.1 Isolation of plasmid DNA (Sambrook *et al.,* 1989)

Small-scale isolation of plasmid DNA (Birnboim and Doly, 1979)

A single bacterial colony was inoculated into 5 ml LB medium, containing an appropriate antibiotic, and incubated at 37°C for 12-16 hours with a shaking speed of 160 rpm. 0.2 ml of this culture was used for glycerol stock and rest of it was centrifuged at 4000 x g for 10 min. The pellet was resuspended in 100 μl of resuspension solution P1 (Invitrogen). The bacterial cells were lysed with 200 μl of lysis solution P2 (Invitrogen), incubated at RT for 5 min and then neutralised with 150 μl of neutralisation solution P3 (Invitrogen). The precipitated solution was incubated at RT for 5 min and centrifuged at 13000 x g at RT. The supernatant was transferred into a new tube, where 1 ml of 100% ethanol was added to precipitate the DNA. Then it was incubated for 30 min at RT, centrifuged at full speed for 20 min, and finally the pellet was washed with 350 μl of 70% ethanol and after air-drying dissolved in 30 μl of dH$_2$O.

P1: 50 mM Tris/HCl, pH 8.0; 10 mM EDTA; 100 μg/ ml RNase A

P2: 200 mM NaOH; 1% SDS

P3: 3 M Potassium acetate, pH 5.5

Large-scale preparation of Endotoxin free plasmid DNA using the Qiagen Maxi Kit

A single clone was inoculated into 5 ml LB medium, containing an appropriate antibiotic. The preculture was incubated for 12 hours at 37°C with shaking. Then it was diluted 500 times in 100 ml of the same medium and incubated overnight at 37°C with shaking. Next day it was centrifuged at 6000 x g for 15 min. The pellet was resuspended in 5 ml of solution P1 and cells were lysed with P2 and P3 as described above. The precipitated solution was centrifuged at 20000 x g for 30 min at 4°C. Meanwhile, the column (Qiagen-tip), that was provided with the maxi preparation kit, was equilibrated with 10 ml of QBT solution. After centrifugation, the lysate was poured into this equilibrated column to allow the DNA to bind with the resin present on the bottom of the column. The column was then washed twice with 10 ml of solution QC. Finally, the DNA was eluted with 5 ml of QF

solution. For precipitation of the DNA, 3.5 ml of isopropanol was added, mixed thoroughly and then centrifuged at 14000 x g for 30 min at 4°C. The obtained pellet was washed with 70% ethanol and dissolved in 100 μl of TE buffer.

QBT: 750 mM Sodium chloride; 50 mM MOPS pH 7.0; 15 % Ethanol; 0.5 % Triton X-100

QC: 1 mM Sodium chloride; 50 mM MOPS pH 7.0; 15 % Ethanol

QF: 1.25 M Sodium chloride; 50 mM Tris/HCl pH 8.5

2.2.1.2 Isolation of genomic DNA

Isolation of genomic DNA from tissue samples (Laird *et al.,* 1991)

1 cm of the mouse tail was incubated in 700 μl of lysis buffer I containing 35 μl proteinase K (10 μg/μl) at 55°C overnight in Thermomixer 5436. The tissue lysate was centrifuged at 14000 x g for 15 min and the supernatant was transferred into a new e-cup. Then, DNA was precipitated by adding an equal volume of isopropanol, mixed by inverting several times and centrifuged at 14000 x g at RT for 15 min. DNA was washed with 1 ml of 70% ethanol, dissolved in 50-100 μl of dH_2O and incubated at 60°C for 10 min.

Isolation of genomic DNA from cultured cells

Cells were washed with PBS and incubated overnight in 500 μl of lysis buffer II at 37°C. Next, equal volume of isopropanol was added, mixed by inverting several times and incubated for 10 min at RT. Then, centrifuged for 15 min at maximal speed. After washing the pellet with 70% ethanol, the DNA was dissolved in 80 μl of dH_2O and incubated at 60°C for 10 min.

2.2.1.3 Isolation of total RNA from tissue samples and cultured cells

Total RNA isolation reagent is an improved version of the single-step method for total RNA isolation. The composition of reagent includes phenol and guanidine thiocyanate in a mono-phase solution. 100-200 mg of tissue sample was homogenised in 1 ml of TRI Reagent by using an e-cup homogeniser. The sample volume did not not exceed 10% of the volume of reagent used for the homogenisation. To isolate total RNA from cultured cells, 350 μl of reagent was added to the Petri dish (6 cm). Cells were homogenised with a rubber scraper and the lysate was transferred into a microcentrifuge tube, where it was incubated at 4°C for 5 min to permit the complete dissociation of nucleoprotein complexes. Then, 0.2 ml of chloroform was added, mixed vigorously, and stored at 4°C for 10 min. After

centrifugation at 12000 xg for 15 min at 4°C, the upper aqueous phase was transferred into a new tube. The RNA was precipitated by adding 0.5 ml of isopropanol. Finally, the pellet was washed twice with 75% ethanol and dissolved in 30-80 μl of RNase free water (DEPC-dH$_2$O).

2.2.2 Determination of nucleic acid concentration

The concentration of nucleic acids was determined spectrophotometrically by measuring absorption of the samples at 260 nm. The quality of nucleic acids i.e. contamination with salt and protein was estimated by ratio of absorbance 260nm/280 nm. The correct value of the ratio is 1,8 for DNA and 2,0 for RNA.

2.2.3 Determination of transgene integration – GenomeWalker Universal Kit

GenomeWalker Kit helps to find unknown genomic DNA sequences adjacent to a known sequence. First step was to construct pools which consist of adaptor-ligated genomic DNA fragments (i.e. libraries). Thereafter, primary PCR was done by using outer adaptor primer (AP1) provided in the kit and outer gene-specific primer (EvaL1_GenomeWalk_F1 for EvaL1 line). Diluted primary PCR mixture was then used as a template for nested PCR with a nested adaptor primer (AP2) provided in the kit and nested gene-specific primer (EvaL1_GenomeWalk_F2). The obtained result was a major PCR product from at least three of four libraries. All fragments were sequenced. The one, which began with a known sequence at the 5' end of EvaL1_GenomeWalk_F2 primer and extended into the unknown adjacent genomic DNA, was further cloned, sequenced and compared to mouse genome sequence.

The procedure was exactly followed according to manufacturer's protocol (GenomeWalker Universal Kit – User Manual, cat. no. 638904, Clontech).

2.2.4 Gel electrophoresis

Gel electrophoresis is the technique which enables separation of nucleic acids and proteins in an electrical field according to their mobility which is directly proportional to macromolecule's charge to mass ratio.

MATERIALS AND METHODS

2.2.4.1 Agarose gel electrophoresis of DNA

Agarose gels were used to run nucleic acid molecules from as small as 50 bases to more than 20 kb, depending on the concentration of the agarose. Usually, 1 g agarose was added to 100 ml of 0.5 x TBE buffer and boiled in the microwave to dissolve the agarose, then cooled down to about 60°C before adding 3 μl of ethidium bromide (10 mg/ml). This 1% agarose gel was poured into a horizontal gel chamber.

2.2.4.2 Agarose gel electrophoresis of RNA (Hodge, 1994)

mRNA molecules often have complementary regions that can form secondary structures. Therefore, RNA was pre-treated with formaldehyde and formamide in order to denature the secondary structure of RNA and it was run on an agarose gel containing formaldehyde. 1.25g of agarose was added to 100 ml of 1 x E buffer and dissolved by heating in a microwave. After cooling it to about 60°C, 25 ml of formaldehyde (37%) was added, stirred and poured into a vertical gel chamber. RNA samples (10 – 30 μg) were mixed with double volume of sample buffer, then denatured at $65^{o}C$ for 10 min and chilled on ice. After adding loading buffer (equal volume to RNA sample), the gel was loaded and run at 70-80V at $4^{o}C$ for 4 – 5 hours.

Sample buffer/ 1 sample: 2 μl 10x E buffer; 3 μl 37% formaldehyde; 8 μl 40% formamide;

Loading buffer: 40 μl 1% ethidium bromide in 500 μl standard loading buffer

2.2.4.3 SDS-PAGE gel for separation of proteins

NuPage 4-12% Bis-Tris gel is SDS-PAGE gel with 4-12% percentage gradient what allows more efficient separation of proteins. 20.5 μl of whole protein lysate was mixed with 7.5 μl 4 x NuPage sample buffer and 2 μl 1M DTT. Then, the samples were denatured in $95^{o}C$ for 10 min and chilled in ice. The gel electrophoresis was run in 1 x MOPS buffer or 1 x MES buffer (Invitrogen). As a weight marker, a pre-stained molecular weight standard (See Blue Plus2, Invitrogen) was loaded. The gel was run at 100 V for 2 – 3 hours at RT.

MATERIALS AND METHODS

2.2.5 Purification of DNA fragments from agarose gel

To extract and purify DNA of 70 bp to 10 kb in length from agarose gels, QIAquick gel extraction kit (Qiagen) was used. Up to 400 mg agarose can be processed during single isolation. 3 volumes of QG buffer were added to an agarose gel piece and then incubated at 50°C for 10 min. After the gel slice was dissolved, the solution was applied to a QIAquick column and centrifuged for 1 min. The flow through was discarded and the column was washed with 0.75 ml of PE buffer. After drying, the column was placed into a fresh microcentrifuge tube. To elute DNA, 50 μl of dH_2O was applied to the centre of the QIAquick membrane and the column was centrifuged for 1 min.

2.2.6 Enzymatic modifications of DNA

2.2.6.1 Restriction of DNA

Restriction enzyme digestions were performed by incubating double-stranded DNA with a restriction enzyme in amount of max. 1/10 reaction volume in a buffer recommended by the supplier, and at the optimal temperature for the specific enzyme. Standard digestions included 2-10 U enzyme per 1 μg DNA. Usually incubation time was 1-3 hours at 37°C. For genomic DNA digestion, the reaction solution was incubated overnight at 37°C.

2.2.6.2 Ligation of DNA fragments

The cloning of an insert DNA into a vector (digested with appropriate restriction enzyme) was carried out in the following ligation reaction mix in total volume of 10 μl:

- 30 ng vector DNA (digested)
- 50-100 ng insert DNA (1:3, vector: insert ratio)
- 1 μl ligation buffer (10x)
- 1 μl T4 DNA ligase (5 U/μl)

The reactions were performed at 4°C overnight.

MATERIALS AND METHODS

2.2.6.3 TA-Cloning (Clark, 1988; Hu, 1993)

Taq polymerase and other DNA polymerases have a terminal transferase activity that results in the non-template addition of a single nucleotide to the 3' ends of PCR products. In the presence of all 4 dNTPs, dATP is preferentially added. This terminal transferase activity is the basis of the TA-cloning strategy. For cloning of PCR products, a pGEMTeasy vector system that has 5'T overhangs was used. The following substances were mixed:

- 50 ng of pGEMTeasy vector
- 150 ng PCR product
- 1 µl of T4 DNA Ligase buffer (x10)
- 1 µl of T4 DNA Ligase

The reactions were done in a total volume of 10 µl and incubated overnight at 4°C.

2.2.6.4 Dephosphorylation

The removal of 5' phosphate groups from DNA was done by using of Antarctic Phosphatase (BioLabs). Dephosphorylation mixture was prepared as follows:

1 µg DNA

2 µl 10x AP buffer

1 µl 5U Antarctic Phosphatase

The mixture of 20 µl was then incubated at 37°C for either 15 (for 5' extension) or 60 min (for 3' extension). Afterwards, the enzyme was inactivated for 10 min in 65°C.

2.2.7 Transformation of competent bacteria (Ausubel *et al.,* 1994)

Transformation of bacteria was done by gently mixing 50 µl-aliquot of competent bacteria (Invitrogen) with 10 µl of ligation reaction. After incubation for 30 min on ice, bacteria were heat-shocked for 45 sec at 37°C and cooled down for 2 min on ice. After adding 450-900 µl of S.O.C. medium, the mixture was incubated at 37°C, 400 rpm, for 1 hour to allow recovery of heat shocked bacteria which then were plated on LB-agar plates.

MATERIALS AND METHODS

2.2.8 Polymerase Chain Reaction (PCR)

In general, the PCR reaction contained the following substances:

- 10 ng DNA
- 1 μl forward primer (10 pmol)
- 1 μl reverse primer (10 pmol)
- 1 μl 10 mM dNTPs
- 5 μl 10 x PCR buffer
- 1.5 μl 50 mM $MgCl_2$
- 0.5 μl *Taq* DNA Polymerase (5 U/□l)
- Up to 50 μl dH_2O

The reaction mixture was placed in a 200 μl reaction tube and placed in a thermocycler. Thermal cycling was carried out for 35 cycles with denaturation at 95°C for 30 sec, annealing at 55-60°C for 30 sec and extension at 72°C for 30 sec. -1 min (depending on the product size).

2.2.8.1 Genotyping PCRs

Flox/-/Δ PCR

Ingredients:		Program:	
H_2O	11,6 μl	94°C – 5 min	
buffer	1,5 μl	94°C – 30 sec.	
$MgCl_2$	0,3 μl	65°C – 50 sec.	35x
dNTPs	0,3 μl	72°C – 30 sec.	
Pelo_F11	0,3 μl	72°C – 7 min	
Pelo_R14	0,3 μl		
PGK_cKO_R1	0,3 μl		
Taq Platinum	0,15 μl		
DNA	0,5 μl		

CreEIIa PCR

Ingredients:		Program:	
H_2O	6,1 μl	94°C – 5 min	
buffer	1 μl	94°C – 30 sec.	
$MgCl_2$	0,3 μl	67°C – 40 sec.	30x
dNTPs	0,2 μl	72°C – 40 sec.	
EllaCre_F	0,6 μl	72°C – 7 min	
EllaCre_R	0,6 μl		
Taq Platinum	0,15 μl		
DNA	0,5 μl		

MATERIALS AND METHODS

Cre PCR (cKO/Stra8 line)

Ingredients:		Program:	
H_2O	20 µl	94^oC – 5 min	
buffer	2,5 µl	94^oC – 45 sec.	
$MgCl_2$	0,75 µl	57^oC – 55 sec.	35x
dNTPs	0,5 µl	72^oC – 1 min 20 sec.	
Stra8_F	0,5 µl	72^oC – 7 min	
Cre_R	0,5 µl		
Taq Platinum	0,15 µl		
DNA	0,5 µl		

CreERT PCR

Ingredients:		Program:	
H_2O	6,8 µl	94^oC – 5 min	
buffer	1 µl	94^oC – 30 sec.	
$MgCl_2$	0,4 µl	56^oC – 30 sec.	30x
dNTPs	0,2 µl	72^oC – 50 sec.	
RosaCreER_F	0,5 µl	72^oC – 7 min	
RosaCreER_R	0,5 µl		
Taq Platinum	0,15 µl		
DNA	0,5 µl		

EvaL1 PCR

Ingredients:		Program:	
H_2O	18 µl	94^oC – 5 min	
buffer	2,5 µl	94^oC – 30 sec.	
$MgCl_2$	1 µl	60^oC – 45 sec.	35x
dNTPs	0,5 µl	72^oC – 30 sec.	
EvaL1_F	1 µl	72^oC – 7 min	
EvaL1_R	0,5 µl		
EvaL1_GenomeWalk_F2	0,5 µl		
Taq Platinum	0,15 µl		
DNA	0,5 µl		

AdamL1, AdamL9, EvaL6

The PCRs were performed according to established protocols for these lines (Buyandelger, 2006).

2.2.8.2 Generation of Southern probes

5'external probe

The probe was generated by Buyandelger (2006).

Internal probe (3'probe, 266bp)

The probe was amplified by PCR as follows:

MATERIALS AND METHODS

Ingredients: Program:
H$_2$O   17,5 µl   94°C – 5 min
buffer   2,5 µl   94°C – 30 sec.
MgCl$_2$ 1 µl   60°C – 50 sec.   35x
dNTPs   1 µl   72°C – 45 sec.
Pelota3'_F2   1 µl   72°C – 7 min
Pelota3'_R2   1 µl
Taq Platinum   0,15 µl
DNA   0,5 µl

The PCR product was subcloned into pGEMTeasy and sequenced. The 266 bp *EcoRI* fragment was purified and used as a probe for Southern blot.

3'external probe (885bp)

It was amplified by PCR as follows:

Ingredients: Program:
H$_2$O   19,8 µl   94°C – 5 min
buffer   2,5 µl   94°C – 30 sec.
MgCl$_2$ 0,5 µl   58°C – 30 sec.   35x
dNTPs   0,5 µl   72°C – 45 sec.
cKO_3'ext_F   0,5 µl   72°C – 7 min
cKO_3'ext _R   0,5 µl
Taq Platinum   0,15 µl
DNA   0,5 µl

The PCR product was subcloned into pGEMTeasy and sequenced. The 885 bp *EcoRI* fragment was purified and used as a probe for Southern blot.

2.2.8.3 Reverse transcription PCR (RT-PCR)

RT-PCR generates cDNA fragments from RNA templates and helps to determine the expression of genes in specific tissues or in different development stages.

1-5 µg of total RNA was mixed with 1 µl of oligo (dT)18 primer (10 pmol/µl) in a total volume of 12 µl. For denaturation the mixture was heated to 70°C for 10 min and then quickly chilled on ice. After a brief centrifugation, the following substances were added to the mixture:

- 4 µl 5 x first strand buffer

- 2 µl 0.1 M DTT

- 1 µl 10 mM dNTPs

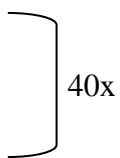- 1 µl RNasin (10 U/µl)

MATERIALS AND METHODS

The reaction was incubated at 42°C for 2 min. Then, 1 µl of reverse transcriptase enzyme (Superscript II, Invitrogen) was added and the mixture was incubated at 42°C for 50 min for the first strand cDNA synthesis. Next, the reaction was inactivated by heating at 70°C for 15 min 1 µl of the first strand reaction was used for the PCR reaction.

2.2.8.4 Quantitive Real-Time PCR

DNA was isolated from transgenic mice tails by the method described above (2.2.1.2.1). Serial dilutions of sample and standard DNA's were made. Standard DNA (a mixture of Founder DNA and two F1 males) was serially diluted to 20, 10, 5, 2.5, 1.25 and 0.625 ng/µl for the generation of standard curve, while each sample DNA (transgenic mice) was diluted to a concentration of 10 ng/µl. Primers were designed to generate amplicons less than 200 bp, thus enhancing the efficiency of PCR amplification. Real-Time quantitative PCR was performed using QuantiTect SYBR Green PCR Master mix (Quiagen) in an ABI Prism 7900HT sequence detection system. Each reaction was run in triplicate and the melting curves were analysed to ensure that only a single product was amplified. 18S primers were used for the normalisation of each DNA sample. Quantitative real-time PCR reactions of DNA specimens and standards were conducted in a total volume of 10 µl with 5 µl of 2 x QuantiTect SYBR-Green PCR-Master-Mix, 1 µl of each forward and reverse primer in a final concentration of 9 µM and 2.5 µl of DNA.

The following cycling parameters were used:

2 min 50°C

15 min 95°C

15 sec 95°C

30 sec 60°C   40x

30 sec 72°C

15 sec 95°C

15 sec 60°C melting curve

15 sec 95°C

Standard curves of the threshold cycle number versus the log number of copies of genes were generated for transgenic integration sites and were used to extrapolate the number of integration sites of transgene. Quantitative Real-Time PCR results were reported

as the number of transgenic allele in comparison to transgenic allele in founder mouse. The samples were normalized by reference to 18S gene.

2.2.8.5 Quantitive Real-Time RT-PCR

In general Quantitative Real-Time RT-PCR for mRNAs was performed as for DNA (2.2.2.8.3). cDNA synthesis was done according to section 2.2.8.2 with preceding DNAse treatment. 5 µl 2x QuantiTect SYBR-Green PCR-Master-Mix, 1 µl Forward Primer (9µM), 1 µl Reverse Primer (9µM), 0.3µl MgCl2 (50mM) and 1µl of cDNA (in a 1/20 dilution) were mixed with RNase free water to a total volume of 10 µl. The following PCR program was used:

2 min 50°C

15 min 95°C

15 sec 95°C

30 sec 55°C   } 40x

30 sec 72°C

15 sec 95°C

15 sec 60°C melting curve

15 sec 95°C

Primer sequences are provided in section 2.1.9. *Sdha* was used as endogenous reference. For standard curves, a mixture of NMRI testes cDNA and cKO/Stra8_Cre testes cDNA was used. Selection of the appropriate sample for the standard curve was based on preliminary experiments testing detection of expression of each gene by RT-PCR (2.2.8.2). Reliability of Real-time PCR data was also assessed in connection with the respective dissociation curves.   `

2.2.9 Protein manipulation methods

2.2.9.1 Isolation of total protein lysate

Approximately 100 mg of tissue was homogenised in 200 - 500 µl lysis buffer A. Then, the samples were treated with ultrasound on ice 2 x 1 min, centrifuged at 8000 x g for 20 min at 4°C and the supernatant was aliquoted in several microcentrifuge tubes. The tubes were frozen in liquid nitrogen and stored at -80°C.

MATERIALS AND METHODS

5 x 10^6 cells/ml were washed with cold phosphate buffered saline (PBS) and resuspended in 50 - 200 µl of lysis buffer A. The cells were left on ice for 30 min, treated with ultrasound on ice 2 x 30 sec and centrifuged at 24000 x g for 20 min at 4^oC. The supernatant with protein extract was either used immediately or stored at -80^oC for later use.

2.2.9.2 Determination of protein concentration (Bradford, 1976)

To determine the protein concentration, Bio-Rad protein assay was employed. The BSA stock solution of 1 mg/ml was diluted in order to obtain standard dilutions in range of 10 µg/ml to 100 µg/ml. The dye reagent concentrate (Bio-Rad Laboratories GmbH) was diluted 1:5 with H_2O and 2 µl sample were added. The absorption of the color reaction was measured at 595 nm in a spectrophotometer.

2.2.10 Blotting techniques

2.2.10.1 Southern blotting of DNA (Southern, 1975)

After electrophoresis of DNA, the gel was treated with 0.25 M HCl for depurination for 20 – 30 min, with denaturation solution for 30 min and neutralisation solution for 45 min. The transfer of the DNA to the nitrocellulose membrane was done in a Turbo-Blot apparatus (Schleicher & Schuell, Dassel). About 25-28 Whatman filter papers (GB 003) were layered on a Stack Tray, followed by 4 Whatman filter papers (GB 002) and 1 Whatman filter paper (GB 002) soaked with 20 x SSC. The equilibrated nitrocellulose filter, that was also soaked with 20 x SSC, was laid on the top. The agarose gel, treated as described above, was placed on the filter and was covered with 3 Whatman filter papers GB 002 soaked with 20 x SSC. The buffer tray was filled with 20 x SSC. Finally a wick, which was soaked with 20 x SSC, and the wick cover were put on top of the blot. The transfer was carried out for overnight. Finally, after disassembling of the blot, the DNA was fixed onto the filter by baking at 80°C for at least 2 hours.

MATERIALS AND METHODS

2.2.10.2 Northern blotting of RNA

The procedure performed for the transfer of RNA onto a nitrocellulose filter was the same as described above (2.2.10.1). However, the gel did not need to be denatured, but was transferred directly onto the filter.

2.2.10.3 Western blotting of protein (Gershoni and Palade, 1982)

After electrophoresis of proteins, the SDS PAGE gel and the PVDF membrane were moistened with transfer buffer. Four pieces of filter paper were soaked in transfer buffer and placed on the semi dry transfer machine's lower plate. Then, wet membrane and the gel were put, avoiding any air bubbles. Another four soaked Whatman papers were placed on the pile to complete the sandwich model. The upper plate was placed over this sandwich and the transfer was carried out at 3.5 mA/cm^2 for 1 hr.

After blotting, the gel was stained with Comassie blue overnight at RT in order to check the amount of proteins which were not transferred.

2.2.11 "Random Prime" method for generation of ^{32}P labeled DNA (Denhardt, 1966; Feinberg and Vogelstein, 1984)

RediprimeTM II Random Prime Labeling System (Amersham Pharmacia) was used for labelling of DNA probes. The method depended on the random priming principle developed by Feinberg and Vogelstein (1984). The reaction mix contained dATP, dGTP, dTTP, Klenow fragment (4-8 U) and random oligodeoxyribonucleotides. Firstly, 25-50 ng DNA were denatured in a total volume of 46 μl at 95°C for 10 min and quickly chilled on ice for 5 min. After pipetting the denatured probe into RediprimeTM II Random Prime Labelling System cup, 4 μl of [α-32P] dCTP (3000 Ci/mmol) were added to the reaction mixture. The labelling reaction was carried out at 37°C for 45 min. The labelled probe was purified from uncorporated [α-32P] dCTP by using illustra^{TM}Probe Quant^{TM} G-50 Micro Cloumns (GE Healthcare).

MATERIALS AND METHODS

2.2.12 Non-radioactive dye terminator cycle sequencing

Non-radioactive sequencing was performed with the Dye Terminator Cycle Sequencing-Kit (ABI PRISM). The reaction products were analysed with automatic sequencing equipment, MegaBase DNA Sequencer. For the sequencing reaction, four different dye labelled dideoxy nucleotides were used (Sanger *et al.,* 1977), which, when exposed to an argon laser, emit fluorescent light that can be detected and interpreted.

The reaction was carried out in a total volume of 10 μl containing 1 μg plasmid DNA or 100-200 ng purified PCR products, 10 pmol primer and 4 μl reaction mix (contained dNTPs, dideoxy dye terminators and *Taq* DNA polymerase). Elongation and chain termination took place during the following program in a thermocycler: 4 min denaturation followed by 25 cycles at 95°C, 30 sec; 55°C, 15 sec, annealing; 60°C, 4 min, elongation. After the sequencing reaction, the DNA was precipitated with 1/10 volume 3 M sodium acetate and 2.5 volume 100% ethanol and washed in 70% ethanol. The pellet was dissolved in 4 μl of loading buffer, denatured at 95°C for 3 min, and finally loaded on the sequence gel.

2.2.13 Hybridisation of nucleic acids (Denhardt, 1966)

A membrane for hybridization was equilibrated in 2 x SSC and transferred to a hybridisation bottle. After adding 12 ml of Rapid-hyb buffer (GE Healthcare) and sheared denatured salmon DNA, the membrane was incubated for 2 hours in the hybridisation oven at 65°C. Then, the labelled probe was denatured at 95°C for 10 min, chilled on ice for 5 min, and added to the hybridisation solution. The hybridisation was carried out overnight in the oven. Next day, the filter was washed for 10 min with 2 x SSC, then with 2 x SSC containing 0.2% SDS at 65°C for 10 – 20 min. Finally, the membrane was washed with 0.2 x SSC containing 0.1 % SDS at the hybridisation temperature. After drying the filter, it was sealed in Saran wrap and exposed to autoradiography overnight at -80°C. The film was developed in X-Ray Automatic Processor Curix 60.

MATERIALS AND METHODS

2.2.14 Histological techniques

2.2.14.1 Tissue preparation for paraffin-embedding

The freshly prepared tissues were fixed in Bouin's solution or 4% (w/v) paraformaldehyde for 6 - 24 hours to prevent alterations in the cellular structure. The dehydration process was accomplished by passing the tissue through a series of increasing alcohol concentrations, i.e. 70%, 80%, 90%, 96%, 100% ethanol for 1 hour at RT and isopropanol overnight. Later, the alcohol was removed from the tissue by incubation in 25%, 50%, 75% and 100% xylene. Next step was incubation of the tissues in paraffine at 60°C for 12-24 hours. Before embedding, the paraffin was changed at least three times. Finally, the tissue was placed in embedding mold and melted paraffin was poured into the mold to form a block. The block was cooled and became ready for sectioning.

2.2.14.2 Sections of the paraffin block

Paraffin blocks were clamped into the microtome (Hn 40 Ing., Nut hole, Germany). The thickness of the section was 5 μm. The sections were floated on 40°C water to allow actual spread. Then, they were put onto slides. After complete drying at 37°C, slides were stored at 4°C for further analysis.

2.2.14.3 Immunofluorescence staining

For mouse tissues:

Tissue sections were incubated twice for 10 min in xylene to remove the paraffin. Then, they were re-hydrated in a decreasing ethanol series (100%, 96%, 70%, 50%, and 30%) for 2 min each. For immunofluorescence staining, the sections were washed in PBS and then incubated with a blocking solution containing 10% goat serum and 0.02% Tween-20 in PBS for 2 hours at RT. Then, they were incubated with primary antibodies for overnight in a humidified chamber at 4°C. Subsequently, they were rinsed three times for 5 min in PBS and an appropriate secondary antibody was put for 1 hour. Finally, the slides were washed three times for 5 min in PBS and the nuclei were counterstained with DAPI. Immunostaining of the sections was examined using a fluorescence equipped microscope (BX60; Olympus).

MATERIALS AND METHODS

For cells:

Cells were fixed in 4% paraformaldehyde in PBS for 15 min at 4^oC , rinsed in PBS and incubated in 50 mM NH_4Cl (PBS) for 10 min at RT. After washing in PBS (2 x), the cells were 3 x washed in 0,2% Triton X-100 (PBS) for 4 min. Next, the primary antibody with appropriate dilution was applied for overnight at 4^oC. Cells were washed 2x in 0,2% Triton X-100 (PBS) for 4 min and incubated with Cy3- conjugated IgG for 1 hour at RT. One drop of mounting medium with DAPI was dispensed onto the slides after washing with PBS. Fluorescent cells were visualised with Olympus BX60 microscope.

2.2.14.4 Phalloidin staining of cells

Cells were washed twice in PBS for 5 min, fixed for 15 min (4^oC) in 4% paraformaldehyde and washed 3 times in PBS. Then, they were incubated for 1 hour in phalloidin (diluted 1:1000) conjugated with Cy3 and washed 3 times in PBS. The slides were mounted with DAPI-containing medium.

2.2.14.5 Alkaline phosphatase staining of cells

Cells were washed with PBS, fixed for 30 sec. with fixation solution (Sigma) and washed with dH_2O for 1 min. Incubation with staining solution was applied for 15 min in RT. Next, the cells were washed for 2 min in water and incubated with neutral red for 10-20 sec. Afterwards, they were washed in tapped water and left for drying.

2.2.14.6 Hematoxylin-eosin (H&E) staining of the histological sections

Tissue sections were first incubated three times in xylene for 3 min each, followed by incubation in 100% for 3 min, 95% and 80% ethanol for 2 min each. Thereafter slides were washed in dH_2O for 5 min and stained for 3 min in hematoxylin. The staining was followed by rinsing with deionised water and washing in tap water for 10 min. The treated slides were dipped fast in acid ethanol (1ml concentrated HCl in 400 ml 70% ethanol) for 8-12 times to destain and in amonium water (0,25%), rinsed in tap water for 2 min and in deionised water for 2 min, stained in eosin for 1 min and then incubated in 70%, 80%, 90%, 95% and 100% ethanol for 2 min each. Finally, the stained slides were incubated in xylene for 15 min and mounted with Eukitt-quick hardening mounting medium.

MATERIALS AND METHODS

2.2.14.7 Apoptosis detection

ApopTag Peroxidase Apoptosis Detection Kit was used for analysis of apoptotic cells in testis sections (5 μm). The sections were firstly deparafinized, dehydrated and washed 2 x 5 min in PBS. Next, the slides were incubated for 15 min at RT in 20 μg/ml Proteinase K and washed 2 x 2 min in dH_2O. To block endogenous peroxidase, tissues were incubated in 3 % H_2O_2 for 5 min at RT. After 2 x 5 min washing in PBS, the tissues were covered for 10 sec. with equilibration buffer. Next, Working Strength TdT Enzyme (30% enzyme in reaction buffer) was applied for 1-hour incubation at 37^oC in darkness. To stop the reaction, the slides were incubated for 10 min shaking at RT in Stop/Wash buffer (1:34 in dH_2O) and then washed 3 x 1 min with PBS. Next step was incubation with anti-digoxigenin for 30 min at RT in darkness and washing 4 x 2 min with PBS. Then the slides were stained with Working Strength Peroxidase Substrate (2% DAB Substrate in DAB Dilution buffer) for 6 min at RT, washed 3 x 1 min and 1 x 5 min with dH_2O. They were covered by AquaPolyMount liquid.

2.2.15 Eukaryotic cell culture methods

The cells were cultured at $37°C$ in a humidified incubator with 5% CO_2.

2.2.15.1 Preparation of MEFs feeder layers

A frozen aliquot of MEFs was quickly thawed at $37°C$ and transferred to 10 ml MEF medium. After centrifugation at 1000 x g for 5 min, the cell pellet was gently resuspended in 10 ml MEFs medium and plated on a 50 ml culture flask. Cells were incubated at $37°C$ in 5% CO_2. When the cells formed a confluent monolayer after three days, they were trypsinised, transferred to five 10 cm dishes and grown until they formed confluent monolayer, or directly treated with mitomycin C (1mg/ml) for 3 hours. Then, the cells were washed twice with 10 ml PBS, resuspended with 10 ml medium and centrifuged. Next, they were resuspended in MEFs medium and plated onto dishes, which were pretreated with 0.1% gelatine for 30 min. The feeder cells were left to attach by incubation overnight at $37°C$, 5% CO_2 or used after 2 hours of incubation. Before adding ES cells on the feeder layer, the medium was changed to ES cell medium.

MATERIALS AND METHODS

2.2.15.2 Trypsinisation of eukaryotic cells

Cells were washed twice with sterile PBS and incubated in minimal amount trypsin-EDTA (0.5 g/l trypsin, 0.2 g/l EDTA) at 37°C for 5 min. Trypsin was inhibited by addition of growth medium, in which the cells were subsequently resuspended. The enzyme was removed by centrifugation at 1000 x g for 3 min. Cells were resuspended in an appropriate volume of cell culture medium and transferred into a new flask/plate with medium.

2.2.15.3 Cryopreservation and thawing of eukaryotic cells

Trypsinised cells were spun down (1000 x g for 5 min) in 4 ml of growth medium. The supernatant was aspirated and the cells were resuspended in freezing medium (DMEM, 20% FCS, 10% DMSO). Aliquots of the cells were kept for 2 days at -80°C and then stored in liquid nitrogen. For revitalisation, frozen cells were quickly thawed and cells were inoculated in a suitable amount of growth medium, centrifuged and plated.

2.2.15.4 Isolation and handling of primary mouse embryonic fibroblasts (MEFs)

In order to isolate mouse embryonic fibroblasts (MEFs), pregnant female mice were sacrificed at 13-15 p.c. by cervical dislocation. Uterine horns were dissected and placed into a Petri dish containing PBS. Then each embryo was separated from its placenta and surrounding membranes. Embryo heads were taken for genotyping and the whole gastric system was removed. Such prepared embryos were sheared, put in 10 ml of trypsin-EDTA (1-2ml per embryo) and incubated for aprox. 5 min. An obtained cell suspension was transferred to 10 ml falcon tube and about 2 volumes of fresh medium was added, then cenrifugated at 1000 x g for 5 min and plated out at 1 embryo equivalent per 10 cm dish. Medium was changed the following day.

2.2.15.5 Growth of ES cells on feeder layer

One aliquot of frozen ES cells was quickly thawed at 37°C and cells were transferred to a 12 ml tube containing 6 ml ES cell medium. After centrifugation, the cell pellet was resuspended in 5 ml ES cell medium and plated on 6 cm dishes containing feeder layer. Next day the medium was changed. The second day, cells were washed with PBS, treated with 2

ml trypsin/EDTA at 37°C, 5% CO_2 for 5 min, resuspended with 5 ml ES medium and centrifuged. The cell pellet was resuspended in 10 ml ES cell medium and distributed either to 5 or 6 dishes (6 cm) or to 2 dishes (10 cm) containing feeder layers. The cells were passaged every second day as described above.

2.2.15.6 Differentiation of ES cells

Random differentiation by generation of embryoid bodies (EBs)

After trypsinization, cells were transferred to sterile bacterial dish, where they were cultured in 10 ml ES medium without LIF for 10 days. Afterwards, EBs were either collected for analysis or trypsinized and plated on gelatin-coated 6-well plates in 2 ml medium without LIF.

Neuronal differentiation (Kawasaki et al., 2000)

Undifferentiated mouse ES cells were expanded on gelatin-coated cell culture dishes in Glasgow minimal essential medium (GIBCO-Invitrogen, Karlsruhe, Germany) containing 1% fetal calf serum (FCS), 10% knockout replacement, 2 mM glutamine, 0.1 non essential amino acids, 1 mM sodium pyruvate, 0.1 mM 2-mercaptoethanol, 2000 U/ml leukemia inhibitory factor (GIBCO). The neuronal differentiation was induced in a culture on mitomycin C-inactivated PA6 feeder cells. The differentiation medium was composed of G-MEM supplemented with 10% KSR, 2 mM glutamine, 1 mM sodium pyruvate, 0.1 mM nonessential amino acids, and 0.1 mM 2-mercaptoethanol. ES cells were cultured on PA6 feeder cells in differentiation medium for 8 days before it was replaced with induction medium and cultured for an additional 6 days. The induction medium consisted of G-MEM including N-2 supplement (GIBCO), 100 μM tetrahydrobiopterin (Sigma), 200 μM ascorbic acid, 2 mM glutamine, 1 mM sodium pyruvate, 0.1 mM nonessential amino acids, and 0.1 mM 2-mercaptoethanol. After 4 days of differentiation, the medium was changed daily. On day 14 of the culture cells were analyzed.

MATERIALS AND METHODS

2.2.16. Production of targeted embryonic stem cell clones

2.2.16.1 Electroporation of ES cells

ES cells, which have grown for two days in 10 cm dishes, were trypsinised. The cell pellet was washed in 20 ml PBS, centrifuged and resuspended in 1 ml PBS. The 0.8 ml of cell suspension was mixed with 40 μg of linearised DNA-construct and transferred into an electroporation cuvette. The electroporation was performed at 240V, 500μF with the Bio-Rad gene pulserTM apparatus. After electroporation, the cuvette was placed on ice for 20 min. The cell suspension was transferred from cuvette into 20 ml of ES cell medium and plated onto two 10 cm dishes containing feeder layers. The medium was changed every next day. Two days after the electroporation, the drugs for selection were added (active G418 at 400μg/ml and gancyclovir at 2 μM). The medium was changed every day. After about eight days of selection, drug resistant colonies have appeared and were ready for screening by Southern blot analysis.

2.2.16.2 Growing ES cells for Southern blot analysis

The drug resistant colonies that were formed after about eight days of selection were picked with a drawn-out Pasteur pipette under a dissecting microscope. Each colony was transferred into a 24-well plate containing feeders and ES cell medium. After 2 days, the ES cells were trypsinised with 100 μl trypsin for 5 min and resuspended in 500 μl ES cell medium. Half of the cell suspension in each well was transferred to a well on two different 24-well plates, one gelatinised plate, and the other containing feeder cells (master plate). The gelatinised plate was used for preparing DNA and the master plate was kept frozen.

2.2.17 Flow cytometry (FACS) procedure for apoptosis detection and cell surface staining (Kanwar et al. 2008)

1×10^6 cells per measurement were washed in 5-ml tubes with PBS and resuspended in 100 μl PBS before cell surface staining with 1 μg of the respective antibodies: anti-CD3 (clone CT-CD3, rat IgG2a, phycoerythrin [PE]-labeled; Caltag Laboratories, Hamburg, Germany), anti-CD4 (clone CT-CD4, rat IgG2a, PE or tricolor [TC]-labeled; Caltag), anti-CD8a (clone CT-CD8a, rat IgG2a, fluorescein isothiocyanate [FITC] or PE-labeled), anti-

MATERIALS AND METHODS

CD8b (clone CT-CD8b, rat IgG2a, PElabeled; Caltag), anti-CD19 (clone 6D5, rat IgG2a, FIT C-labeled; Caltag), anti-CD25 (clone 7D4, rat IgM, FITClabeled, Becton Dickinson), anti-CD45R/B220 (clone RA3-6B2, rat IgG2a, PE-labeled; Caltag). TC-conjugated streptavidin (SA1006, Caltag) was used as the secondary reagent. Appropriate isotype controls were purchased from Caltag Laboratories. The cells were stained for 45 min at 4°C before being washed and resuspended in 200 µl PBS.

Exposure of phosphatidylserine as a membrane parameter of apoptosis was determined by staining cells for 45 min at 4°C in binding buffer (10 mM HEPES/NaOH, pH 7.4, 140 mM NaCl, 2.5 mM $CaCl_2$) with 5 µl annexin V-FITC (Becton Dickinson) in combination with 1 µg/ml propidium iodide (Sigma) to distinguish early apoptotic from late apoptotic or necrotic cells. The cells were resuspended in 200 µl annexin binding buffer before measurement. DNA histograms were obtained after propidium iodide staining of cells fixed in ethanol as described previously (Ormerod et al. 1992; Dressel et al. 2000). Flow cytometry was performed on a FACScan flow cytometer with CellQuest software (Becton Dickinson, Heidelberg, Germany); 10,000 to 50,000 cells per sample were counted.

2.2.18 Production of chimeras by injection of ES cells into blastocysts

The standard procedure is to inject 10-20 ES cells from 129/Sv, which are recombinant for the targeted locus, into the blastocoel cavity of recently cavitated blastocysts that have been recovered by flushing the uteri of day 4 pregnant mice (C57BL/6J). After injection, embryos are cultured for a short period (2-3 hrs) to allow re-expansion of the blastocoel cavity and then transferred to the uterine horns of day three pseudopregnant mice. Pseudopregnant females are obtained by mating 6-8 weeks old oestrous females with vasectomised males. Chimeric mice have been generated in Max Planck Institute for experimental medicine.

2.2.19 Detection of chimerism and mice breeding

Chimeric males (and sometimes females) are bred to wildtype mice to ascertain contribution of the ES cells to germline. Once a germline chimera has been identified, the first priority will be to obtain and maintain the targeted allele in living animals. The chimeras were bred with C57BL/6J.

MATERIALS AND METHODS

2.2.20 Preparation of cKO ESCs from cKO mice

Uterus was isolated from pregnant (E3.5) female and both its horns were cut to open it. Next, it was flushed with M2 medium through opened horns to wash out the blastocysts onto the plate. Then, the blastocysts were collected and transferred to KO medium on gelatine-pretreated plate. After 4 days, one could observe ESCs growing on the layer of trophoblast cells. The clones were picked and plated into separate wells of 24-well plate with feeder layer, they were cultured in ES medium. To confirm their genotype, genomic DNA was isolated and genotyping PCR was performed.

2.2.21 Tamoxifen (TAM) treatment of mice

The adult mice were injected intraperitoneally with 1 mg / day for 5 days. 10-day-old and 15-day-old mice were injected with 0.2-0.3 mg dose per day depending on the weight.

Preparation of tamoxifen

50 mg TAM were suspended in 500 µl 100% ethanol. Next, 4 ml of sunflower oil was added and it was mixed till powder was dissolved. An obtained solution (1mg/100 µl) was aliquoted and stored in -20°C max. for 4 weeks.

2.2.22 Hydroxytamoxifen (OHT) treatment of generated cKO ESCs

Cells were treated with 1 µM OHT for 2 days what resulted in complete silencing of floxed pelota allele.

2.2.23 Generation of teratomas in SCID mice

SCID (Severe Combined Immuno Deficiency) mice, resident in the Institute of Human genetics in Göttingen, were injected with 10^{6} ES cells suspended in 200 µl PBS. The injection was done subcutaneously.

MATERIALS AND METHODS

2.2.24 Bone marrow transplantation

Bone marrow of TAM-treated cKO mice was isolated by flushing femoral bones of TAM-treated mice. After washing in PBS, the cells were counted. $3x\ 10^6$ cells were intravenously injected to immune-defficient mice, resident in the institute.

2.2.25 Fertility test of Stra8 mice

To check fertility of deficient mice, they were bred with wild type mice. If female mouse became pregnant it meant that mutant male was fertile. The offsprings were counted to estimate if subfertility appeared.

2.2.26 Preparation of adaptor oligos

Sequences of linkers were designed as follows:

Linker containing LoxP site

5' AGCTTGGTACCATAACTTCGTATAGCATACATTATACGAAGTTATGAATTCA 3'

5' AGCTTGAATTCATAACTTCGTATAATGTATGCTATACGAAGTTATGGTACCA 3'

KpnI/Tsp509I linker

5' GACTGTCGACACT 3'

5' AATTAGTGTCGACAGTGGTAC 3'

SpeI/XhoI/NotI linker

5' CTAGTACTACTACTCTCGAGACTGC 3'

5' GGCCGCAGTCTCGAGTAGTAGTA 3'

Both oligonucleotides (8 μl 10 μM of each) of each linker were subsequently annealed in 45 μl of 1x annealing buffer in following program:

94°C – 4 min; 85°C – 4 min; 75°C – 4 min; 70°C – 4 min; 68°C – 10 min; 65°C – 10 min; 62°C – 10 min; 60°C – 10 min; 58°C – 10 min; 56°C – 10 min; 53°C – 4 min; 37°C – 15 min Then the reaction mixture was placed on ice ready to be ligated (5 μl) with desired clone.

MATERIALS AND METHODS

2.27 Computer analysis

For the analysis of the nucleotide sequences, programs like BLAST, BLAST2, MEGABLAST and other programs from National Center for Biotechnology Information (NCBI) were used (www.ncbi.nlm.nih.gov). For protein studies ExPASy tools (www.expasy.ch) were used. Mouse genome sequence and other analysis on mouse genes, transcripts and putative proteins were done in Ensembl database (www.ensembl.org).

RESULTS

3. RESULTS

3.1. Generation and characterization of pelota conditional knockout mouse

The lethality of pelota conventional knockout embryos (Pelo$^{-/-}$) at postimplantation stage became an essential obstacle to determination of pelota function in different developmental processes, such as organogenesis, gametogenesis and tumorgenesis. Furthermore, we were not able to establish Pelo-deficient cell lines, which can help to describe the molecular role of Pelo in stem cell self-renewal and RNA decay. To overcome this early lethality of Pelo$^{-/-}$ mice, we have generated a conditional knockout mouse model using Cre/LoxP system to inactivate pelota in a tissue-specific and time-controled manner (Lakso et al., 1992; Pichel et al., 1993).

We have constructed a pelota conditional knockout (cKO) allele, where the exons 2 and 3 are flanked with two LoxP elements. We expected that insertion of these elements in introns 1 and 3 would not disrupt the expression of floxed Pelo allele (Pelo^{F}) and thereby Pelo$^{flox/flox}$ (allele flanked by LoxP sites) mice would develop normally. To silence the gene, that is to excise the LoxP-flanked region of Pelo^{F} allele, we have generated three mouse lines by introduction of three transgenic Cre recombinase alleles in the genome of Pelo$^{F/F}$ or Pelo$^{F/-}$ (*Fig. 3*).
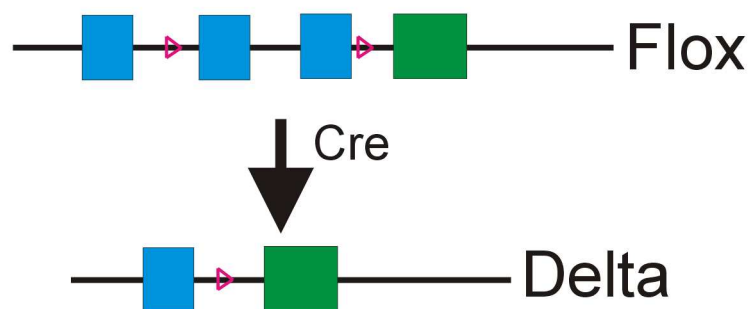
Figure 3. Simplified scheme of conditional knockout (cKO) system
Blue squares represent pelota exons, whereas green one is a symbol of Neo cassette. Pink triangles stand for LoxP sites, which are recombined upon Cre recombinase activation.

EIIaCre recombinase is expressed under the control of adenovirus EIIa promoter (Lakso et al., 1996). It is active in oocytes and shortly after fertilization (Dooley et al., 1989).

RESULTS

Therefore, we expected that Cre-mediated recombination would occur at one-cell stage and effectively delete LoxP-flanked Pelo fragment (Williams-Simons and Westphal, 1999). The $Pelo^{F/F}EIIaCre$ line was generated in order to determine whether obtained $Pelo^{\Delta/\Delta}$ or $Pelo^{\Delta/-}$ embryos would die at E7.5 mimicking the classical knockout mouse ($Pelo^{-/-}$) phenotype.

Second Cre recombinase helped us with functional characterization of pelota in spermatogenesis. The transgenic Stra8-Cre allele (generated by Dev and Shirneshan) was introduced into the second line. The recombinase is expressed under Stra8 (<u>st</u>imulated by <u>r</u>etinoic <u>ac</u>id gene <u>8)</u> promoter. Its expression is limited to spermatogonia (Oulad-Abdelghani et al., 1996; Baltus et al., 2006). We expected that excision of floxed pelo allele would occur in spermatogonia and their derivative cells.

For spatiotemporal inactivation of $Pelo^{F/F}$ allele we used ubiquitously expressed Rosa26-CreERT knock-in allele (available in the Institute of human genetics). The Cre recombinase is fused with the ligand-binding domain of human estrogen receptor (ERT) that binds tamoxifen (TAM) but not estrogen. The floxed pelota allele can be excised in various tissues and cultured cells after administration of tamoxifen to animals. The mouse line allows the study of the effects of pelota disruption on development of different tissues. It also enabled us to establish $Pelo^{F/F}CreERT$ embryonic stem cells (ESCs) for identification of the role of PELO in proliferation and differentiation.

3.1.1. Generation of a conditional knockout (cKO) construct

The 12.5-kb-long genomic fragment (containing the pelota gene and its flanking regions) was used for the generation of the pelota cKO construct. To clone a 5' region of the construct, a 1622 bp *PstI/EcoRI* fragment composed of third exon (*clone 1 in Fig. 4A*) was cloned into pBluescript vector (*clone 2 in Fig. 4B*). Next, clone 1 was digested with *SpeI* and *PstI* enzymes in order to obtain 1573 bp fragment containing part of first exon and the whole second exon. After cloning into pGEMTeasy vector, clone 3 (*Fig. 4C*) was digested with *HindIII*, dephosphorylated and ligated with a linker containing LoxP element (*pink triangle in Fig. 4D*) and *KpnI/EcoRI* restriction sites (*clone 4, Fig. 4D*). To ligate both fragments possessing exons, a *SpeI/PstI*-digested insert of clone 4 was ligated into clone 2 resulting in clone 5 (*Fig.4E*).
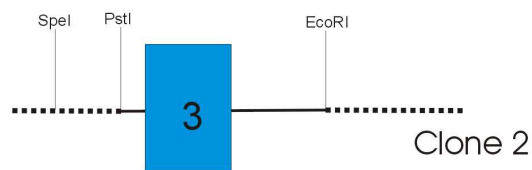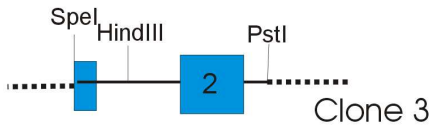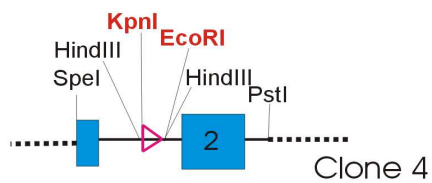
RESULTS

A

EcoRI　　PstI　　PstI　　SpeI　HindIII　　PstI　　EcoRI PstI SpeI

1 1　　2　　3

5' REGION [6052 bp]

[1573 bp]

[1622 bp]

Clone 1

B

SpeI　PstI　　EcoRI

3

Clone 2

C

SpeI HindIII　　PstI

2

Clone 3

D

KpnI EcoRI
HindIII　HindIII
SpeI　　　PstI

2

Clone 4

E

SpeI　　　PstI　　EcoRI　SalI

1　　2　　3

Clone 5

F

KpnI　XhoI SalI　　EcoRI　　　SpeI　　NotI

1

5' linker
SalI　　Tsp509I/EcoRI

Clone 6

RESULTS

Figure 4. The scheme representing cloning strategy for generation of 5' region of conditional knockout construct.
A – clone 1; B – clone 2; C – clone 3; D – clone 4; E – clone 5; F – clone 6; G – clone 7, EcoRI* - inactivated EcoRI site; H – clone 8; I – clone 9. Dotted lines stand for vector sequences; pink triangle is a symbol of LoxP site; red lines – linker sequence; detailed description of the figures in the text.

To construct 5' region, clone 1 (*Fig. 4A*) was digested with *EcoRI* and *SpeI*. The obtained 6052-bp-long fragment was subcloned into pBluescript (*clone 6 in Fig. 4F*). To enable further cloning, one needed to exclude *EcoRI* and *XhoI* sites from clone 6. To reach the goal, a *KpnI/Tsp509I* linker containing *KpnI*, *SalI* and *Tsp509I* sites was designed (*Fig. 4F*). It was cloned into clone 6 digested with *KpnI* and *EcoRI*. *Tsp509I* end is compatibile with *EcoRI*, but such ligation leads to inactivation of the *EcoRI* site in clone 7 (*Fig.4F, G*). Subsequently, another linker (*SpeI/XhoI/NotI*) was cloned into *SpeI/NotI* digested clone 7 (*clone 8 in Fig. 4H*). *SpeI/SalI* fragment from clone 5 (*Fig. 4E*) was isolated and cloned in *SpeI/XhoI*-digested clone 8 to give clone 9 (*Fig. 4I*). *SalI* and *XhoI* restriction sites are compatibile in an analogous way to *EcoRI* and *Tsp509I*, so *XhoI* site was eliminated from the final clone 9 (*Fig. 4I, marked in red*).

Next step was the generation of 3' homologous region. Clone 1 (*Fig. 4A*) was digested with *EcoRI* and a 3.3kb-long fragment was subcloned into pBluescript (*Fig. 5A*). To exclude *SpeI* site from multicloning site of clone 10, it was digested with *BamHI* and *NotI*, filled-up by T4 Polymerase and blunt-end ligated (*Fig. 5B*). To elongate the 3' arm it was necessary to amplify a 1.47 kb fragment which is localized 3' downstream from 3.3kb

RESULTS

region. After amplification (by using 3'regionA_F and 3'region_R primers), the 1.47 kb fragment was inserted into pGEMTeasy vector to generate clone 12 (*Fig. 5C*). Sequencing of the product confirmed the lack of mutations. To finish the 3' arm of the construct, *SpeI/XhoI* fragment of clone 11 was ligated with clone 12 (*clone 13 in Fig. 5D*).
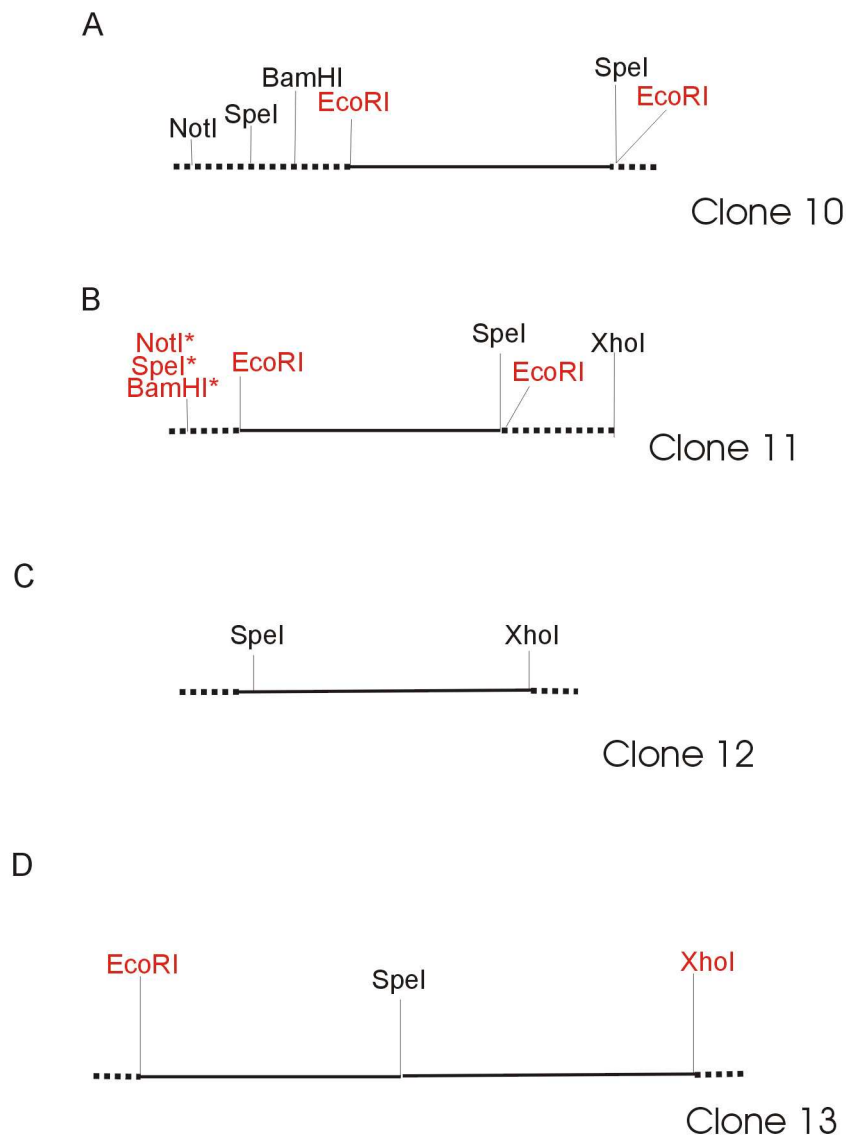

Figure 5.* The scheme representing cloning s*trategy for generation of 3' homologous region of conditional knockout construct.
A – clone 10; B – clone 11, NotI*/SpeI*/BamHI* - removed restriction sites; C – clone 12; D – clone 13. Dotted lines stand for vector sequences; detailed description of the figures in the text.

RESULTS

Last step of the construct preparation was cloning of both generated regions into final vector pPNT4. *SalI/NotI* fragment of clone 9 (*Fig. 3I*) was inserted upstream from the LoxP site of the vector, whereas *EcoRI/XhoI* insert from clone 13 (*Fig. 5D*) was introduced downstream from neomycin phosphotransferase (*Neo*) gene. Downstream from 3' arm in the vector, Herpes simplex virus thymidine kinase (*TK*) gene was located what enabled negative selection of embryonic stem cells (ESCs) transfected with the construct (*Fig. 6*).
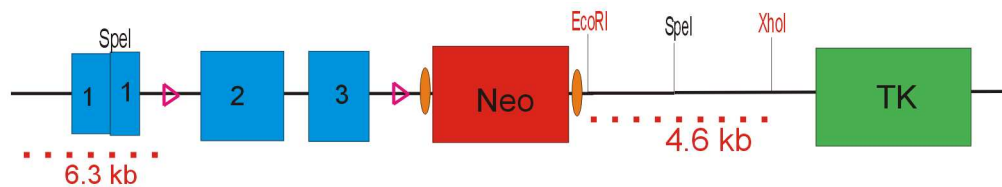
Figure 6. Final conditional knockout construct.
Exons 2 and 3 are flanked by LoxP elements (pink triangles). The neomycin cassette (Neo) is flanked by Flp/FRT elements (orange ovals). Red dotted lines stand for homologous arms of the construct; TK – thymidine kinase.

3.1.2. Isolation of homologous recombinant ESC clones

R1 ES cells were trypsinized, washed and suspended in PBS. Approximately 2×10^7 cells/ml were mixed with 40 μg linearized construct (digested with SalI) and the mixture was electroporated at 240V and 500 μF using a Bio-Rad Gene Pulser apparatus. The transfected cells were plated on G418–resistant mouse embryonic fibroblasts (MEFs) and cultured in nonselective medium for 36 hours. Then selective medium was applied for 10 days. Afterwards, resistant clones were picked and further cultured on 24-well plates for DNA isolation and cell freezing.

To find a correct homologous recombinant ESC clone, DNA of 100 ESC clones were screened by Southern analysis using 5' external probe (*Fig. 7*). After DNA digestion with *EcoRI*, a 15 kb band was expected for the wild type allele and a 13 kb band for the flox allele (*Fig. 7*). I found 42 clones that gave correct results. Four of them were selected for further analysis. *BsrGI-* and *AseI*-digested DNA was hybridized with 3' external and internal probe, respectively (*Fig.7*). As shown in *Fig. 8*, ESC clone no. 22 and 60 turned out to be correct, bands of expected size were detected (*Fig. 8B, C*). To confirm the absence of additional insertion of cKO construct in other loci of ESC genome, *BsrgI*-digested DNA of the clones was hybridized with the probe for Neomycin cassette. The expected result was obtained – single band of 15.2 kb (*Fig. 8D*). An internal probe recognized a 7kb fragment

(Flox allele) and a 5.2kb fragment (wild-type allele) in *AseI*-digested DNA, what further confirmed the lack of another insertion. The clone 60 was chosen for blastocyst injection.
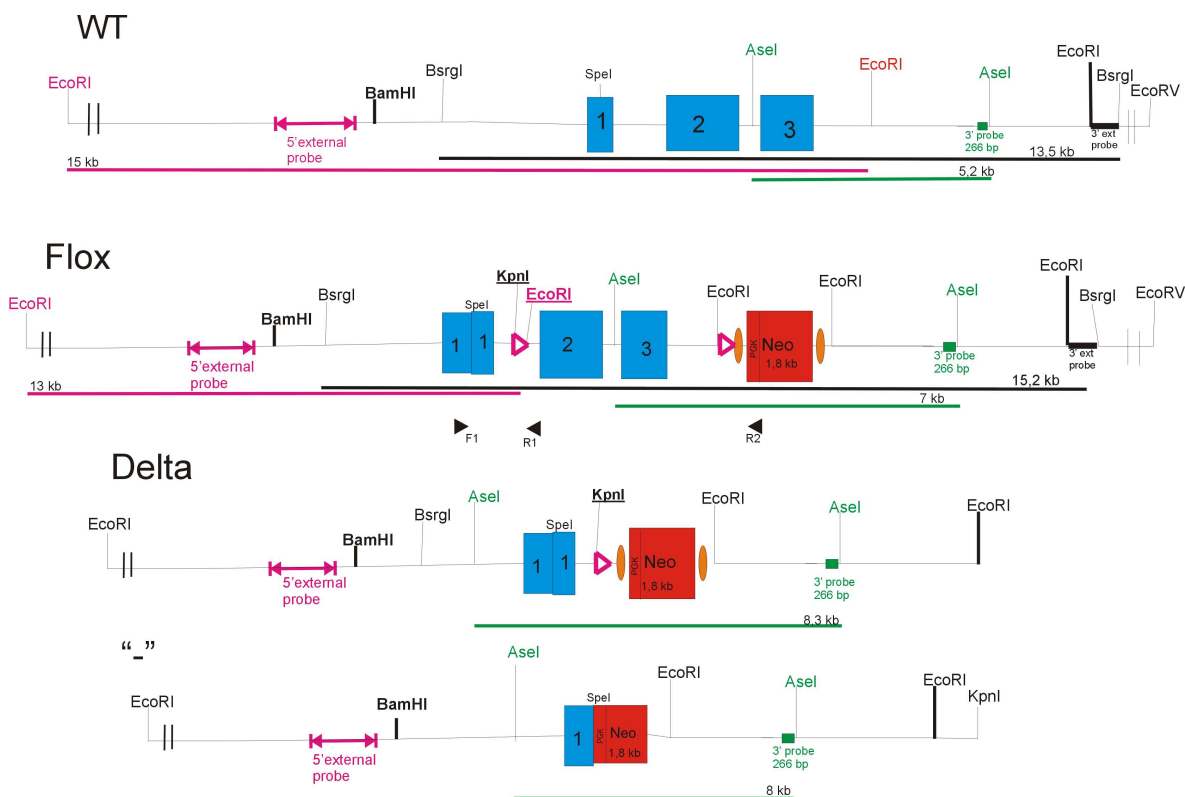

Figure 7. A schematic diagram of conditional knockout (cKO) allele
*WT – wild type allele; **Flox** – conditional knockout allele; **Delta** – cKO allele after deletion of floxed region between LoxP sites (pink triangles); **"-"** – classical knockout allele. The hybridization of EcoRI-digested genomic DNA with the 5'external probe results in a 15-kb band for WT and a 13-kb band for the Flox allele (pink color); BsrGI-digested DNA hybridized with 3'ext probe results in 13.5-kb band for WT and 15.2-kb band for Flox allele (black color);bands obtained by hybridization of AseI-digested DNA with the internal probe (3' probe, 266bp) are marked in green color. Primers used in genotyping: F1 = Pelo_F11, R1 = Pelo_R14 and R2 = PGK_cKO_R1 are marked by black arrow heads.*

RESULTS
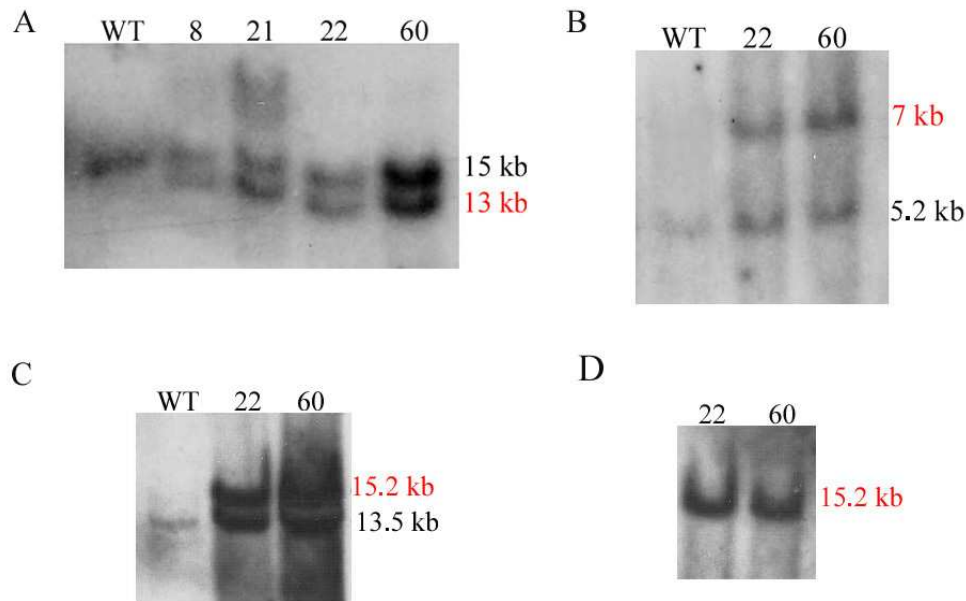
Figure 8. Southern analysis of ESC clones transfected with conditional knockout construct.
A – DNA digested with EcoRI and hybridized with 5' external probe; B – DNA digested with AseI and hybridized with internal probe (3' probe,266bp); C – DNA digested with BsrGI and hybridized with 3' external probe; D – DNA digested with BsrgI and hybridized with Neo probe. Red colour – size of mutant band.

In summary, hybridization of external probes showed correct homologous recombination of the 5' and 3' arms of the construct, whereas results obtained from internal and Neo probes confirmed that there was only one integration site of the cKO construct.

3.1.3. Generation of chimeric mice

Recombinant ES cells were injected into blastocysts derived from C57Bl/6J mouse strain in Max Planck Institute for experimental medicine in Göttingen. The blastocysts were then transferred into pseudopregnant CD1 females. I obtained 7 chimeric males from clone no. 60, chimerism of which ranged from 20 to 100%, and 4 chimeric males from clone no. 22 with chimerism between 10 and 80%. Two chimeras (90-100%) from each line were bred with C57Bl/6J females. All of them transmitted the cKO allele to their offsprings. For determination of the genotypes in F1 generation, a set of PCR primers were designed (*Fig. 7*), which amplify 376 bp-long band for flox allele and 330 bp-long fragment for wild type allele (*Fig. 9*).
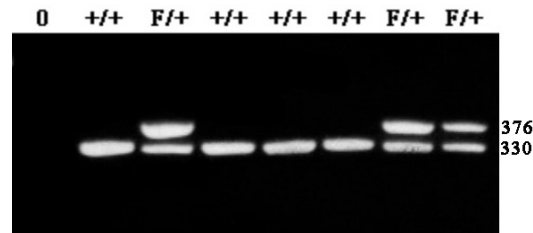
RESULTS

Figure 9. Genotyping PCR for F1 generation of Pelota cKO mice.
376bp – flox allele; 330bp - wild-type allele. PCR conditions are presented in chapter 2.2.8.1.

Mice of F1 generation (Pelo$^{F/+}$) displayed no abnormalities – they were healthy and fertile. When bred together ($\male$Pelo$^{F/+}$ x $\female$Pelo$^{F/+}$), they yielded Pelo$^{F/F}$ offspring which were viable and fertile as well. These results revealed that the introduction of neomycin cassette and LoxP elements into introns of pelota gene did not disrupt its expression.

3.1.4. Generation of an ESC line

For more comprehensive studies of pelota influence on differentiation and cell cycle progression, we generated a Pelo$^{F/-}$CreERT embryonic stem cell line. To establish the ESC line, blastocysts (E3.5) were isolated from Pelo$^{F/-}$CreERT females mated with Pelo$^{F/-}$ CreERT males. After 4 days of blastocyst culture, when the proliferating inner cell mass (ICM) caused a break of zona pellucida, one could observe trophoblast cells attached to the bottom and ICM growing on them. Such generated ESCs were genotyped - clone 9 (Pelo$^{F/-}$ CreERT) and 1 (Pelo$^{F/F}$) were chosen for further experiments. To induce Cre-mediated silencing of pelota gene, both clones were treated with 1 μM hydroxytamoxifen (OHT) which is more suitable for cultured cells than tamoxifen applied for mice treatment. A genotyping PCR showed that one-day presence of OHT in medium was sufficient to excise the floxed region from the allele of mutant cells (*Fig. 10*). OHT did not influence viability and differentiation ability of control cells (Pelo$^{F/F}$). It proved that applied OHT concentration was not toxic to the cell.

Pelota deletion was also demonstrated by Northern analysis (*Fig. 11*). Pelota RNA is clearly visible in control and mutant ESCs which were not treated with OHT. After addition of OHT into the medium, pelota expression is stopped in the mutant cells while in control cells lacking recombinase it is not affected.
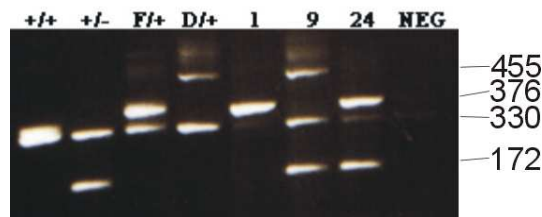
RESULTS

Figure 10. Genotyping PCR for OHT-treated ESCs.
1 – ESC control clone 1; 9 – ESC mutant clone 9; 24 – ESC control clone F/- without CreERT; NEG – negative control for PCR. Wild type band visible in ESC lanes comes from feeder layer (mouse embryonic fibroblasts), on which ESCs are cultured. Size of products: "-" band – 172bp; "+" band – 330bp; flox band (F) – 376bp; delta band (D) – 455bp
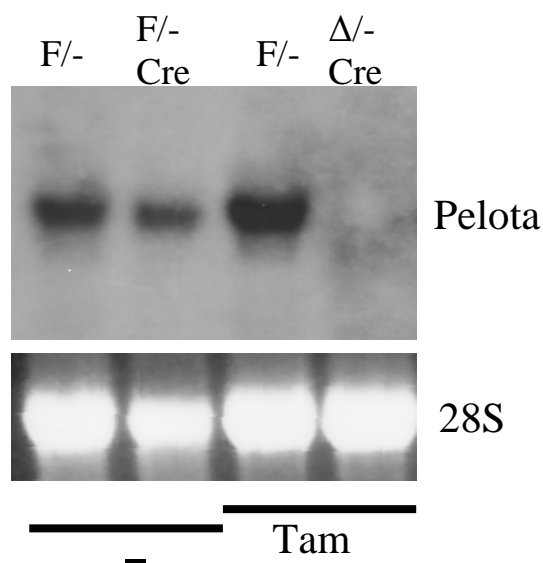

Figure 11. Northern analysis of pelota expression in OHT-treated and untreated ESCs.
F/- are control cells because they do not possess CreERT recombinase. First 2 samples are not treated and 2 last are OHT-treated ESCs. The good quality of RNA is demonstrated in the picture of the gel by RNA of 28S subunit.

Pelota-deficient cells did not exhibit any growth impairment – their morphology did not differ from control ESCs. They were successfully preserved in the culture.

3.1.5. Conditional knockout system– verification of recombination efficiency by generation of cKO/EIIaCre mouse line

To examine the recombination efficiency of floxed pelota allele and to determine whether the deletion of Pelota during early embryogenesis results in a phenotype similar to that of classical knockout mice, we have introduced a non-inducible EIIaCre recombinase

RESULTS

allele into the genome of cKO mice (Lakso et al., 1996). The Cre recombinase allele is controlled by adenovirus EIIa promoter which is activated in one-cell stage embryo. Therefore, we expected that floxed pelota allele would be recombined at zygote stage.

The breeding strategy was as follows: we bred heterozygous $Pelo^{+/-}$ mice with $Pelo^{+/+}$ $EIIaCre^{T/-}$ transgenic animals to obtain $Pelo^{+/-}$ EIIaCre which were further bred with $Pelo^{Flox/+}$. The mice were genotyped by using two PCRs (*Fig. 12*) to determine the genotype of pelota locus and the presence of transgenic EIIaCre allele.
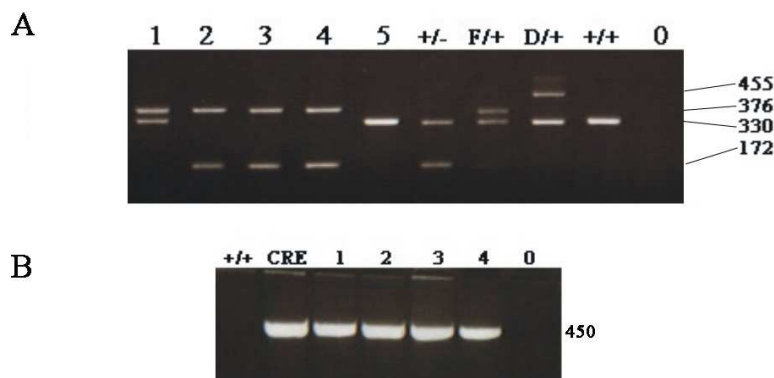
Figure 12. Genotyping PCRs for cKO/EIIa mice
*A – flox/-/Δ PCR for determination of the genotype of pelota locus, **B** – EIIa PCR demonstrating the presence of EIIaCre allele. 1: $Pelo^{F/+}CreEIIa$ mouse, 2-4:$Pelo^{F/-}CreEIIa$, 5: $Pelo^{+/+}$. Size of products of flox/-/ Δ PCR: 455bp – deleted allele; 376bp – flox (F) allele; 330bp – wild-type allele; 172bp – classical KO allele. Size of transgene band: 450bp. Primers were designed in transgene sequence what explains lack of the band in wild-type animal (+/+). PCR conditions are presented in chapter 2.2.8.1.*

We predicted that $Pelo^{Δ/-}CreEIIa$ offsprings would die at early embryonic stage. There were no $Pelo^{Δ/-}EIIaCre$ animals out of 219 genotyped mice of F1 generation. According to Mendelian ratio, $Pelo^{Δ/-}EIIaCre$ should constitute 12.5% of all offsprings in the breeding of $Pelo^{+/-}Cre^{T/-}$ and $Pelo^{F/+}$ (*Table 1*). Moreover, this genotype was also not found in further generations (180 mice tested).

Table 1. Statistics of genotypes obtained in F1 generation from cKO/EIIaCre mouse line

$Pelo^{+/-}Cre^{T/-}$ x $Pelo^{F/+}$							
F1 generation	+/+	+/-	F/+	F/-	+/+ T/-	+/- T/-	Δ/+ T/-	Δ/- T/-
Mendelian ratio	1	1	1	1	1	1	1	1
Mice number (out of 219)	33	29	25	41	36	29	26	**0**
Percentage (%)	15.1	13.2	11.4	18.7	16.4	13.2	11.9	**0**

RESULTS

The results clearly demonstrated that Cre-mediated recombination efficiently excises pelota-flanked region in one-cell stage of mouse development, i.e. Pelo$^{\Delta/-}$ EIIaCre died during prenatal stages (like Pelo$^{-/-}$). To obtain more evidence, embryos (E8.5) from breeding of Pelo$^{\Delta/+}$CreEIIa mice were genotyped. None out of 7 isolated embryos was Pelo$^{\Delta/\Delta}$ EIIaCre. Three deciduas were found empty and degenerated. It indicated that the absorption of dead embryos had occured. These results suggest that Pelo$^{\Delta/-}$CreEIIa have a phenotype similar with classical pelota knockout mice (Adham et al., 2003).

3.1.6. The role of Pelota in germ cell development - testis-specific cKO/Stra8-Cre mouse line

To analyze Pelota impact on spermatogenesis, we introduced a Stra8-Cre recombinase allele to the genome of Pelo$^{F/F}$ cKO mice. Expression of Stra8 is germ-cell-specific and has been reported in spermatogonia (Oulad-Abdelghani et al., 1996) and premeiotic germ cells of embryonic ovary (Baltus et al., 2006). According to Stra8 expression, we expected that pelota would be exclusively deleted in spermatogonia and we would be able to verify pelota involvement in self-renewal of germ stem cells.

3.1.6.1 Generation of Pelo$^{F/-}$Stra8-Cre mouse

Heterozygous Pelo$^{+/-}$ mice were bred with transgenic Pelo$^{+/+}$Stra8-Cre$^{T/-}$ to obtain Pelo$^{+/-}$Stra8-Cre mice, which were further bred with Pelo$^{F/F}$ mice. We genotyped the offsprings using flox/-/Δ PCR amplifying all alternatives of Pelo allele and PCR demonstrating presence/lack of Stra8-Cre in mouse genome (*Fig.13*). In F2 generation we detected all expected genotypes (*Table 2*). Pelo$^{flox/-}$Stra8-Cre mice, which are the actual model for study of spermatogenesis in pelo-deficient mice, were also found. It indicates that Pelo^{F} allele is not recombined in somatic cells.
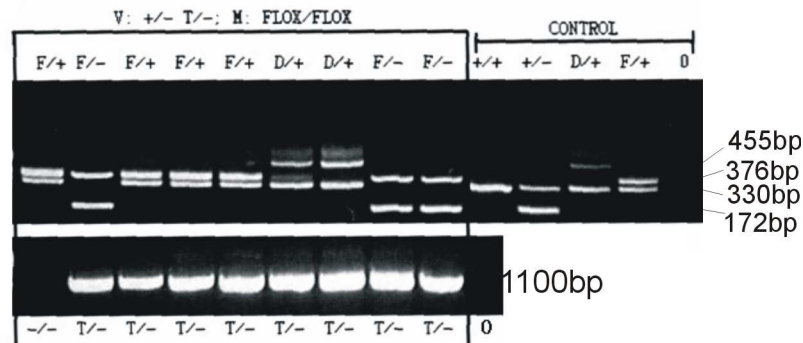
RESULTS

Figure 13. Genotyping PCRs for cKO/Stra8-Cre line.
The figure shows pictures of PCR products loaded on gel. PCR flox/-/Δ products are PeloΔ (455bp), PeloF (376bp), Pelo+ (330bp), Pelo- (172bp). Transgene-specific band is 1100bp long. Primers were designed in transgene sequence what explains lack of the band in wild-type animal. PCR conditions are presented in chapter 2.2.8.1.

Table 2. Statistics of male genotypes obtained in F2 generation from cKO/Stra8-Cre mouse line

Pelo$^{+/-}$Stra8-Cre$^{T/-}$ x Pelo$^{F/F}$				
F2 generation	F/+	F/-	F/+Cre	F/-Cre
Mendelian ratio	1	1	1	1
♂ Number (out of 66)	14	17	19	16
Percentage (%)	21.2	25.8	28.8	24.2

However, by genotyping the mice of this line we found 9 males and 5 females which were Pelo$^{Δ/+}$Cre. It suggests that Stra8-Cre-mediated recombination occurs in some somatic cells. Intrestingly, no chimeric Pelo$^{Δ/F/-}$Stra8-Cre offspring was detected. To examine the Cre recombination range resulting in pelota deletion, DNA from various tissues of two Pelo$^{Δ/+}$Stra8-Cre animals was isolated and genotyped. The mosaic genotype was found in all studied organs (*Fig. 14*). The result suggests that Cre recombinase under Stra8 promoter is activated during early embryogenesis of some animals and then contributes to pelota excision by Cre-mediated recombination of floxed allele. The absence of Pelo$^{F/Δ/-}$Stra8-Cre animals may be caused by early embryonic lethality of this genotype.
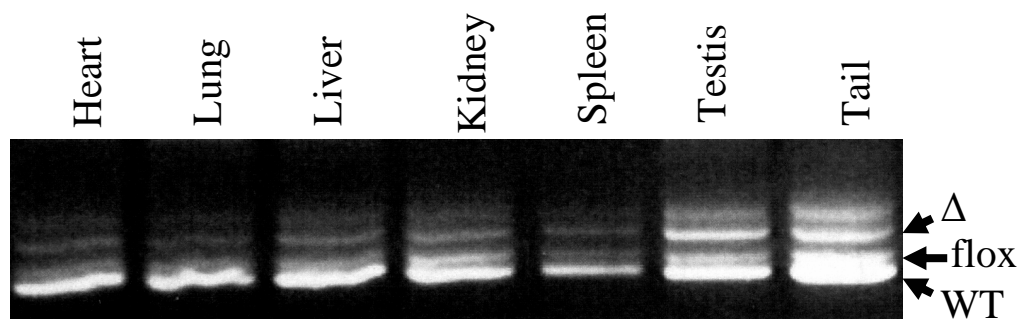
RESULTS

Figure 14. Genotyping of different organs derived from Pelo$^{\Delta/+}$Stra8-Cre animal
DNA from different organs was isolated by the same method as from tail DNA (chapter 2.2.1.2.) and it was genotyped with PCR flox/-/Δ.

3.1.6.2. Histological analysis of testes during postnatal development

In order to check if Stra8-Cre-mediated pelota deletion influences spermatogenesis, we isolated testes of 6-week-old males for histological study (*Fig. 15*). Hematoxilin and eosin (H&E) staining revealed that spermatogenesis is impaired in 70% of seminiferous tubules of Pelo$^{F/-}$Stra8-Cre. The diameter of the tubules is significantly smaller than in wild type and Leydig cells are hyperproliferated. Germ cell differentiation is arrested at premeiotic stage in most affected tubules where few number of pachytene spermatocytes and round spermatids were observed. Additionally, one could notice numerous vacuoles. In normal tubules of mutant testes, spermatogenesis was found to progress fairly normal to elongated spermatids.
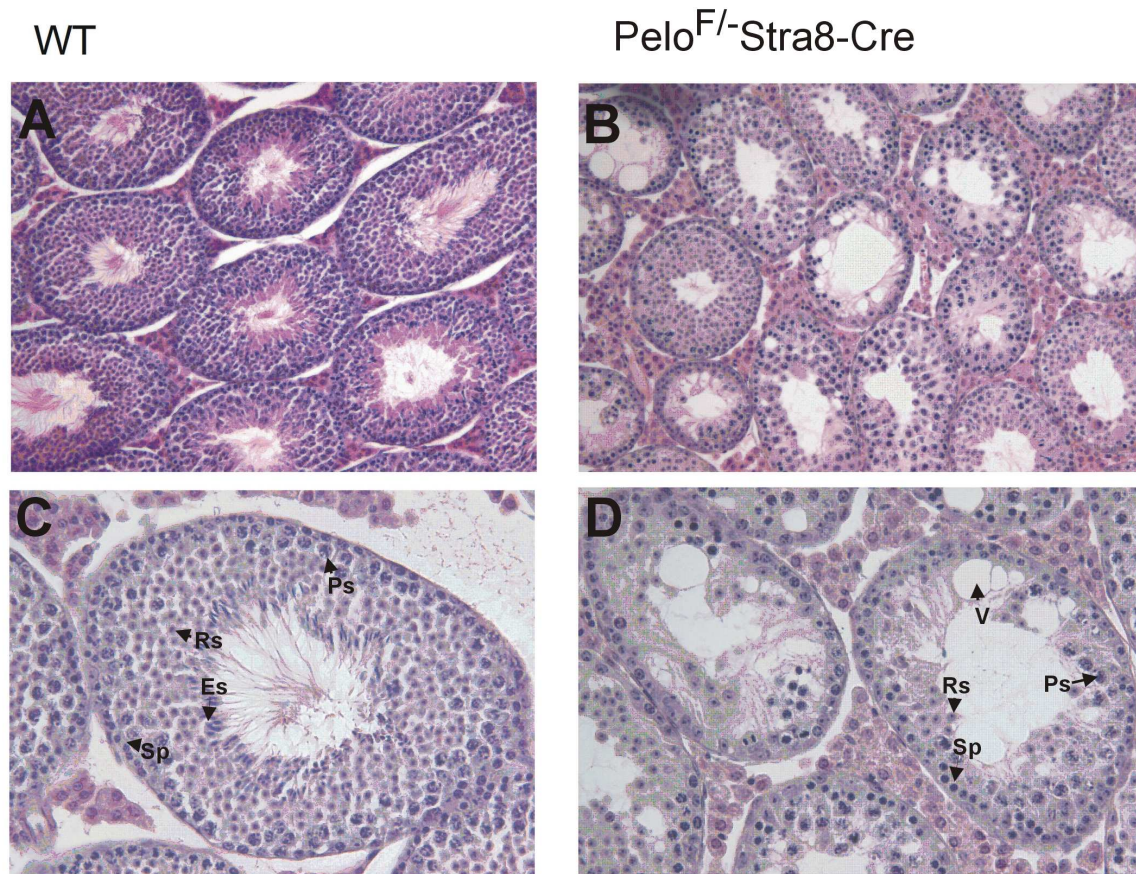
RESULTS

WT   Pelo$^{F/-}$Stra8-Cre

Figure 15. H&E staining of testis sections from wild-type and Pelo$^{F/-}$Stra8-Cre mice.
Testes were isolated from 6-week-old animals of cKO/Stra8-Cre line. A, C – wild-type testis; B, D – Pelo$^{F/-}$Stra8-Cre testis. Sp – spermatogonia; Ps – pachytene spermatocytes; Rs – round spermatids; Es – elongates spermatids; V – vacuoles. A,B – 10 x magnification; C, D – 20 x magnification.

     To define the onset of pelota influence on spermatogenesis in Pelo$^{F/-}$Stra8-Cre, we characterized the first wave of germ cell differentiation in testes of wild-type and mutant mice. We isolated testes from 5-, 10-, 15-, 20- and 25-day-old animals, fixed and stained them with hematoxilin and eosin.

     Analysis of cross sections of 5- and 10-day-old wild-type and mutant testes revealed no striking differences (*Fig.16A-D*). At day 10 of spermatogenesis, primary spermatocytes appear. The number of germ cells seems to be slightly reduced compared to the wild type. At day 15, the differentiation reaches the stage of pachytene spermatocytes (*Fig. 16E*). In mutant testes, we observed a drastic reduction in the number of pachytene spermatocytes in some tubules, while the other tubules displayed the depletion of all meiotic germ cells (*Fig. 16F*). Germ cell development results in round spermatids at the day 20 (*Fig17A*). However, in mutant testes the germ cells were developmentally arrested at the stage of pachytene

WT
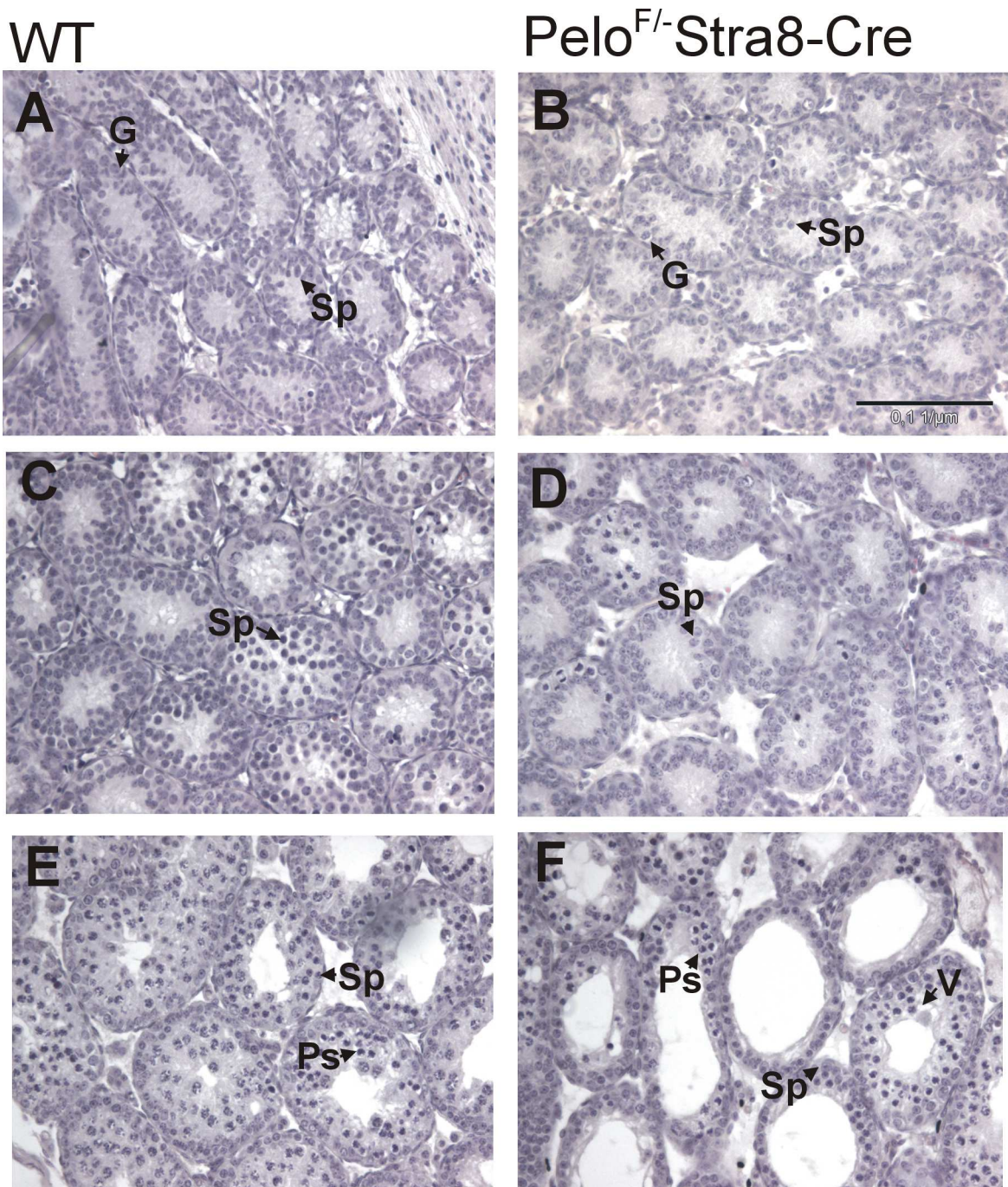
Pelo^{F/-}Stra8-Cre

Figure 16. H&E staining of 5-, 10- and 15-day-old testis sections from wild-type and Pelo^{F/-}Stra8-Cre mice.
A, C, E – wild-type testis; B, D, F – Pelo^{F/-}Stra8-Cre testis. G – gonocytes; Sp – spermatogonia; Ps – pachytene spermatocytes; V – vacuoles. Photos were taken in 20 x magnification).

spermatocytes (*Fig. 17B*). At day 25 the first round of spermiogenesis proceeds and elongated spermatids appear (*Fig. 17C*). While mutant testes displayed severe depletion of germ cells, pachytene spermatocytes and round spermatids were strongly reduced in number,

RESULTS

and vacuolization of Sertoli cells was more pronounced (*Fig. 17D*). These results suggest that spermatogenesis is disrupted at premeiotic and/or early meiotic stages.
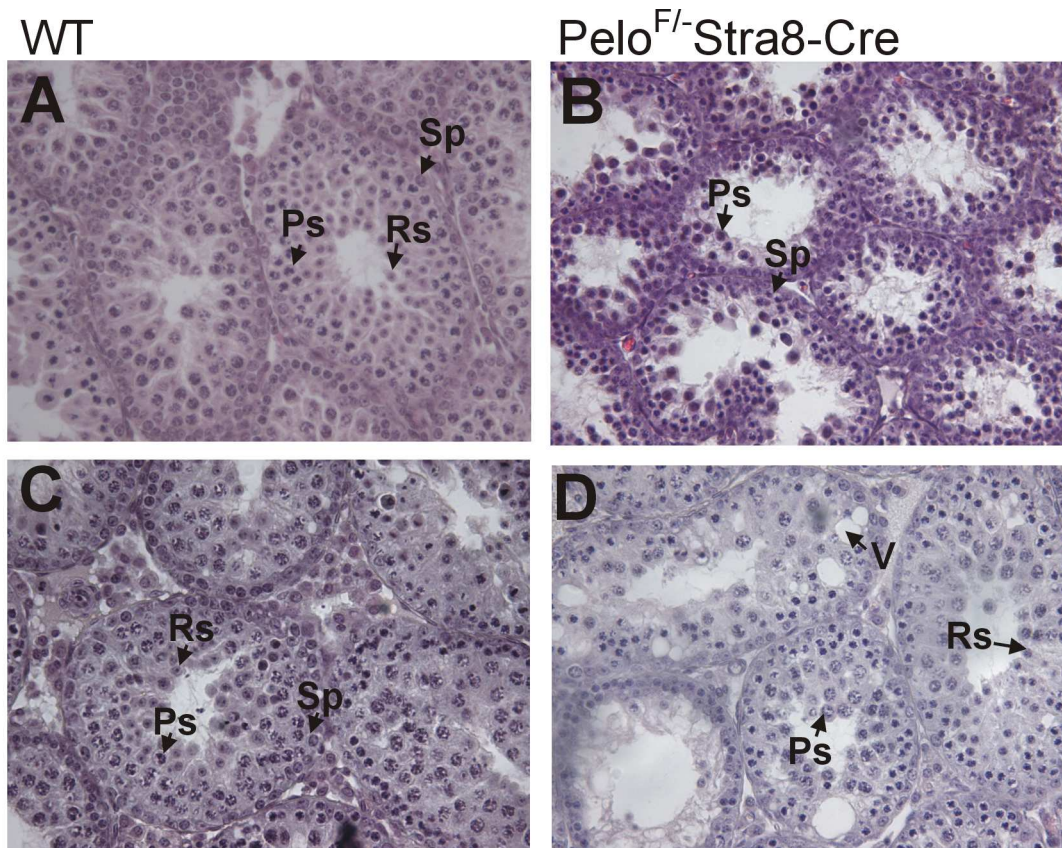

Figure 17. H&E staining of 20- and 25-day-old testis sections from wild-type and Pelo[F/-] Cre mice.

20-day-old testes are presented in picture A and B. 25-day-old testes are shown in picture C and D. A, C – wild-type testis; B, D – Pelo[F/-]Cre testis. Sp – spermatogonia; Ps – pachytene spermatocytes; Rs – round spermatids; V – vacuoles; Gc – monster cells. Photos were taken in 20 x magnification.

Due to severe impairment of spermatogenesis and loss of cells in particular tubules, we performed a TUNEL-assay (the terminal deoxynucleotidytransferase-mediated dUTP-Biotin nick end labeling) in order to verify if enhanced apoptosis is the reason of germ cell depletion. We examined the apoptosis levels in testes of 5-, 10-, 15-, 20 and 25-day-old mice (*Fig. 18*). In comparison to control mice (wild-type), Pelo[F/-]Stra8-Cre did not show any difference in apoptosis level until postnatal day 10. However, starting with day 15 we could observe a significant increase in number of apoptotic cells, most of which seemed to be in the meiotic prophase. Hence, enhanced level of apoptosis may be the cause of germ cell depletion in mutant testes.
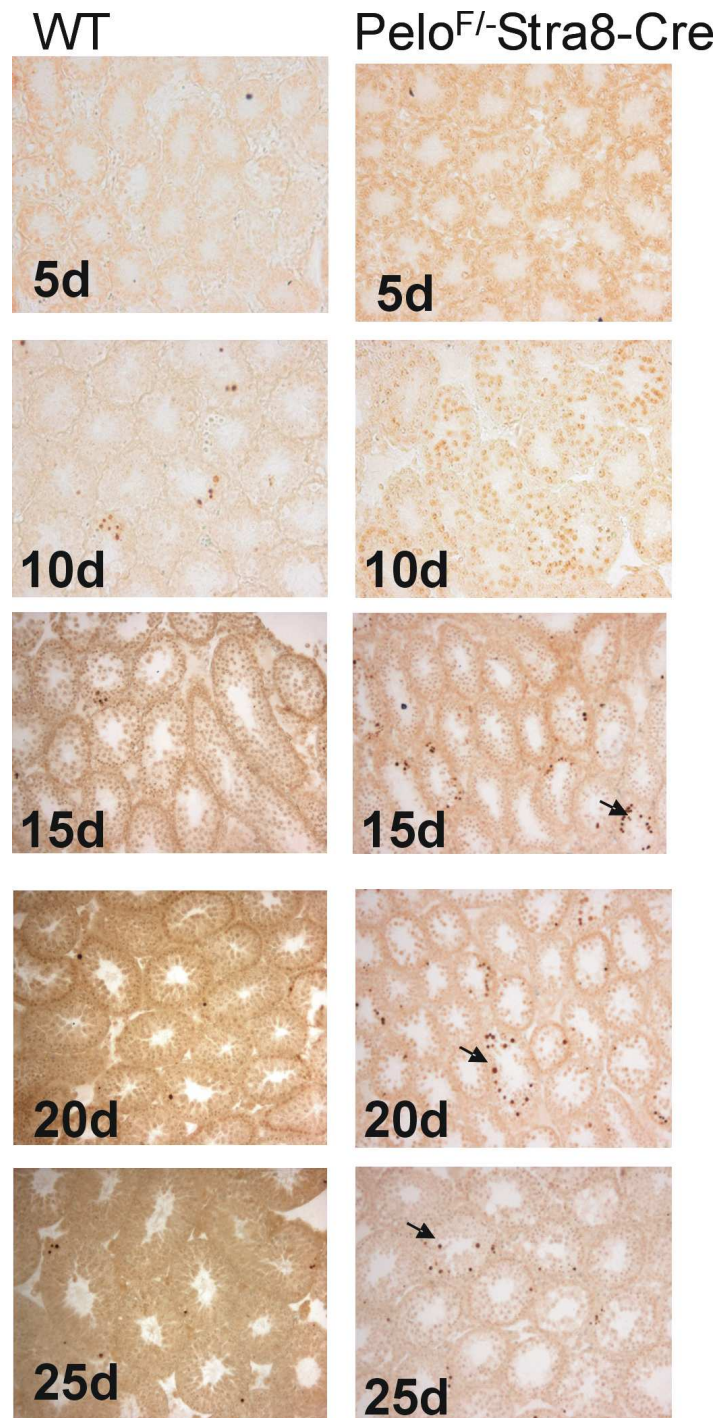
Figure 18. Apoptosis analysis of testis sections from wild-type and and Pelo$^{F/-}$Stra8-Cre mice.

Testes were isolated from 5-, 10-, 15-, 20- and 25-day-old mice. Left panel – wild-type testes; right panel – Pelo$^{F/-}$Stra8-Cre testes. The arrows indicate apoptotic cells. Photos were taken in 20 x magnification.

RESULTS

3.1.6.3. Spermatogenesis of Pelo^{F/-}Stra8-Cre mice is affected at premeiotic stages

To determine the developmental stage, at which spermatogenesis is arrested in mutant testis, we performed immunohistochemical analysis using premeiotic (Hsp-110, GCNA1) and meiotic (HSPA4L) markers.

HSP110 protein is expressed ubiquitously, but its highest level is observed in gonocytes. Immunohistochemical analysis of 5- and 10-day-old testes with antiHSP110 antibody revealed that the number of HSP110-positive cells exhibits a twofold reduction in tubules of 5-day-old Pelo$^{F/-}$Stra8-Cre mice in comparison to the control (*Fig.19A,B*).
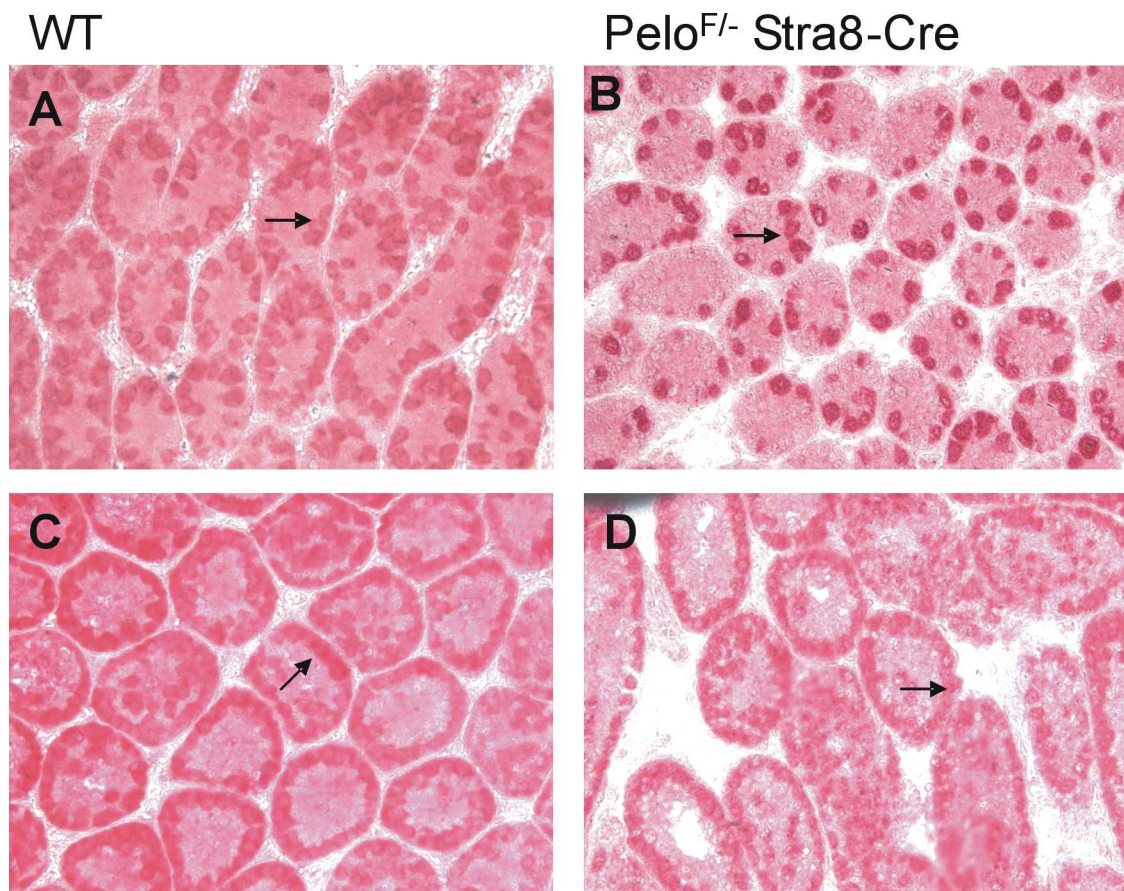

Figure 19. Immunohistochemical analysis of Hsp110 in testis sections from wild-type and Pelo$^{F/-}$Stra8-Cre mice at day 5 and 10 of spermatogenesis
Testes were isolated from 5- and 10-day-old mice. A – wild-type testis; B – Pelo$^{F/-}$Stra8-Cre testis. The arrows show spermatogonia. Photos were taken in 20 x magnification.

Reduction of germ cells was also visible at day 10, but exact estimation of cell number was impossible at that stage due to staining quality (*Fig.19C,D*).

The second premeiotic marker that we used, was GCNA1 (germ cell nuclear antigen). It is highly expressed in spermatogonia and primary spermatocytes (Enders and May, 1994).

RESULTS

We performed GCNA1 staining on 5-, 10- and 15-day-old testis sections of mutant and control mice (*Fig. 20, 21*) to further confirm the premeiotic impairment of spermatogenesis. In 5-day-old testes we could see no significant difference in number of GCNA1-positive cells between the mutant and the conltrol (*Fig. 20A-D*). Staining was specific for cells localized as spermatogonia in the tubules. However, at the age of 10 day we found app. 24% of germ cell-depleted tubules in testes of $Pelo^{F/-}$Stra8-Cre mice (*Fig. 20F, H*), where no GCNA1-positive cells could be detected. In the control all seminiferous tubules contained spermatogonia and primary spermatocytes stained with GCNA1 (*Fig. 20E, G*).

In testes of 15-day-old control mice, GCNA1-positive cells, i.e. spermatogonia and spermatocytes, constituted peripheral multi-cell layer in each tubule (*Fig. 21A, C*). Mutant testes were composed of reduced number of GCNA1-stained cells. We found a significant increase of seminiferous tubules, which lacked GCNA1-positive germ cells in mutant testes (*Fig. 21B, D*).
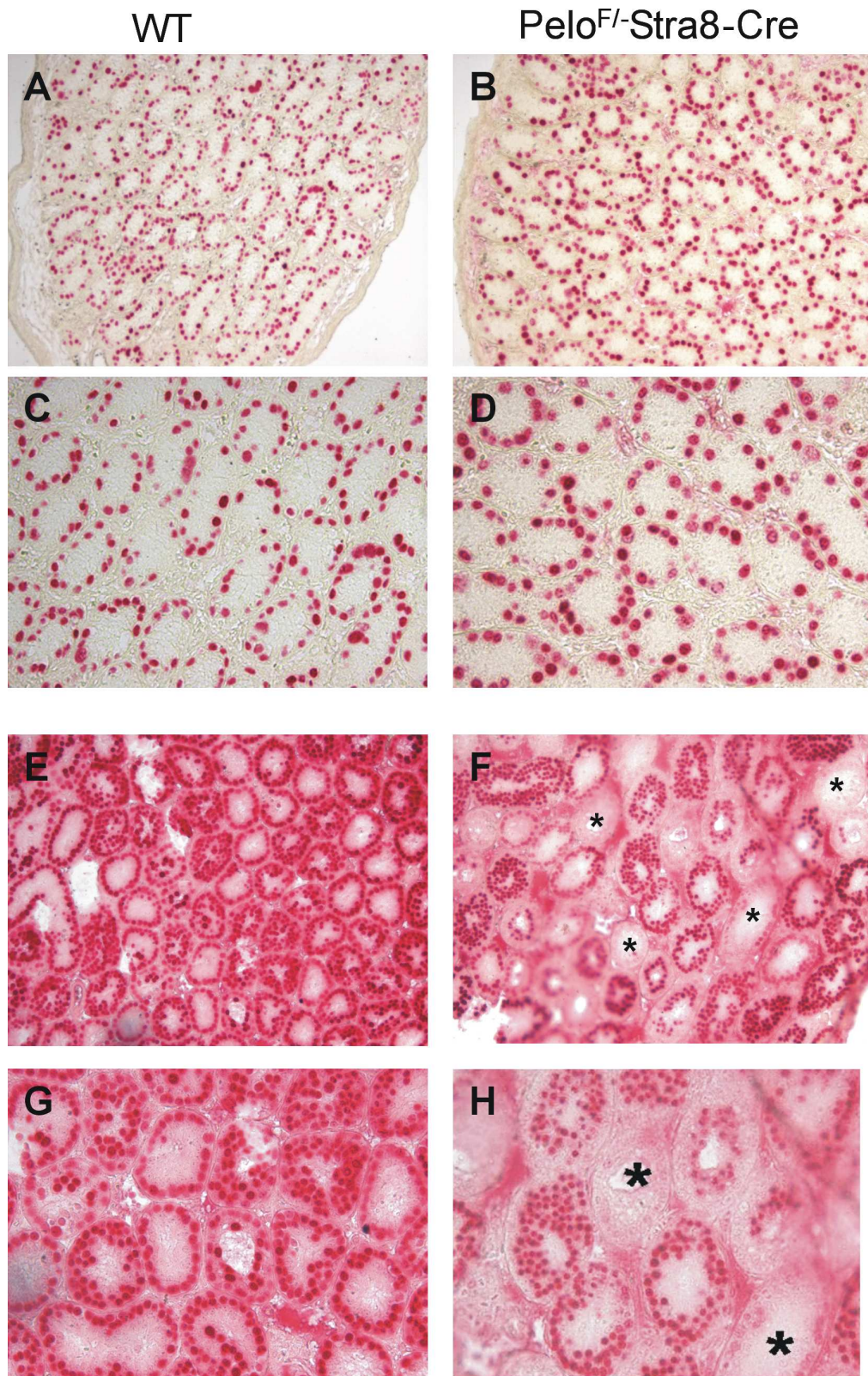
RESULTS

Figure 20. Immunohistochemical analysis of GCNA1 in testis sections from wild-type and Pelo$^{F/-}$Cre mice at day 5 and 10 of spermatogenesis.

Testes were isolated from 5- (A-D) and 10-day-old (E-H) mice. Wild-type testes are presented in the left panel (A, C, E, G), whereas Pelo$^{F/-}$Stra8-Cre testes are demonstrated in the right panel (B, D, F, H). Stars stand for tubuli devoid of spermatogonia. Photos were taken in 10 and 20 x magnification.
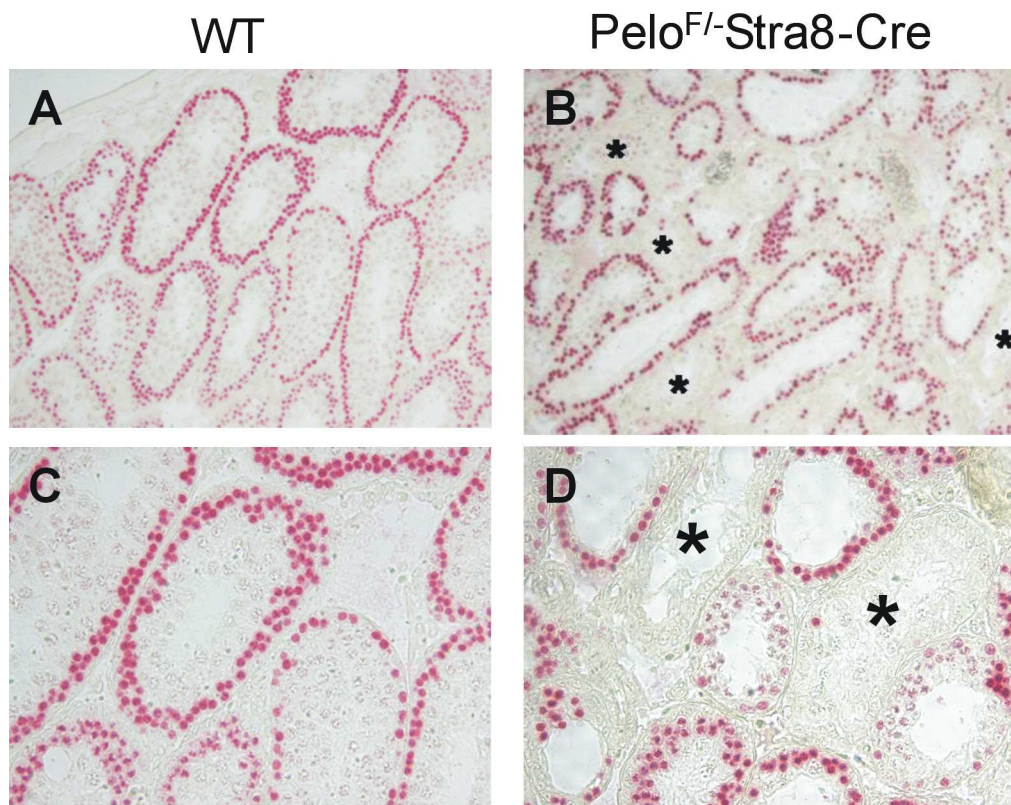
RESULTS

WT   **Pelo$^{F/-}$Stra8-Cre**

Figure 21. Immunohistochemical analysis of GCNA1 in testis sections from wild-type and Pelo$^{F/-}$Cre mice at day 15 of spermatogenesis.
Testes were isolated from 15-day-old mice. A, C – wild-type testis; B, D – Pelo$^{F/-}$Stra8-Cre testis. Star stands for degraded tubuli. Photos were taken in 10 and 20 x magnification.

We used a specific antibody against HSPA4L (heat shock 70kDa protein 4-like /Apg1) for immunohistochemical analysis of testis sections from 15-day-old mice. HSPA4L is expressed from late pachytene spermatocytes and all germ cell stages thereafter (Held et al., 2006). We detected the number of tubules containing HSPA4L-positive cells in mutant testes as compared to wild type is reduced (*Fig. 22A,B*)

On the basis of these immunohistochemical results, we can assume that PELO depletion results in the arrest of spermatogenesis in the premeiotic stage.
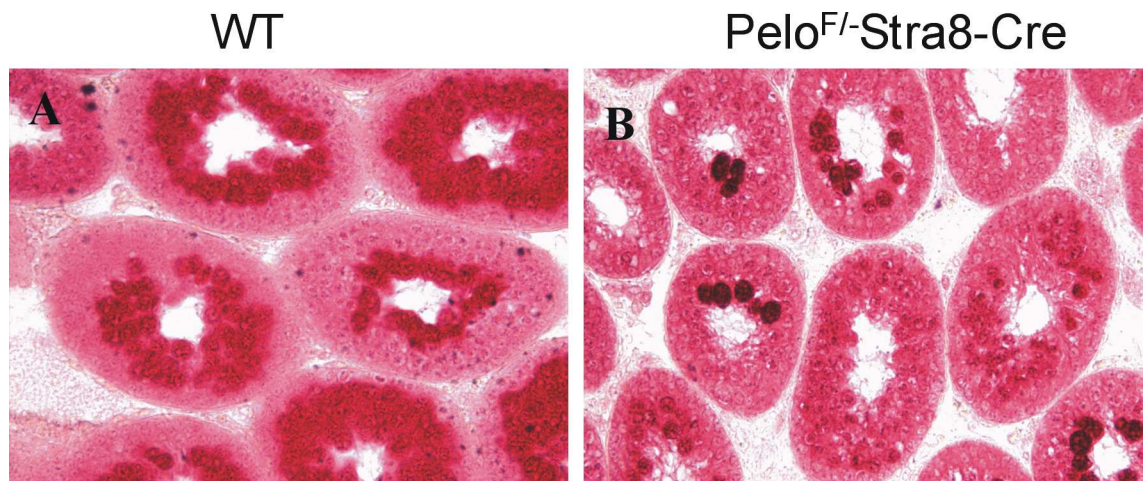
RESULTS

Figure 22. Immunohistochemical analysis of APG1 in testis sections from wild-type and Pelo^{F/-}Cre mice at day 15 of spermatogenesis.

3.1.6.4. Quantitative expresion analysis of premeiotic markers in Pelo$^{F/-}$Stra8-Cre mice

For further verification of the germ cell developmental stage disrupted in mutant testes, we examined the expression of various premeiotic molecular markers by quantitative RT PCR (qRT-PCR). We prepared testis cDNA from 5-, 10-, 15- and 20-day-old mice and used it in real time PCR analysis by means of primers specific for genes expressed in undifferentiated spermatogonia (Plzf and Sox3), differentiated spermatogonia (c-Kit) and early meiotic stages (Stra8). The results were standarized to relative expression in reference to expression of housekeeping gene - SDHA (succinate dehydrogenase complex subunit A). The analysis of the marker expression was performed using 2-3 testes of each stage and each genotype.

Plzf and Sox3 genes are expressed in undifferentiated spermatogonia (Raverot et al., 2005). The relative expression of both markers was reduced in 5- and 10-day-old mutant testes compared to the control. Except for decreased expression of Plzf gene in 15-day-old mutant testes, there were no significant differences in the transcript level of both markers between mutant and control testes at 15- and 20-day-old testes (*Fig. 23*).

Analysis of c-Kit, exclusively expressed in differentiated spermatogonia (Schrans-Stassen et al., 1999), revealed no difference in relative expression between mutant and control testes of all studied developmental stages (10-, 15-, 20-day-old) apart from mutant 5-day-old testes, where it was reduced (*Fig. 24*).
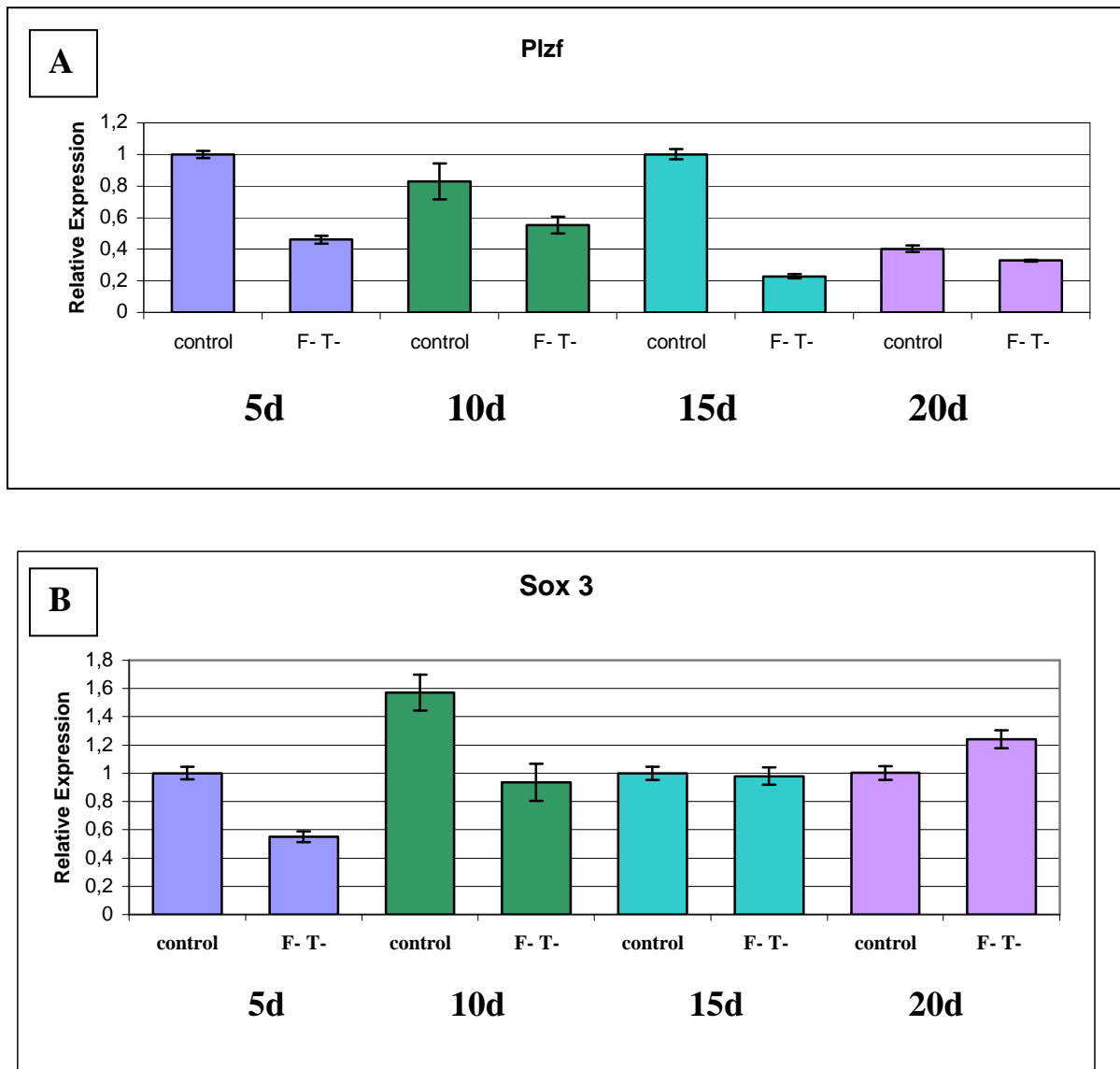
RESULTS

Figure 23. Relative levels of Plzf (A) and Sox3 (B) mRNA expression in testes of Pelo/Stra8-Cre mice during first wave of spermatogenesis.

Values represent relative level of Plzf and Sox3 in testes of 5-, 10-, 15- and 20-day-old animals (5d, 10d, 15d, 20d). Expression levels were normalised to the expression of endogenous control (Sdha). 2-3 biological replicates were used for each stage and genotype.
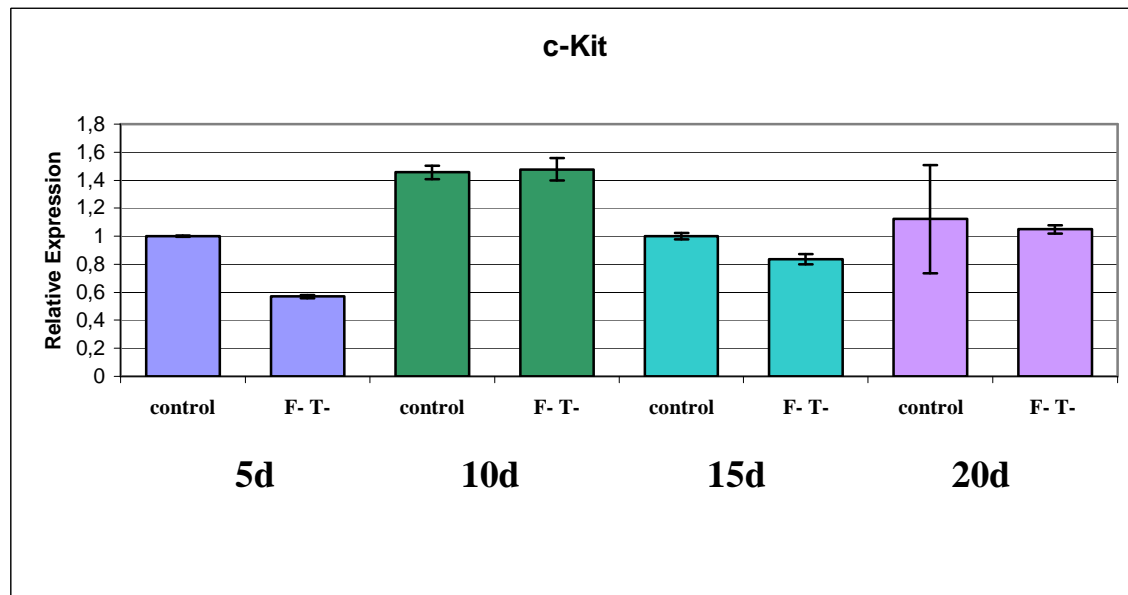
RESULTS

c-Kit

Figure 24. Relative levels of c-Kit mRNA expression in testes of Pelo/Stra8-Cre mice during first wave of spermatogenesis.
Values represent relative levels of c-Kit in testes of 5-, 10-, 15- and 20-day-old animals (5d, 10d, 15d, 20d). Expression levels were normalised to the expression of endogenous control (Sdha). 2-3 biological replicates were used for each stage and genotype.

Dazl, Ddx4 and Stra8 genes are specifically expressed in spermatogonia and early primary spermatocytes (Ruggiu et al., 1997; Toyooka et al., 2000; Zhou et al., 2008). Analysis of the expression profile during postnatal development showed that expression of these genes was relatively low in 5-day-old wild-type and mutant testes. In day 10, when the first wave of spermatogenesis progresses to leptotene spermatocytes in wild-type testes, a drastic increase in mRNA levels of all three genes was observed in mutant as well as in wild-type testes. However, in mutants it was significantly lower. At days 15 and 20 the expression level is sharply decreased in both genotypes (*Fig. 25*). The evident reduction in mRNA level of Dazl, Ddx4 and Stra8 led us to assumption that leptotene is a first stage that is affected during the first wave of spermatogenesis in Pelo^F/-Stra8-Cre mice.
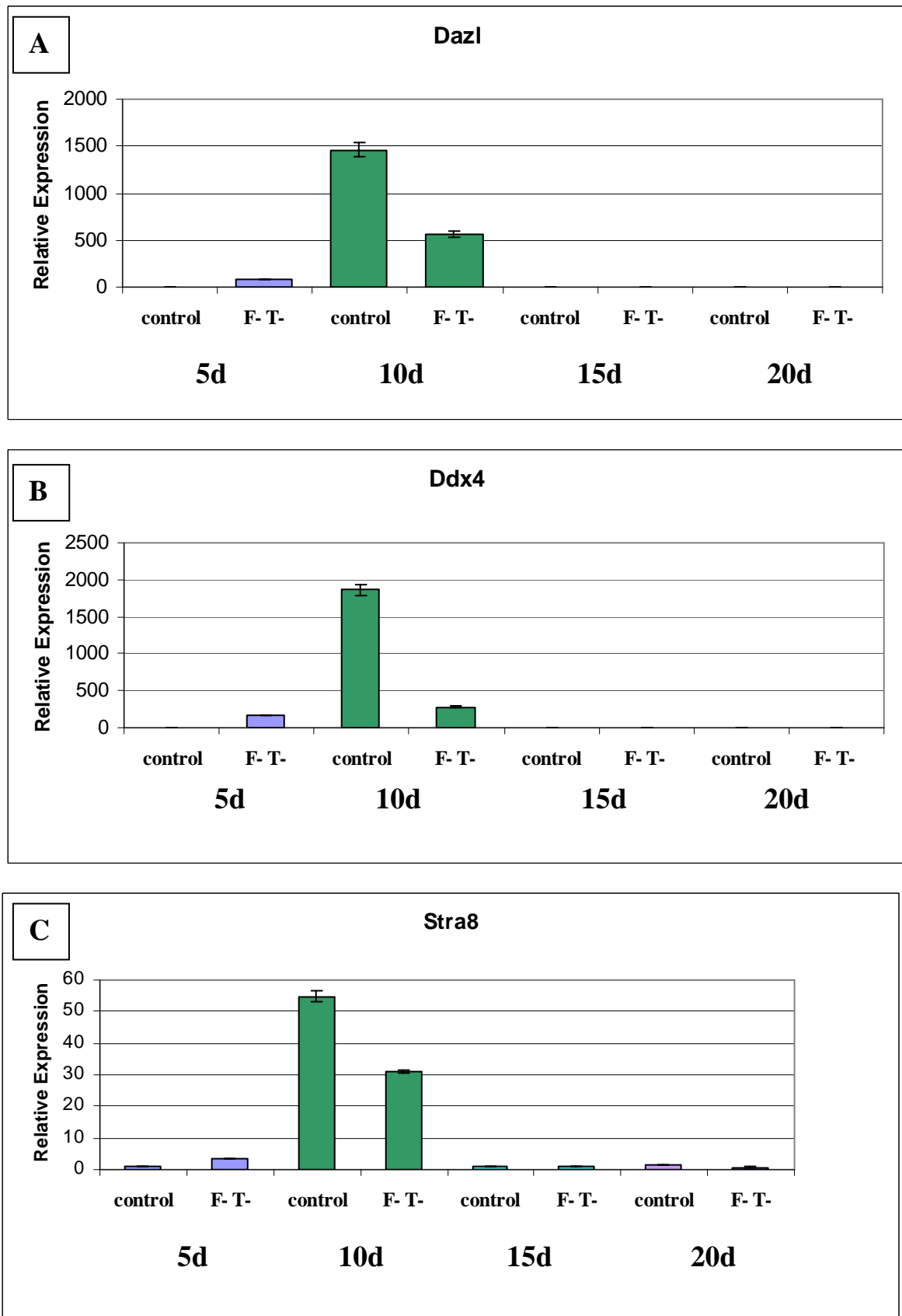
Figure 25. Relative levels of Dazl (A), Ddx4 (B) and Stra8 (C) mRNA expression in testes of Pelo/Stra8-Cre mice during first wave of spermatogenesis.

RESULTS

Values represent relative level of Dazl and Ddx4 in testes of 5-, 10-, 15- and 20-day-old animals (5d, 10d, 15d, 20d). Expression levels were normalised to the expression of endogenous control (Sdha). 2-3 biological replicates were used for each stage and genotype.

3.1.6.5. Analysis of Pelo$^{F/-}$Stra8-Cre fertility

The histological and molecular analysis of mutant testes suggests spermatogenesis impairment at early stages (premeiotic germ cells). However, germ cell differentiation progresses normally in some seminiferous tubules of mutant testes. To study the consequences of the impairment on fertility of mutant mice, at the age of 8 weeks three males and three females Pelo$^{F/-}$Stra8-Cre were bred with wild-type animals. The number of offsprings was counted and is presented below (*Table 3*).

Table 3. Results of fertility test for Pelo$^{F/-}$Stra8-Cre mice

Pelo$^{F/-}$Stra8-Cre	Litter size (mean)	Litter number	General number of offsprings
♂	9.2	9	83
♀	12.4	8	99

The fertility test showed that examined animals were fertile and there was no decrease in amount of offsprings in single litter. The mean litter size of mutant females was comparable with wild-type mice which deliver 14 offspring on average.Whereas mutant males produced a slightly reduced number of offsprings.

3.1.7. Tamoxifen-dependent pelota deletion in cKO/CreERT mouse line

To study pelota function in postnatal develpment of mammals, we have generated a system for spatiotemporal inactivation of floxed pelota allele. We introduced ubiquitously expressed Rosa26_CreERT knock-in allele to the genome of Pelo$^{F/F}$ and Pelo$^{F/-}$ mice. The CreERT recombinase is also ubiquitously expressed, but is not translocated to nucleus. The migration occurs upon application of tamoxifen (TAM), which binds to mutated estrogen receptor (ERT) binding site, fused with Cre recombinase. The system allows for excision of

the floxed pelota allele in various tissues and cultured cells after administration of tamoxifen to animals or hydroxytamoxifen (OHT) to the cells. In absence of the substance, the recombinase is not able to be transported into the nucleus what disables its function. This mouse model allows us to study pelota's role in proliferation and differentiation events during mouse development.

To generate the cKO/CreERT line, we mated heterozygous $Pelo^{+/-}$ mice with transgenic $Pelo^{+/+}CreERT$ mice to obtain $Pelo^{+/-}CreERT$. Such mice were further bred either with $Pelo^{F/+}$ or with $Pelo^{F/F}$. From those crossings we achieved the actual genotype, i.e. $Pelo^{F/-}CreERT$, which after tamoxifen application will yield $Pelo^{\Delta/-}CreERT$. Two types of PCR were used for determination of the genotypes: flox/-/Δ PCR which amplify wild-type (+), knockout (-), flox (F) and recombined (Δ) alleles (*Fig. 12A*) and CreERT PCR for Cre recombinase allele (*Fig. 26*).

Figure 26. Genotyping PCR for CreERT recombinase.
The figure presents the genotyping of 3 CreERT-positive mice (1-3) where transgenic allele (290bp) was detected. Primers are designed in transgene sequence what explains lack of the band in wild-type animal. PCR conditions are presented in chapter 2.2.8.1.

$Pelo^{F/F}CreERT$ and $Pelo^{F/-}CreERT$ after TAM-treatment will be mentioned as mutant mice ($Pelo^{\Delta/\Delta}CreERT$ and $Pelo^{\Delta/-}CreERT$, respectively). For the control we used mice either with Pelo wild-type allele ($Pelo^{F/+}CreERT$ or $Pelo^{+/-}CreERT$) or without CreERT recombinase ($Pelo^{F/F}$, $Pelo^{F/-}$ and $Pelo^{+/-}$).

3.1.7.1. TAM treatment of $Pelo^{F/-}CreERT$ mice

Originally, TAM treatment was applied (0.5mg/30g) to adult mutant males (n=8), adult mutant females (3) and control mice (n=5) by intraperitoneal injections for 5 subsequent days. After two weeks from last TAM application, one male was taken for histological analysis. However, all analyzed tissues were morphologically similar to the control. The Cre-mediated Pelo deletion had appeared, but was incomplete (data not shown). The mice did not exhibit any apparent disorder.

RESULTS

Due to the fact that Pelota was shown to be involved in cell division (Castrillon et al., 1993; Ebenhart and Wasserman, 1995; Xi et al., 2005) we have decided to treat young animals which still are in the phase of somatic growth. Therefore, 15-day-old mice were injected with TAM for 5 days. 2 days after last application of tamoxifen, we weighed the mice for next 9 days (*Fig. 27A*). The data indicate shown that $Pelo^{\Delta/\Delta}CreERT$ animals exhibit growth impairment what might be correlated with mitotic cell division disorder.
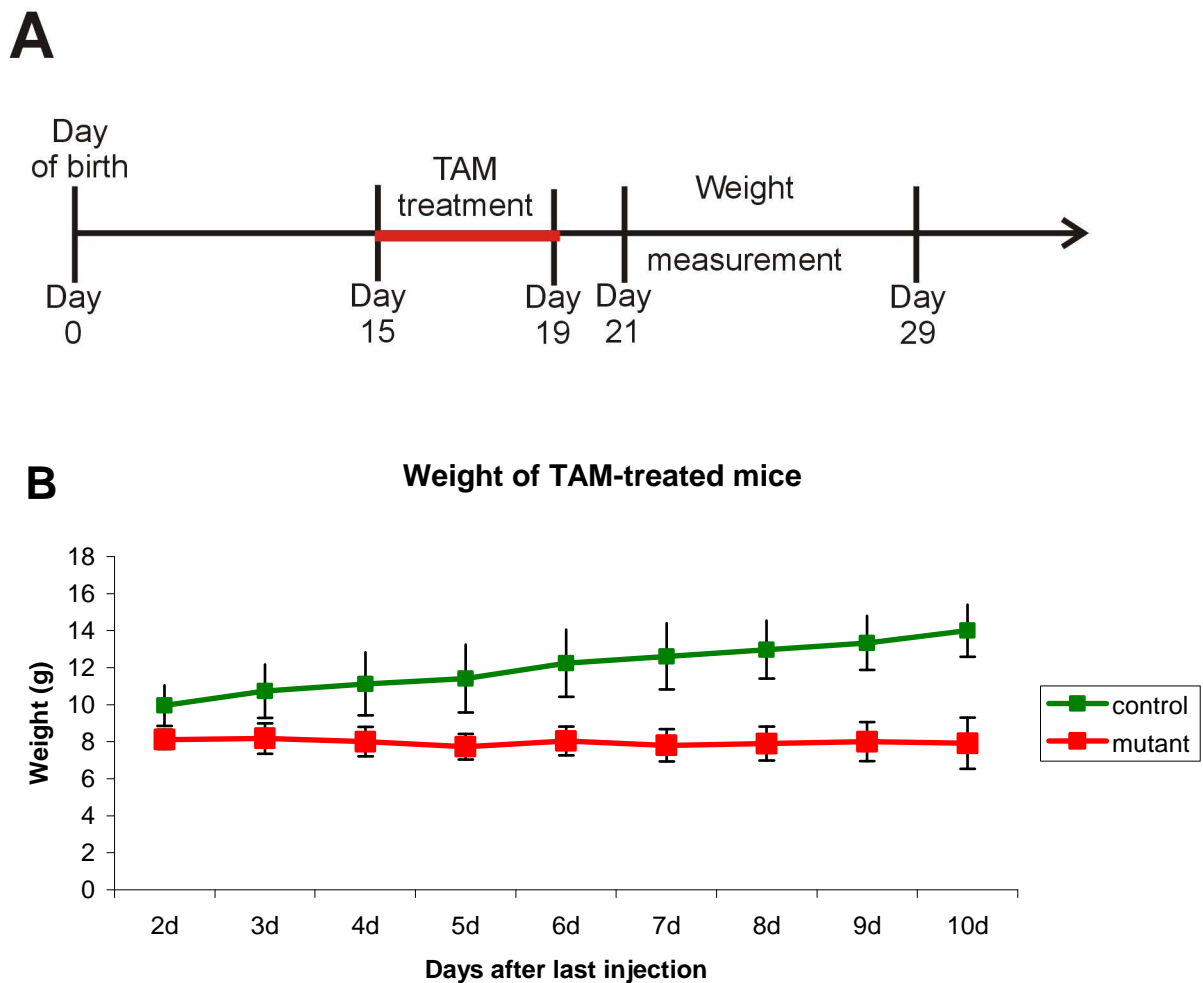
A

B

Figure 27. Weight gaining of mice treated with TAM at the age of 15 days.
The mice were treated for 5 days and the weight measurement was started 2 days after last injection and lasted for 9 days (A). The data were collected from 6 mutant (Pelo$^{\Delta/\Delta}$CreERT or Pelo$^{\Delta/-}$CreERT) and 11 control animals (B).

To verify whether the observed phenotype results from recombination of floxed pelota allele, DNA from various organs of mutant mice was isolated and genotyped (*Fig. 28*). It turned out that TAM-induced pelota deletion occurs in all examined tissues at high extent. Partial deletion was detected in heart, lung, stomach and kidney. Only brain is hardly affected what can be caused by blood-brain barrier blocking tamoxifen transport.
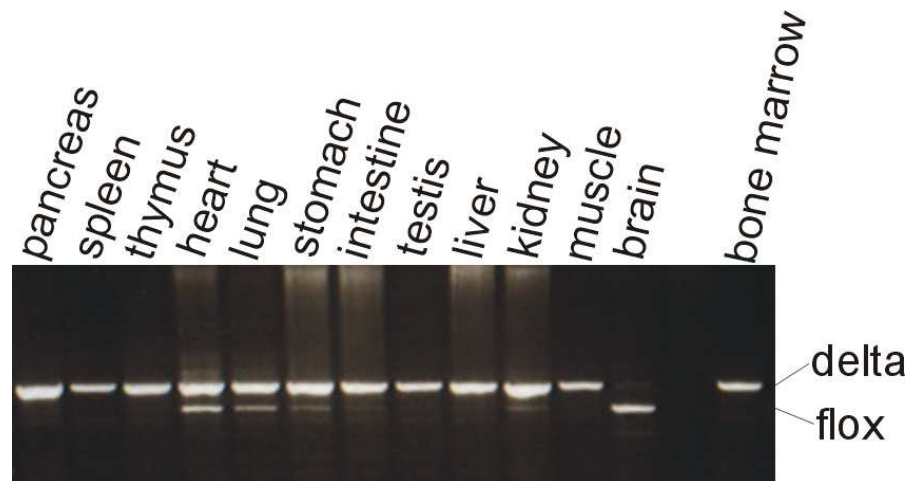
Figure 28. Genotyping PCR of organs from Pelo^{Δ/-}CreERT mouse
Size of products: delta – 455bp; flox – 376bp. PCR conditions are presented in chapter 2.2.8.1.

Approximately 50% of mutant animals died within 3 weeks after the treatment. It suggests that effective pelota ablation is a severe disturbance in mouse physiology. Nonetheless, 50% of Pelo$^{\Delta/-}$CreERT mice were able to survive, so that we could study their phenotype in detail.

3.1.7.2. Effects of pelota deletion in Pelo$^{\Delta/-}$CreERT animals

One month after TAM-application, some symptoms were found in mutant mice. Apart from their reduced weight, Pelo$^{\Delta/-}$CreERT mice have begun to loose hair in the neck area and nose, their eyes have become dry (*Fig. 29*). Additionally, their tails have looked raspy with peeling skin. In the course of the time, the bare skin developed erosive lesions in the neck, nose and around the mouth. In contrast, control mice remain healthy although they have been kept together with mutants in the same cages. It ruled out the possibility that tamoxifen is toxic as well as any contagious factor is responsible for the phenotype.
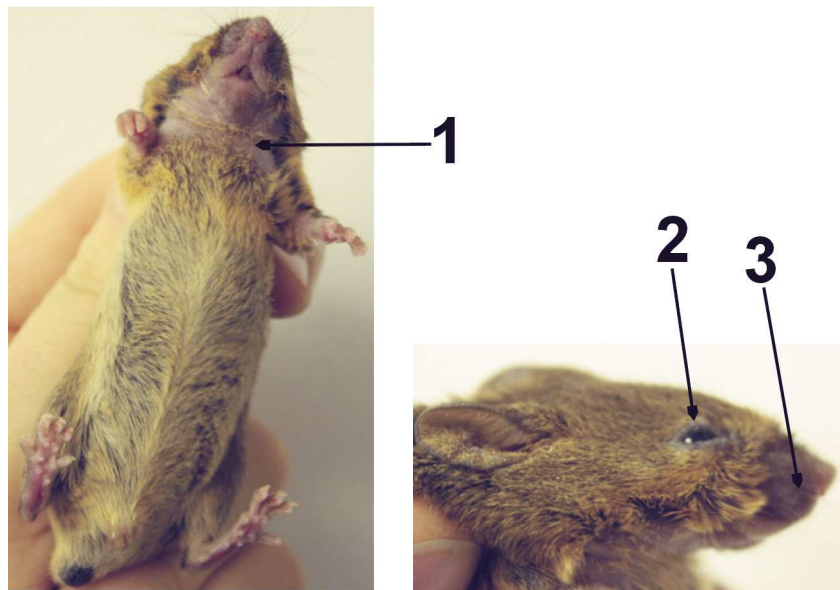
RESULTS

Figure 29. Apparent symptoms of pelota deletion in Pelo$^{\Delta/-}$CreERT mouse.
1 – loss of hair in neck area; 2 – dry eyes; 3 – hairless and swollen nose.

Dissection of mutant mice 2-3 months after TAM-treatment revealed that their thymus and testes are extremely reduced. Histological analysis of diverse tissues of Pelo$^{\Delta/-}$ CreERT has disclosed some abnormalities. H&E staining of skeletal muscle has shown that diameter of skeletal cells is decreased in mutant mice in comparison to the control, but the number of cells seems to be unaffected (*Fig. 30*). This reduction in size is probably associated with growth retardation of mutant animals.
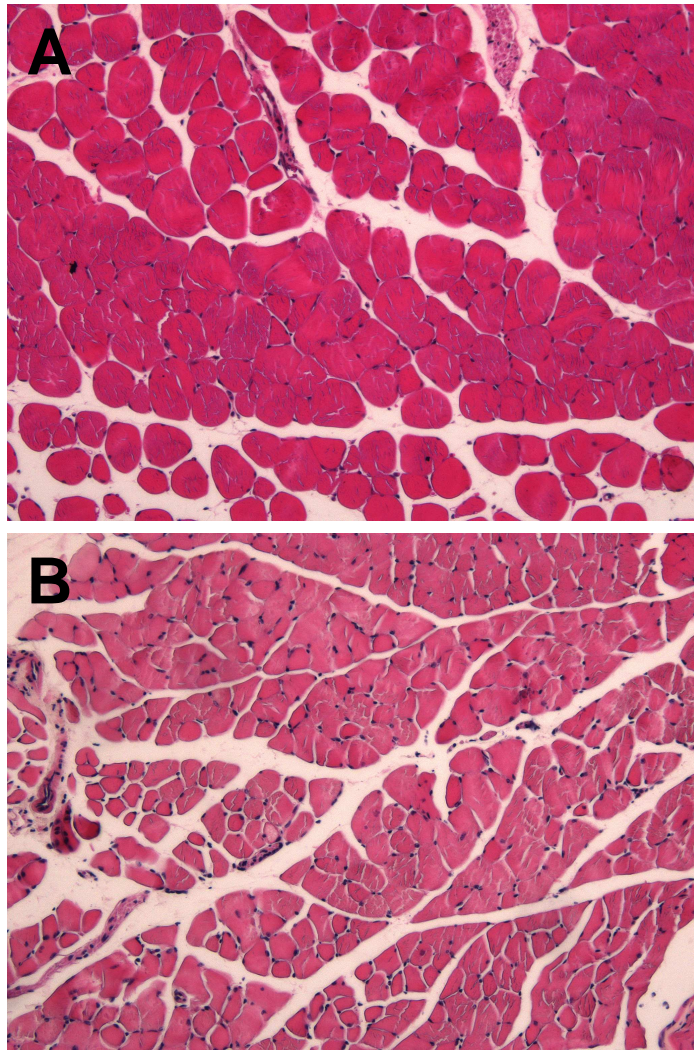
RESULTS

Figure 30. H&E staining of skeletal muscles isolated from Pelo$^{\Delta/-}$CreERT
A – wild-type muscles; B – mutant muscles. Photos were taken under 10 x magnification.

Histological analysis of testes revealed a severe effect of pelota depletion. In 2-month-old wild-type testes we could observe all stages of spermatogenesis, i.e. spermatogonia, primary spermatocytes, round spermatids, elongated spermatids and spermatozoa (Fig. 31A). However, in mutant testes 2 months after TAM treatment spermatogenesis was completely arrested. In seminiferous tubules, one could find only Sertoli cells which fill out the whole lumen. Tubules were reduced in size, so it caused increase of Leydig cells number (*Fig. 31B*).

This phenotype appears already in mutant testes 2 weeks after TAM treatment (at the age of 30 days) what suggests that pelota plays a critical role in a first round of spermatogenesis.
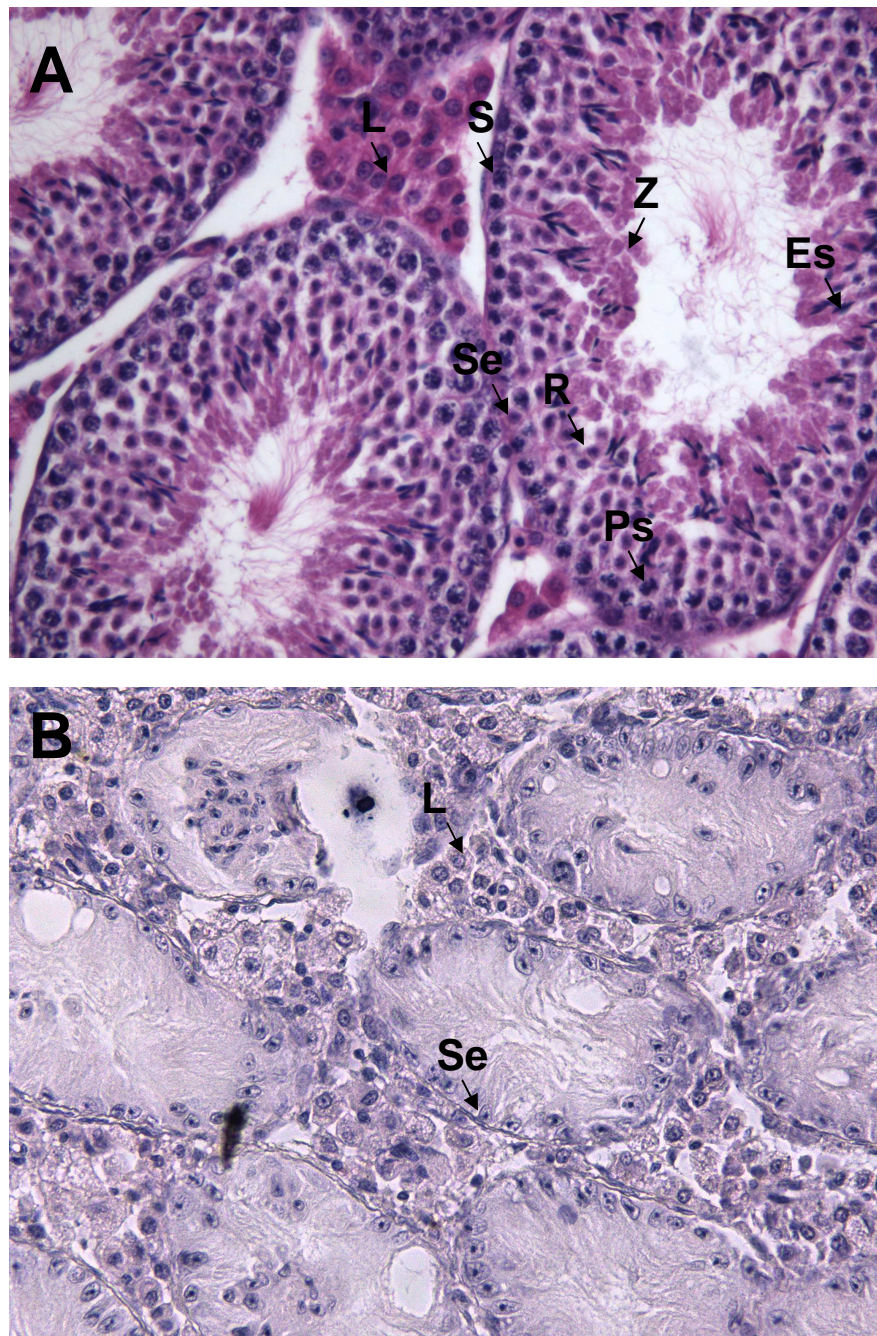
Figure 31. H&E staining of testes isolated from Pelo^{Δ/Δ}CreERT and wild- type mice.
A – wild type; B – mutant. Abbreviations: L – Leydig cells; S – spermatogonia; Ps – primary spermatocytes; Rs – round spermatids; Es – elongated spermatids; Z – spermatozoa; Se – Sertoli cells. Photos were taken under 20 x magnification.

A piece of bare skin from neck area was isolated and stained with H&E. In wild type, the epidermis is relatively thin in comparison to dermis (*Fig. 32A*). Epidermis consists of keratinocytes – cells which are arranged in 5 layers. The most outer layers are composed of flattened cells which have no nuclei. However, in the skin of the mutant we could observe hypertrophia of keratinocytes (hyperkeratosis) which infiltrate the dermis. The keratinocytes
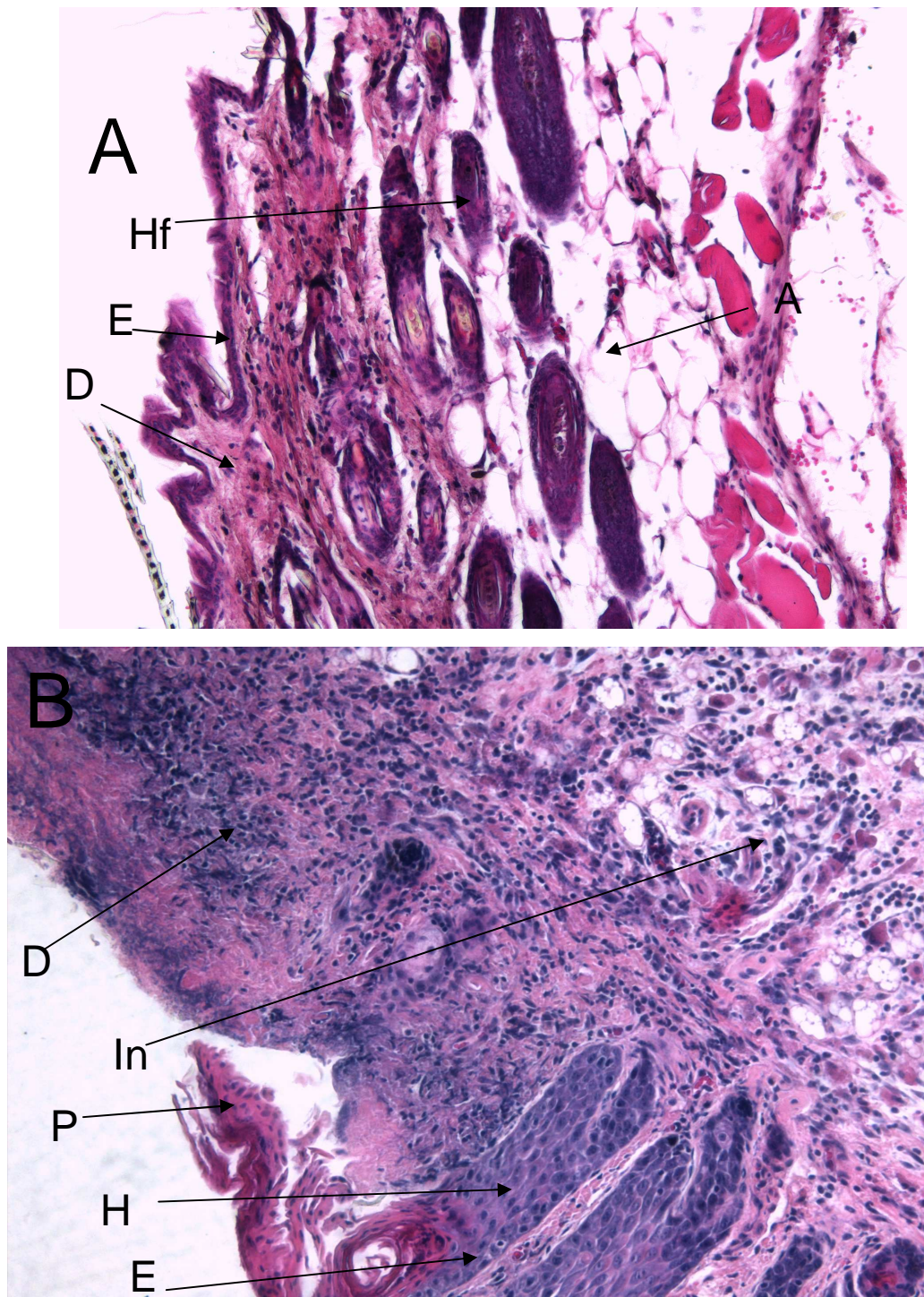
Figure 32. Disorders observed in Pelo^{Δ/-}CreERT skin structure
Skin was isolated from control (A) and Pelo^{Δ/-}CreERT mouse (B). Hf – hair follicle (A); E – epidermis; D – dermis; A – adipocytes(A); In – inflammatory region(B); P – parakeratosis(B); H – hyperkeratosis(B).

from outer layer were found to possess nuclei (parakeratosis) – this process is common for diseases related to excessive proliferation of epithelium. Additionally,

RESULTS

symptoms of a chronic inflammatory response appear in deeper layers of the skin. Histological studies of kidney also revealed lymphocyte-rich inflammatory cell infiltration (data not shown).

Other tissues of the mutant mice (such as spleen, liver, stomach, heart, intestine, ovary) were also studied, but they did not display such a pronounced phenotype. The effect of pelota deletion on different organs still requires thorough studies. The impaired development of thymus beside these histological observations implies putative defects in the immune system of $Pelo^{\Delta/\Delta}$ mice.

The thymus is an organ where thymocytes mature into T cells, which respond to foreign antigens, but do not recognize self-antigens (Goldrath and Bevan, 1999; Miller, 2002; Starr et al., 2003). We suspected that pelota depletion affects the maturation of T cells. Therefore, we have analyzed cell surface markers for B and T cells isolated from thymus (*Table 4.*) and spleen (*Table 5.*) of mutants (n=4) and controls (n=4) using flow cytometry. The thymus and spleen cells were prepared and stained with fluorescence-conjugated monoclonal antibodies, which recognize different cell surface markers (*Materials & methods, 2.2.17.*). The analyzed cell number was 11 ± 4 x 10^7 for control thymus and 11 ± 5 x 10^7 for control spleen. The amount of mutant cells was reduced to 0.8 ± 0.7 x 10^7 in thymus, and 5.5 ± 2.5 x 10^7 in spleen.

We have found a strongly reduced level of $CD4^+CD8^+$ double positive, $CD4^+CD8^-$, $CD8^+CD4^-$ single positive and CD3-positive cells (T lymphocytes). The number of double-negative ($CD4^-CD8^-$) cells, i.e. thymocyte progenitors derived from hematopoietic stem cells, was 6-fold increased in all mutants. It is extremely noticeable in mutant 2' (*Table 4.*), where these cells constituted a vast majority of tested cell population. The decrease of differentiating and mature stages of T cells indicate that after Pelota protein is deleted, the further differentiation of thymocytes is disrupted and the stage of double negative cells is accumulated. It explains high susceptibility to infections of all mutant mice.

RESULTS

Table 4. The number of T cells (various developmental stages) in thymus of TAM-treated animals (Pelo^{Δ/Δ} CreERT and Pelo^{Δ/-} CreERT)
The animals treated with TAM at the age of 6 weeks were analysed 1 month after treatment. The mice which were injected at the age of 15 days, were examined 2 weeks after treatment. The thymus of mutant 3' was strongly reduced and the amount of isolated cells was insufficient for FACS analysis.

Organ	THYMUS				
Age of treated mice	6 weeks		15 days		
Cell surface marker	Control	Mutant	Control	Mutant 1'	2'
DN (double-negative CD4$^-$CD8$^-$ cells)	4.78	**30.59**	11.1±0.6	**15.46**	**98.83**
CD4$^+$CD8$^+$ (differentiating thymocytes)	76.71	**34.86**	60.5±1.6	**77.67**	**0.64**
CD4$^+$CD8$^-$ SP (differentiating thymocytes)	11.91	**28.11**	16.94±0.06	**2.75**	**0.18**
CD8$^+$CD4$^-$ SP (differentiating thymocytes)	5.41	**3.39**	11.3±1	**4.06**	**0**
CD3$^+$ (T cells)	18.08	**11.19**	31.81±6.2	**7.19**	**0.56**

Examination of B cells derived from spleen demonstrated that CD19- and B220-positive cells (B lymphocytes) in Pelo^{Δ/-}CreERT animals are also reduced in number (*Table 5.*) as compared to the controls. CD19 and B220 (CD45) are cell surface markers specific for mature B cells. In some mutant mice we have found a slight increase in number of CD4$^+$CD25$^+$ cells, which recognize autoantigens. This might suggest that mice exhibit autoimmune disorder, but it requires further studies. We detected higher number of CD25$^+$ cells, which are indicators of inflammatory state of the organism as well as NK cells (DX$^+$-positive), which were increased. The amount of T cells, detected in spleen, was variable depending on the individuals.

RESULTS

Table 5. The number of B and T cells in spleen of TAM-treated animals
The animals treated with TAM at the age of 6 weeks were analysed 1 month after treatment. The mice which were injected at the age of 15 days, were examined 2 weeks after treatment. NK cells - natural killer cells.

Organ	SPLEEN						
Age of treated mice	6 weeks		15 days				
	Control	Mutant	Control			Mutant	
Cell surface marker			1 2 3			1'	2'	3'
CD19$^+$ (B cells)	39.09	**11.7**	30.1±14.1			**5.03**	**7.72**	**12.35**
B220$^+$ (B cells)	44.7	**22.85**	33±5			**11.61**	**9.05**	**18.67**
MHCII$^+$ (B cells)	0.12	**0.26**	2.4±2.2			**1.68**	**1.3**	**0.3**
CD25$^+$ (activated B and T cells)	0.72	**1.46**	1.5±0.3			**0.87**	**1.45**	**1.2**
CD4$^+$CD25$^+$	0.69	**1.51**	1.3±0.6			**0.91**	**1.37**	**0.88**
DX5$^+$ (NK cells)	2.79	**6.68**	3.1±0.9			**3.18**	**1**	**2.39**
CD3$^+$ (T cells)	32.29	**9.99**	17.3±18			**5.71**	**6.99**	**20.74**
CD4$^+$ (T cells)	35.07	**49.53**	22.8±16			**12.6**	**11.9**	**18.45**
CD8$^+$ (T cells)	14.77	**13.43**	13.7±10.2			**3.51**	**4.61**	**6.68**

3.1.8. Pelota-deficient ESC line – functional characterization

To study pelota function on a molecular level, we generated a ESC line with flox allele and tamoxifen-activated CreERT recombinase. For all experiments described we used Pelo$^{F/F}$ cells treated with OHT as a control.

To study if pelota deficiency enhances direction of cells to programmed cell death, we performed the annexin-7AAD assay. For control, we used Pelo$^{F/-}$ cells either untreated or treated with OHT and untreated mutant cells (Pelo$^{F/-}$CreERT). Using FACS analysis, we examined early (annexin V staining) and late (7-AAD staining) apoptosis levels in the culture (*Fig. 33*). The percentage of viable cells (*NOT STAINED, Fig. 33*) was predominant in comparison to apoptotic cells. The experiment showed that the number of either dead or apoptotic cells was not increased upon pelota deletion. It demonstrates that pelota deficiency does not influence the proliferation and viability of ES cells.
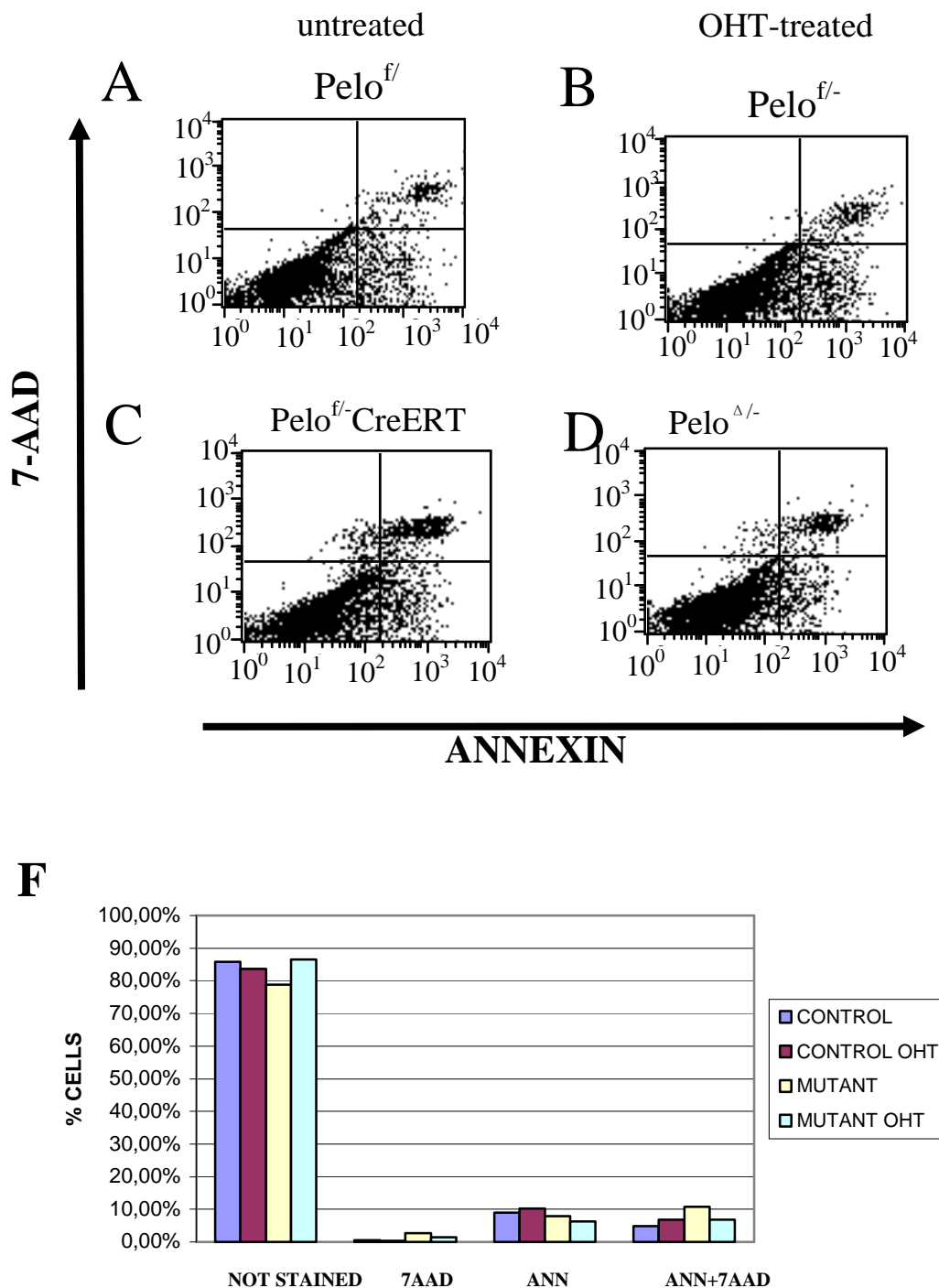
untreated OHT-treated

Figure 33. Flow cytometric analysis of apoptosis level in mutant cells treated with OHT and untreated

FITC-Annexin V/7AAD flow cytometry of an untreated control (A) and mutant (C). OHT-treated cells are presented in B (control) and D (mutant). The lower left quadrant shows viable cells, which exclude 7AAD and are negative for FITC-Annexin V binding. The upper right quadrant contains the nonviable necrotic cells positive for 7AAD and annexin binding. The lower right quadrant represents the apoptotic cells, FITC-Annexin V positive and 7AAD negative, demonstrating cytoplasmic membrane integrity. The graph (F) indicates percentage of all kinds of cells. NOT STAINED - viable cells; 7AAD – single-stained with

RESULTS

7AAD (necrotic cells); ANN – single-stained with annexin (apoptotic cells); ANN+7AAD - double-stained with annexin and 7AAD.

Lack of prominent effect of pelota ablation on proliferation and viability of ESCs led us to check the role of pelota protein in differentiation. Therefore, the cells were cultured in conditions that induce the differentiation process. ESCs were trypsinized, plated on bacteria dishes and left in suspension in the absence of LIF for 10 days. Under these conditions ES cells aggregated and formed embryoid bodies (EBs), in which cells differentiated into the three germ layers – endoderm, mesoderm and ectoderm. We did not observe any differences in morphology between mutant and control cells. EBs were thereafter trypsinized, plated on gelatin-coated dishes and cultured in ESC medium without LIF. We could observe a striking difference in morphology between mutant and control cells. The control cells were differentiated, whereas pelota-deficient cells formed two types of cells spread on the plate: differentiated ones attached to the bottom and ESC-like colonies growing over them. To confirm pluripotent character of the mutant cells, we stained them with alkaline phosphatase (AP), which is an enzyme specific for pluripotent cells. Pelo$^{\Delta/-}$CreERT colonies were AP-positive (*Fig. 34B*).
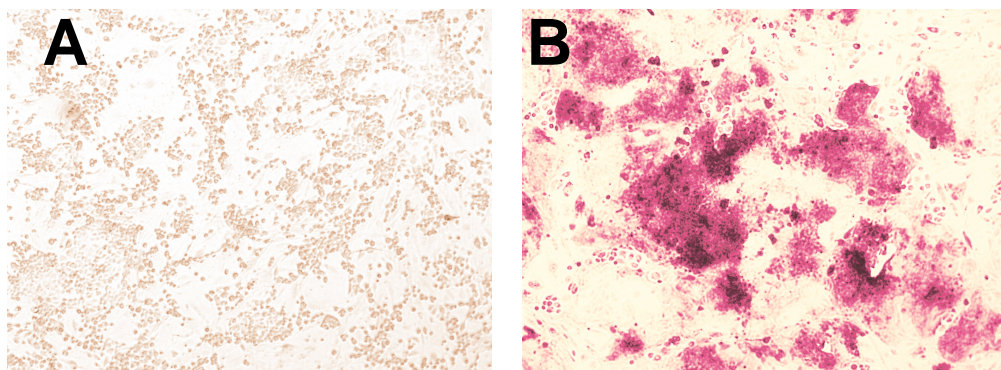

Figure 34. Alkaline phosphatase staining of replated EB-like structures from Pelo$^{\Delta/-}$ CreERT and wild-type cells.
EBs after 10 days of differentiation were trypsinized and plated on gelatine. A – wild type; B – mutant cells.

Further confirmation of pluripotent nature of mutant EBs was determined by expression analysis of essential molecular marker for pluripotency – Oct4 gene, which is downregulated as soon as the cell begins to differentiate. Western blot analysis showed that Oct4 protein is normally expressed in undifferentiated cells (ES1 and ES9), but it was also present in Pelo$^{\Delta/-}$ EBs in contrary to control EBs (*Fig. 35*).
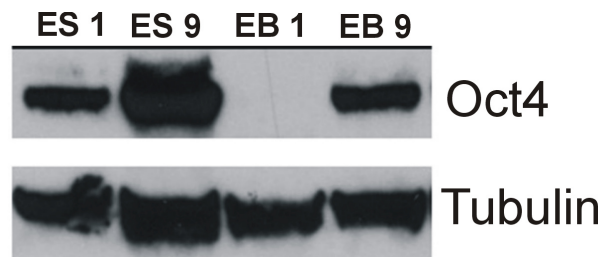
RESULTS

ES 1 ES 9 EB 1 EB 9

Oct4

Tubulin

Figure 35. Western blot analysis of Oct4 expression in differentiated and undifferentiated cKO/CreERT cells.
Picture shows Oct4 protein in undifferentiated mutant (ES9) and control (ES1) cells; differentiated mutant (EB9) and control (EB1) cells.

For further demonstration of Oct4 expression in Pelo$^{\Delta/-}$ EBs, we performed immunohistochemical staining of EBs, which were cultured for 18 days in medium without LIF. The experiment proved that Oct4 protein was still expressed in the mutant cells (*Fig. 36*). Nonetheless, we could find few positive cells also in the control (*Table 6*). There were 21.2% of positive and partially positive cells in the control type, whereas in the mutant such colonies constituted 45.9% of all counted colonies. These data show that Pelo$^{\Delta/-}$ cells failed to differentiate at higher extent than the control.
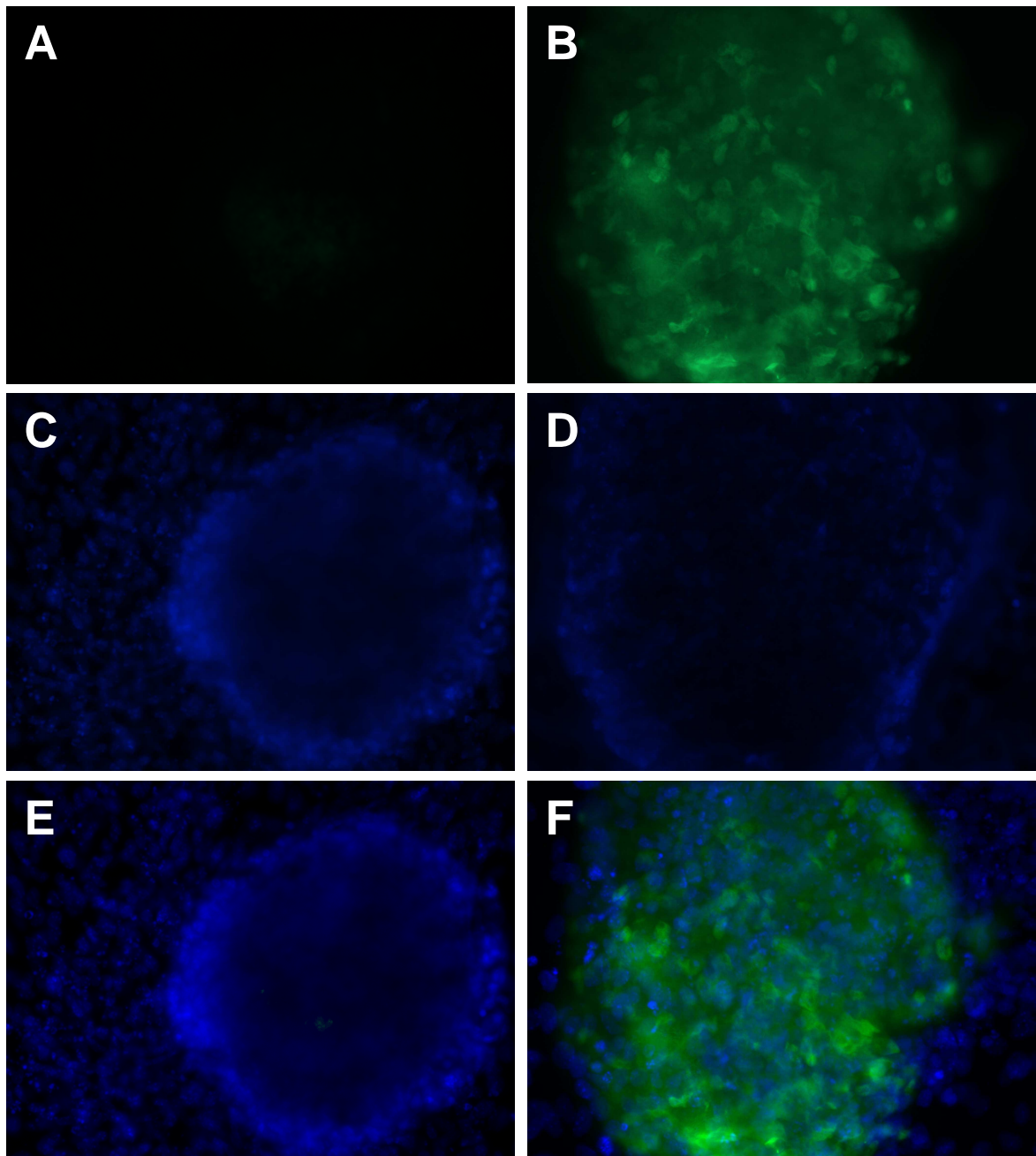
Figure 36. Immunohistochemical analysis of Oct4 expression in differentiated mutant cells

The cells were cultured for 18 days without LIF and then stained with antiOct4 antibody and mounted in medium containing DAPI. A, C, E –control cells; B, D, F – mutant cells. The photos were taken in green fluorescence for visualization of Oct4 and blue- for DAPI.

RESULTS

Table 6. Statistcs for Oct4-positive cells after differentiation.
Cells were plated on 4-chamber slides. The calculations are done for each chamber of the slides with control and mutant cells.

Sort of cell aggregate	Control			$Pelo^{\Delta/-}CreERT$		
	Oct4-positive	Oct4-negative	Partially positive	Oct4-positive	Oct4-negative	Partially positive
No. of aggregates in first chamber / % of aggregates	0 / 0%	21 / 11.7%	2 / 1.1%	3 / 1.5%	21 / 10.8%	8 / 4.1%
No. of aggregates in second chamber / % of aggregates	3 / 1.7%	12 / 6.7%	3 / 1.7%	1 / 0.5%	29 / 14.9%	14 / 7.2%
No. of aggregates in third chamber / % of aggregates	1 / 0.6%	69 / 38.5%	19 / 10.6%	5 / 2.6%	40 / 20.6%	28 / 14.4%
No. of aggregates in forth chamber / % of aggregates	0 / 0%	39 / 21.8%	10 / 5.6%	8 / 4.1%	15 / 7.7%	22 / 11.3%
No. of aggregates in general / % of aggregates in general	**4 / 2.2%**	**141 / 78.8%**	**34 / 19%**	**17 / 8.8%**	**105 / 54.1%**	**72 / 37.1%**

We have then examined the expression of miR-290 cluster – set of microRNAs specifically expressed in pluripotent cells. In wild-type cells, miR-290 was downregulated upon differentiation and loss of pluripotency. However, in pelota-deficient EBs the amount of those small regulative RNAs was upregulated (*Fig. 37*).
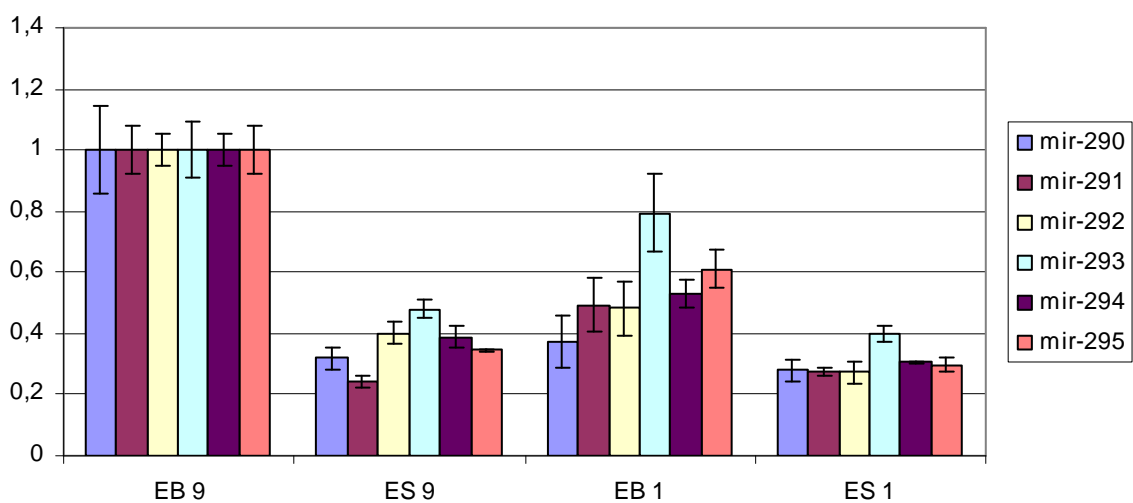

Figure 37. Relative levels of miR-290 cluster expression in $Pelo^{\Delta/-}$ ES cells and embryoid bodies.

RESULTS

Values represent relative levels of microRNAs of miR-290 cluster in undifferentiated control (ES1) and mutant (ES9) ES cell and differentiated cells: the control (EB1) and the mutant (EB9). Expression levels were normalised to the expression of endogenous control (Sdha). 2 technical replicates were done for each microRNA and each cell type. The different colours of bars stand for different microRNAs of miR-290 cluster – explained in the right table.

Results presented above, indicate that the mutant EBs are indeed pluripotent and their differentiation is somehow disrupted. To shed more light on differentiation process in Pelo$^{\Delta/-}$CreERT cells, we determined the potential of mutant ESCs for neuronal differentiation (*Fig. 38*). The experiment did not show any difference between mutant and control cells in their ability to form neurons. In both cases one could observe neuronal cells which were confirmed by immunohistochemical staining with neuron-specific markers – β3-tubulin (TUJ) and tyrosine hydroxylase (TH). As shown in *Figure 38*, TUJ- and TH-positive cells were found in both cell lines. However, the number of mutant cells, which formed neurons seems to be decreased in comparison to control.
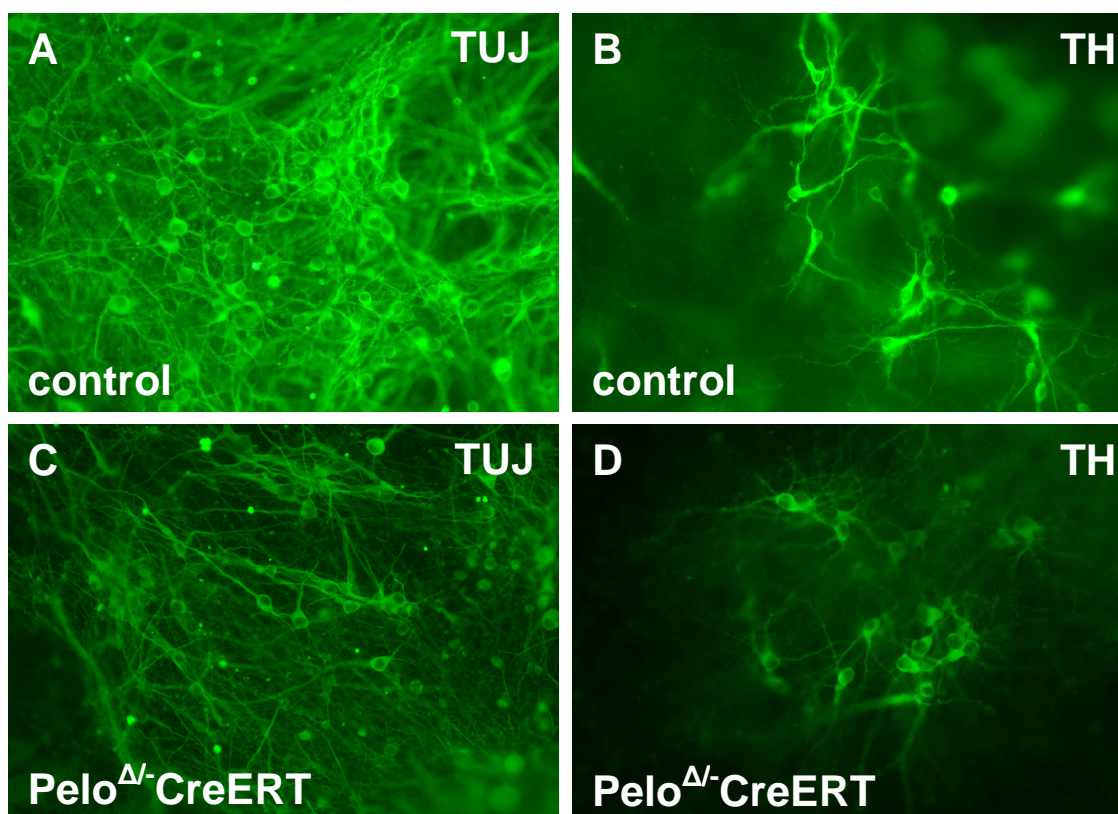

Figure 38. Neural differentiation of mutant and control cells.
The control (A,B) and mutant (C,D) cells were stained with two neuron-specific antibodies: β3-tubulin (TUJ) and tyrosine hydroxylase (TH) and visualized by green fluorescence (FITC).

RESULTS

For investigation of endodermal and mesodermal differentiation ability of mutant cells, we determined the expression level of early and late molecular markers for mesoderm and endoderm development. Eomesodermin is expressed early during mesodermal differentiation (Izumi et al. 2007), whereas vimentin is suggested to be neccesary in advanced stages of mesoderm formation (Rius and Aller, 1992). The expression level of eomesodermin was higher in 10-day-old Pelo$^{\Delta/-}$CreERT EBs than in control EBs (*Fig. 39A*), whereas the vimentin was expressed in mutant EBs on a very low level in contrast to the control (*Fig. 39B*). The data suggest that mesoderm formation is arrested at early stages in Pelo$^{\Delta/-}$CreERT cells. The high expression of vimentin in control EBs suggests that the cells have reached the late stage of mesodermal differentiation, while in the mutant cells the expression of vimentin has not yet been activated due to early-stage arrest. To verify this assumption, the expression level of both markers must be examined in 3-, 5- and 10-day-old EBs.
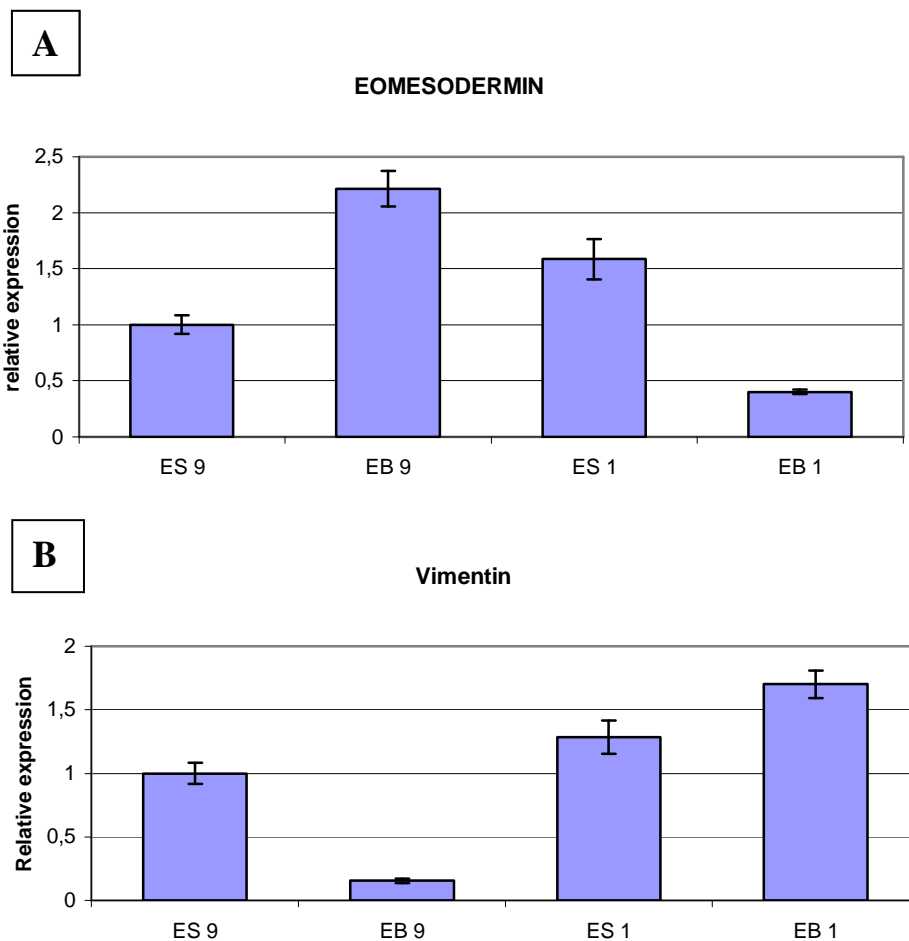
Figure 39. Eexpression profiles of early (A) and late (B) mesodermal markers.
Values represent relative level of eomesodermin and vimentin in 10-day-old mutant (EB9)
and control (EB1) EBs and was compared to the expression in undifferentiated mutant (EB9)

RESULTS

and control (EB1) ES cells. Expression levels were normalised to the expression of endogenous control (Sdha). 2 biological replicates were done for each cell type.

Sox7 and Hnf4 are expressed at early and late stages of endodermal differentiation, respectively (Futaki et al., 2004; Duncan et al., 1997). The expression analysis of these markers in 10-day-old EBs revealed that Sox7 expression level does not differ significantly between Pelo$^{\Delta/-}$CreERT and control EBs and is similar to the level in undifferentiated cells (*Fig. 40A*). Late endodermal marker (Hnf4) exhibits high expression level in 10-day-old control EBs, whereas in undifferentiated cells it is downregulated. In mutant EBs the amount
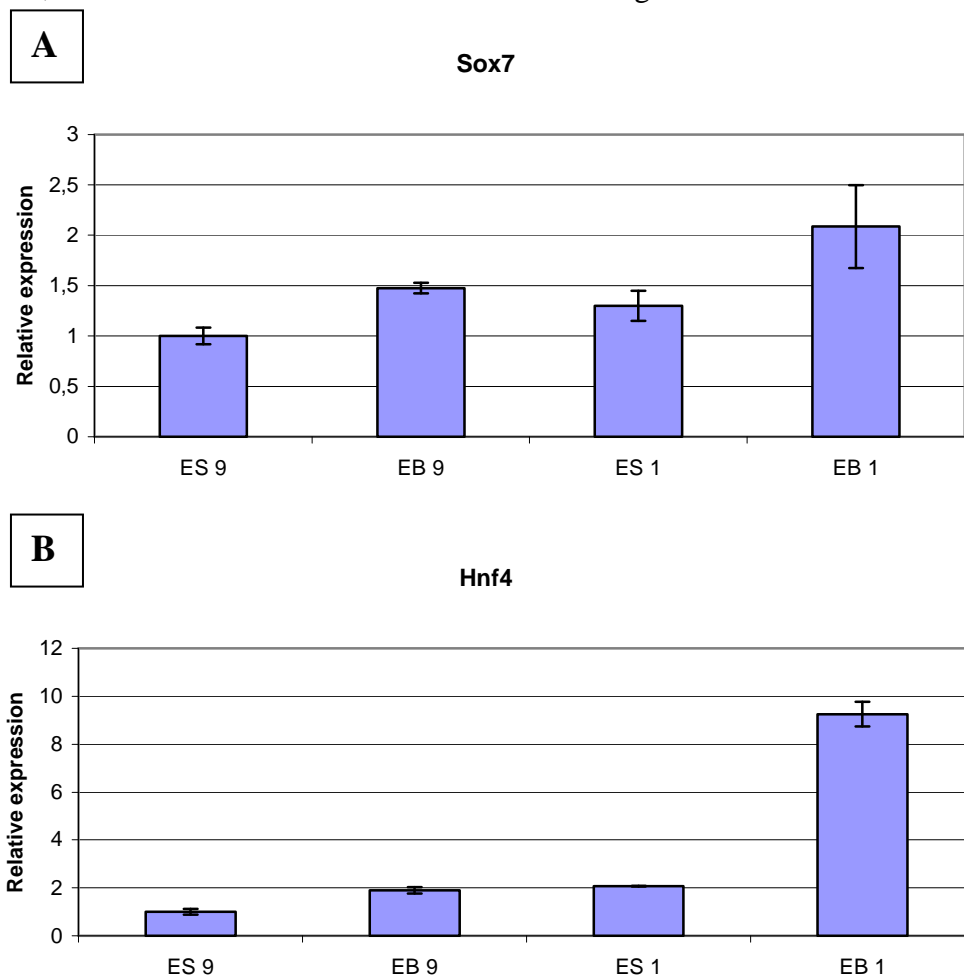
A

Sox7

B

Hnf4

Figure 40. Eexpression profiles of early (A) and late (B) endodermal markers.
Values represent relative level of Sox7 and Hnf4 in 10-day-old mutant (EB9) and control (EB1) EBs and was compared to the expression in undifferentiated mutant (EB9) and control (EB1) ES cells. Expression levels were normalised to the expression of endogenous control (Sdha). 2 biological replicates were done for each cell type.

of Hnf4 transcript is reduced to the level detected in undifferentiated cells. The data suggest that mutant cells fail to form endoderm. Unchanged Sox7 expression may result

RESULTS

from progression to later stages of differentiation, whereas downregulation of Hnf4 may be due to arrest in middle stages of endoderm formation. To evaluate this hypothesis, the expression level of both markers must be done in 3-, 5- and 10-day-old embryoid bodies.

3.2. Transgenic mice overexpressing Pelota

An alternaltive way for demonstration of pelota function in germ cells is a transgenic mouse model. In reference to pelota studies in *Drosophila* ovary (Xi et al., 2005), where depletion of pelota was found to cause loss of self-renewal of germ cells, we suspected that spermatogenesis in mouse testis could be affected as well.

To examine this hypothesis, we studied the phenotype of pelota transgenic animals which had been generated in the institute (Buyandelger, 2006). We analyzed four transgenic lines - two Adam lines (1 and 9) and two Eva lines (1 and 6).

A pelota transgenic allele in Adam lines contains human pelota cDNA under ubiquitin C promoter. The transgene ($Pelo^T$) is specifically expressed in testes (Buyandelger, 2006).
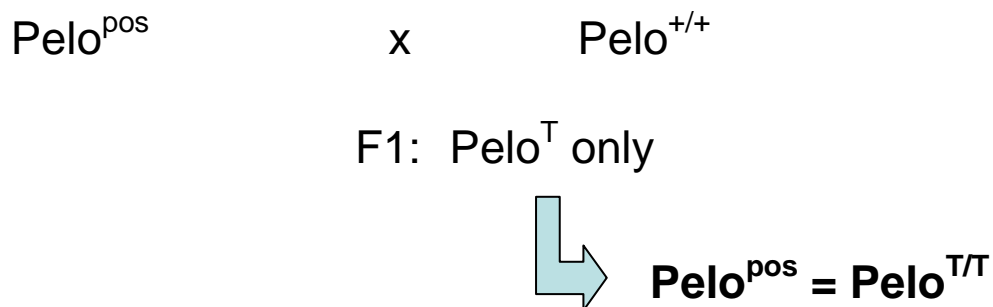
Eva lines possess a transgenic allele composed of human pelota cDNA under the control of the elongation factor 1α promoter. EvaL1 line was shown to exhibit testis-specific $Pelo^T$, whereas the expression of $Pelo^T$ in EvaL6 was detected in all studied tissues (Buyandelger, 2006). It was impossible to analyze the expression pattern of the transgene on protein level, because transgenic PELO protein did not possess any epitope tag (e.g. c-myc) and was therefore undistinguishable from endogenous Pelota protein. Therefore, the studies concerning expression were done on the level of RNA.

3.2.1. Testis-specific transgenic lines

Despite different promoters in Adam and Eva lines, the mice of lines AdamL1, AdamL9 and EvaL1 showed transgene expression restricted to testes. Fertility of males in all lines was not affected, i.e. the mice gave viable offsprings and avarage litter size was comparable to wild type FVB strain: 9±2 animals. We decided to generate lines of homozygous $Pelo^T$ mice. To establish homozygous lines ($Pelo^{T/T}$), we mated $Pelo^T$ mice from F1 generation together. Subsequently, F2 mice were bred with wild type in order to distinguish between $Pelo^T$ and $Pelo^{T/T}$ mice (*Fig. 41*).
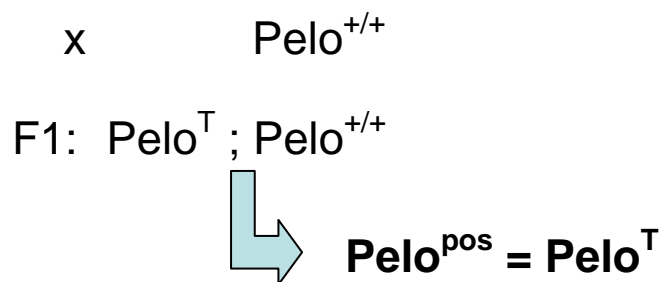
RESULTS

Option I:

$$\text{Pelo}^{\text{pos}} \quad \times \quad \text{Pelo}^{+/+}$$

$$\text{F1:} \ \text{Pelo}^{\text{T}} \ \text{only}$$

$$\Rightarrow \quad \textbf{Pelo}^{\textbf{pos}} = \textbf{Pelo}^{\textbf{T/T}}$$

Option II:

$$\text{Pelo}^{\text{pos}} \quad \times \quad \text{Pelo}^{+/+}$$

$$\text{F1:} \ \text{Pelo}^{\text{T}} \ ; \ \text{Pelo}^{+/+}$$

$$\Rightarrow \quad \textbf{Pelo}^{\textbf{pos}} = \textbf{Pelo}^{\textbf{T}}$$

Figure 41. Scheme of test breedings to identify the homozygous and hemizygous transgenic mice.
Pelo^{pos} stands for mouse that is positive for transgene, whereas $\text{Pelo}^{+/+}$ is a wild type without transgene. Such genotype estimation was done on the basis of at least 2 litters for each positive mouse.

We were able to establish homozygous lines for AdamL1 and AdamL9, whereas test breedings did not reveal any $\text{Pelo}^{\text{T/T}}$ mouse of line EvaL1. Histological analysis of testes isolated from F2 animals of all those three lines demonstrated that pelota overexpression did not influence spermatogenesis in any of the lines (*Fig. 42*). We detected all spermatogenic stages in seminiferous tubules of AdamL1, AdamL9 and EvaL1 animals.
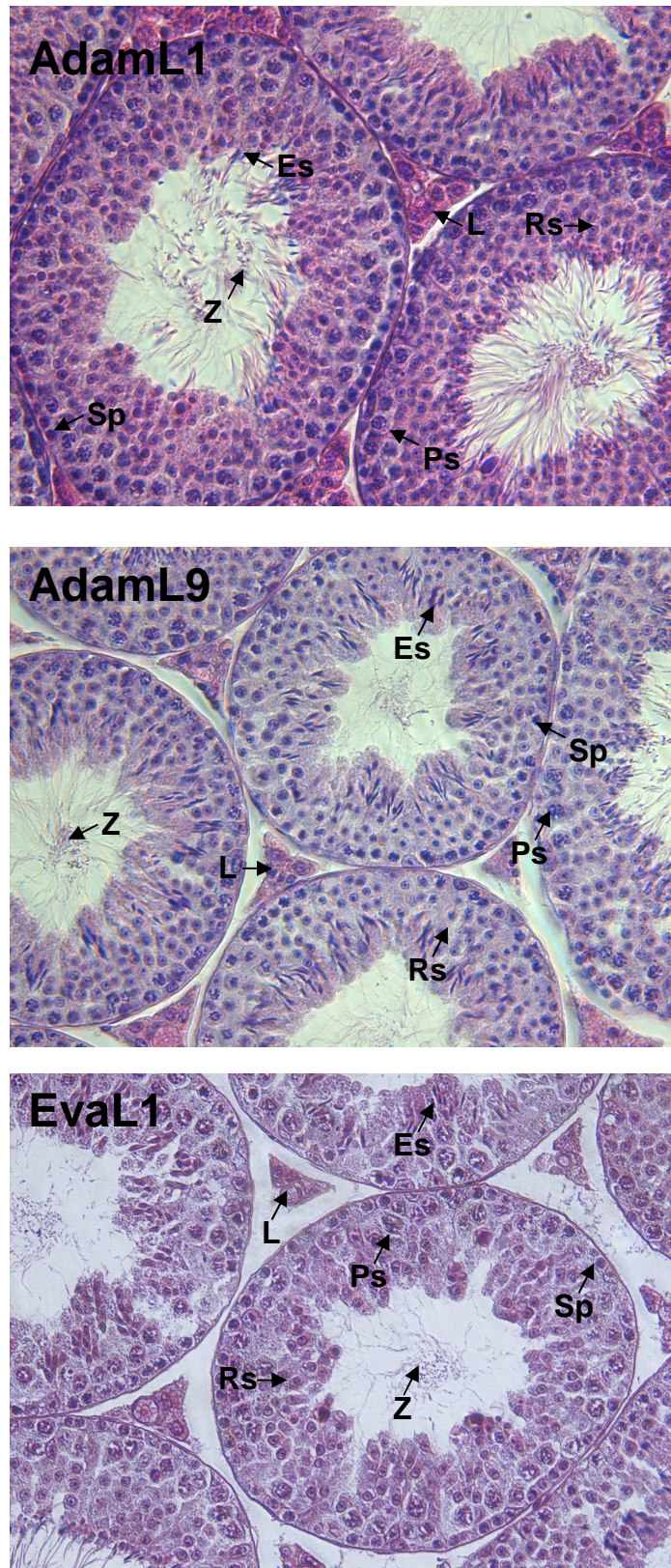
RESULTS

Figure 42. H&E staining of adult testes isolated from AdamL1, AdamL9 and EvaL1.
Sp – spermatogonia; Ps – pachytene spermatocytes; Rs – round spermatids; Z – Spermatozoa; L – Leydig cells. The photos were done in 20x magnification.

RESULTS

The absence of Pelo$^{T/T}$ mice in F2 generation of EvaL1 line led us to assume that the insertion of transgenic allele in the genome might have disrupted a gene, which plays a crucial role during embryogenesis. To determine the integration site of the transgene in EvaL1 genome, we used GenomeWalker Kit (*Materials & methods, 2.2.3*), which allowed us to identify the genomic sequence adjacent to 3'end of transgenic pelota allele. It turned out that pelota construct was recombined into the intronic region of Ror1 (receptor tyrosine kinase-like orphan receptor 1) gene located on chromosome 4. We were able to define the exact integration site of 3' end of the construct. To confirm the integration site, three primers were designed (*Fig. 43*). Two of them were located around the integration site and one was located on 3'end of transgenic construct. The set of these primers was used for genotyping of EvaL1 animals.
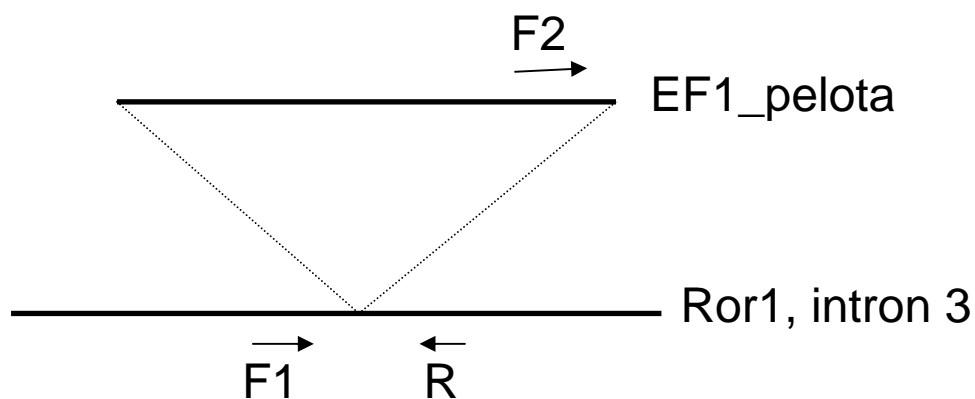

Figure 43. Scheme of pelota construct integration site
The figure presents integration of pelota transgenic allele (EF1_pelota) in the sequence of Ror1 gene, in the intron 3. The arrows show primers which are used for genotyping of EvaL1 animals: F1 – EvaL1_F; F2 – EvaL1_GenomeWalk_F2; R – EvaL1_R

The PCR assay performed by means of designed primers confirmed that determination of integration site was correct. We obtained the expected bands either for wild-type allele or for introduced transgenic allele (*Fig. 44*). It demonstrates that all offsprings obtained from breedings between transgenic mice, were wild-type or heterozygous. Neither of them was Pelo$^{T/T}$.
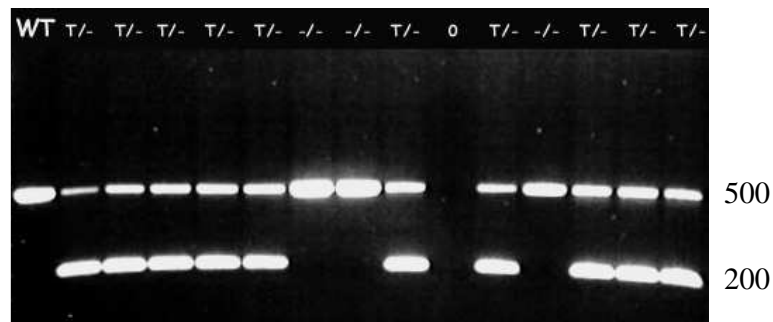
RESULTS

Figure 44. Genotyping PCR for integration site in EvaL1 line
*Wild-type band stands for intron 3 frogment of Ror1 gene without pelota construct
integration amplified by F1 and R primers (Fig. 43), while transgenic allele is amplified by
F2 and R..*

To determine whether the Pelo$^{T/T}$ mice die during embryogenesis, we genotyped embryos at
E15.5 and E17.5 stages. We found Pelo$^{T/T}$ mice in both stages. Analysis of neonatal
offsprings derived from crosses of heterozygous Pelo^T mice revealed that Pelo$^{T/T}$ newborns
died within 24 hour after birth (*Table 7.*).

Table 7. Genotype statistics of newborns which died within 24 hours after birth.

Parents genotype	Pelo^T	x	Pelo^T
Newborns genotype	Pelo$^{-/-}$	Pelo^T	Pelo$^{T/T}$
No. of newborns	17	28	**14**
No. of newborns which died within 24h	1	5	**14**

It could be possible that during recombination process a part of intron/exon sequence
was deleted and Ror1 was disrupted. To prove this hypothesis, Western analysis of proteins
isolated from kidneys of Pelo$^{T/T}$, Pelo^T and Pelo$^{-/-}$ embryos was performed using polyclonal
anti-ROR1 antibody. As shown in *Figure 45.*, the ROR1-specific 105 kDa band was
detected. The protein was present either in wild-type or in Pelo^T kidney-protein extracts,
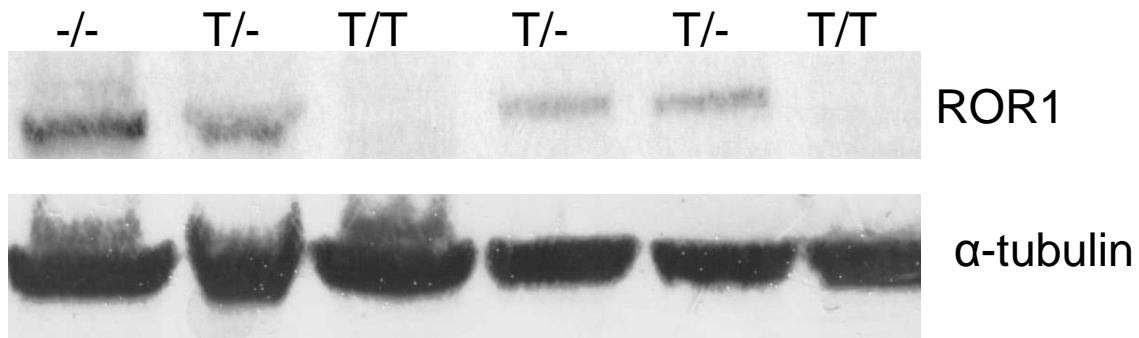whereas in Pelo$^{T/T}$ embryos it was undetectable.

RESULTS

Figure 45. Western analysis for ROR1 protein in EvaL1 mice.
The upper photo presents staining with anti-ROR1 antibody which detects the ROR1 protein in size of 105 kDa. Antibody staining with anti-tubulin (lower photo) demonstrates tubulin protein of 51 kDa which characterizes the quality of proteins used for ROR1 staining.

Lack of ROR1 protein confirmed accidental disruption of this gene by recombination of pelota transgene into Ror1 locus. Ror1 knockout phenotype was published (Nomi et al., 2001). It was reported that Ror1^{-/-} newborns had respiratory problems and died within 24 hours after birth. After observation of EvaL1 newborns, we obtained convergent results.

3.2.2. EvaL6 as a rescue for pelota knockout mice

To study the consequence of Pelo-overexpression on embryonic and germ cell development, our group generated a transgenic mouse line that ubiquitously overexpressed Pelota protein. EvaL6 line was generated by the introduction of the transgenic pelota under EF1 promoter into the wild-type mouse genome (Buyandelger, 2006). The ubiquitous expression of Pelo[T] in EvaL6 mice did not influence mouse viability and fertilty. We generated a homozygous EvaL6 line like described above (*Fig. 41*). The line did not exhibit any apparent phenotype.

These transgenic animals were used to solve the question whether the embryonic lethality of Pelo-deficient mice is due to inactivation of pelota gene or because of position effect resulting from manipulation of pelota locus and consequent change in expression of neighbouring genes.

To verify these possibilities, we introduced the transgenic Pelo allele into the genome of Pelo^{-/-} mice (*Fig. 46*) and proved the ability of Pelo[T] to rescue the embryonic lethality of Pelo^{-/-} mice.

RESULTS

$$\text{Pelo}^{+/-} \quad \text{x} \quad \text{Pelo}^{T/T}$$

$$\text{F1: Pelo}^{+/-T} \quad \text{x} \quad \text{Pelo}^{+/-T}$$

$$\text{F2:} \quad \underline{\textbf{Pelo}^{-/-T}}$$

Figure 46. Strategy of breeding for generation of rescue mouse

Generated Pelo$^{-/-}$Pelo^{T} rescue mice are healthy (*Fig. 47*) what provides evidence that pelota transgenic allele is properly constructed. Moreover, its expression under EF1 promoter is efficient to substitute endogenous Pelota protein and mimic its function in living animal. It confirmed close evolutionary relation between human and murine Pelota protein.

Figure 47. Rescue mouse: Pelo$^{-/-}$Pelo^{T} male

Table 8 demonstrates the genotype statistics of breedings between Pelo$^{+/-T}$ mice, which yielded Pelo$^{-/-T}$ mice. All rescue mice were viable. Their fertility was studied in test breedings. One Pelo$^{-/-T}$ female has already delivered 8 offsprings, while no progeny was obtained from any Pelo$^{-/-T}$ male within 2-month breedings. It indicates that transgenic Pelota protein is also capable of retaining germ cell differentiation and functionality at least in ovaries.

RESULTS

Table 8. Statistical frequency of expected genotypes derived from breedings producing rescue mice

Pelo$^{+/-T}$ x Pelo$^{+/-T}$						
F1 generation	+/+	+/-	-/-	+/+T	+/-T	-/-T
Mendelian ratio	1	1	1	1	1	1
Mice number (out of 52)	8	14	0	5	19	6

DISSCUSSION

4.1. Brief overview of the results

In 2003 pelota function was analyzed in pelota knockout mouse (Adham et al., 2003). The phenotype of homozygous mutants (Pelo$^{-/-}$) is lethal during early stages of embryogenesis (E7.5). Pelo$^{-/-}$ blastocysts fail to expand in growth after 4-day culture. It was hypothesized that inner cell mass displays the defect rather in cell proliferation than in differentiation. The putative role of pelota in differentiation was demonstrated in *Drosophila* ovary, where it is involved in self-renewal of germ stem cells (Xi et al., 2005).

To investigate the function of murine PELO in cell cycle/differentiation, we generated a conditional knockout mouse. On the level of RNA, we demonstrated that tamoxifen-induced recombination of floxed Pelo allele was complete in generated Pelo$^{F/-}$ CreERT ESC line (*Fig. 11*). The procedure was also very efficient in the mouse model, where we detected almost complete deletion of the floxed allele (*Fig. 29*).

The histological analysis showed that spermatogenesis was completely disrupted - all stages of germ cells were absent, only Sertoli cells could be found (*Fig. 31*). For evaluation of PELO effect on spermatogenesis progression, we generated testis-specific knockout mice (Pelo$^{F/-}$Stra8-Cre), where deletion of floxed Pelo region occurs in accordance with Stra8 promoter-derived Cre recombinase expression (*chapter 3.1.6.*). The immunohistochemical analysis of mutant testes unveiled lack of spermatogenic progression since day 15, when meiotic division starts. The quantitative analysis of premeiotic markers revealed that expression of Stra8, Dazl and Ddx4 in 10-day-old testes was alike – all three markers exhibited a drastic increase of transcript level at that time in the control, but in mutant testes we observed twofold reduction (*Fig. 25, 26, chapter 3.1.6.4.*). In case of Plzf, Sox3 and c-Kit, there was no dramatic discrepancy between control and mutant, despite the slight reduction at day 5. It indicates that there was no clear effect of PELO depletion at the stage of either undifferentiated (Plzf and Sox3) or differentiated (c-Kit) spermatogonia. It suggests that the phenotype appeared with onset of spermatogonial differentiation, that is with entry to meiotic division. In addition, we found mosaic mice (Pelo$^{F/\Delta/-}$Stra8-Cre), which displayed incomplete Pelo allele recombination in various somatic tissues, including kidney, liver, heart, spleen, lungs. It indicates that Stra8 expression is transactivated early in embryogenesis. However, we did not find Pelo$^{\Delta/-}$Stra8-Cre mice, what means that this genotype is lethal during embryogenesis, similar to pelota classical knockout.

DISSCUSSION

Handling the well-functioning conditional knockout mouse model, we were able to verify why Pelo null blastocysts were unable to produce the ESC line. We generated Pelo$^{F/-}$CreERT ESC line, where we successfully deleted Pelo (the cell genotype become Pelo$^{\Delta/-}$CreERT) by CreERT recombination (*Fig. 10*). The null cells did not show any proliferative disorder and were well preserved in culture. They also did not exhibit an increased level of programmed cell death. Therefore, we analyzed the differentiation capability of mutant ES cells. The Pelo$^{\Delta/-}$CreERT ES cells turned out to be defective in generating embryoid body structures. The cells showed sustained Oct4 expression and upregulated expression of miR-290 cluster – family of microRNA which is characteristic for pluripotent ES cells (Houbaviy et al., 2003, 2005). To investigate in which germ layer the differentiation failure occurs, we used the mutant cells for neuronal differentiation. The experiment resulted in differentiation of neuronal cells *in vitro*. This indicates that the process of generating ectoderm is unaffected (*Fig. 38*). For analysis of mesoderm and endoderm lineages, we performed quantitative RT PCR by means of early and late markers for both germ layers. In mutant cells subjected to EB formation, the level of early mesodermal marker (eomesoderin, Fig. 39A) was significantly higher that in control EBs, and expression of a late marker (vimentin, Fig. 39B) was strongly reduced. Whereas the early marker for endodermal development (Sox7) did not show any difference between mutant and control, the late marker (Hnf4) was drastically downregulated in mutant cells. From these results we assume that pelota-deficient cells are defective in mesoderm and endoderm formation. To prove our hypothesis we studied differentiation of adult stem cells, i.e. hematopoietic stem cells and spermatogonial stem cells, which are convenient models in the mouse due to continuous differentiation process along the life span of the animal and due to their mesodermal origin.

The analysis of B and T cells isolated from spleen and thymus demonstrated the reduction in number of both kinds of cells. Additionally, in case of T cells we detected a strong increase of double negative cells (CD4$^-$CD8$^-$), which are developmental precursors of mature T cells. However, the following developmental stages, that are double positive (CD4$^+$CD8$^+$), single positive (CD4$^+$CD8$^-$ or CD8$^+$CD4$^-$) and mature T cells (CD3$^+$) were reduced in number (*Table 4.*). This clearly shows the developmental arrest of T cells. However, proliferation of precursor cells was not affected.

To show that mortality of classical knockout mice results from pelota inactivation, we crossed Pelo$^{+/-}$ mice with transgenic Pelo^T mice (*chapter 3.2.2*), which rescued the lethal phenotype. It clearly demonstrates that the lethality originated from pelota inactivation, and it was not the position effect after introduction of the allele into the genome.

DISSCUSSION

In addition, we analyzed transgenic mice which overexpress PELO in testis-specific manner. However, we did not detect any disorder in spermatogenesis. The mice were fertile. This can suggest that PELO protein is subjected to accurate posttranslational regulation in the cell and the excessive amounts of the protein are removed.

4.2. Embryonic stem cell fate shift from pluripotent to differentiated state

Embryonic stem cells are derived from the inner cell mass of the blastocyst (E3.5 in murine embryogenesis) and are capable of giving rise to all three germ layers, what constitutes their pluripotency. The important feature of ES cells is their ability to self-renew, which requires a complex transcriptional profile (Zhou et al., 2006). Some factors were identified to contribute to the pluripotency maintenance, including Oct4, Sox2 and Nanog. The shift of the cell fate to differentiation causes downregulation of the pluripotent markers. For instance, in the cells induced to mesoderm formation, Oct4 is not expressed (Yeom et al., 1996; Yoshimizu et al., 1999).Depletion of the main pluripotent markers stands for the loss of pluripotency. Oct-4-deficient embryos die at blastocyst stage due to loss of pluripotent cells composing inner cell mass (Nichols et al., 1998; Niwa et al. 2000). Sox2-targeted deletion causes a lethal phenotype at peri-implantation stage of embryogenesis. In contrast to Oct4-null mutants, Sox2$^{-/-}$ embryos develop the inner cell mass, but they fail to maintain epiblast cells which are essential for further differentiation of extraembryonic tissues (Avilion et al., 2003). Nanog-deficient ES cells differentiate into extraembryonic endoderm lineage, losing pluripotency (Mitsui et al., 2003). Preservation of pluripotency requires also silencing of genes which are responsible for differentiation initiation. Such inactivation is implemented by means of epigenetic regulation, i.e. chromatin remodeling, histone modifications and DNA methylation (Boyer et al., 2006; Lee et al., 2006). However, the genes of pluripotent markers are also subjected to epigenetic regulation. Such regulation by methylation was reported for Oct4 (Hattori et al., 2004) and Nanog promoters (Deb-Rinker et al., 2005). It was unveiled that <u>N</u>ucleosome <u>R</u>emodeling and histone <u>D</u>eacetylation (NuRD) complex (Xue et al., 1998) is recruited at promoter sequences of the pluripotent markers and is responsible for epigenetic modifications and silencing of the gene expression (Wade et al., 1999; Lan et al., 2002; Crook et al., 2006; Kaji et al., 2006).

The NuRD complex is composed of methyl-binding-domain-related protein 2 and 3 (MBD2/3), histone-binding proteins, chromatin remodeling ATPases, zinc-fingers proteins and histone deacetylases, which form together orchestrated apparatus for epigenetic

DISSCUSSION

modifications (Crook et al., 2006). MBD2 and 3 were identified as core components of NuRD complex (Ng et al., 1999; Zhang et al., 1999). However, it was found that they are mutually exclusive. They reside in two NuRD complexes with distinct core-subunit compositions: MBD2/NuRD and MBD3/NuRD (Le Guezennec et al., 2006). The results of knockout studies for MBD2 and MBD3 indicate that they play nonoverlapping roles in mouse development. Deletion of MBD2 results in relatively mild defects in transcriptional silencing of methylated promoters. The MBD2-knockout mice are viable – this demonstrates that MBD2 is not crucial for mouse development. Unlike MBD2, the deletion of MBD3 causes embryonic lethality (Hendrich et al., 2001).

Due to the fact that it was impossible to establish an ES cell line from Mbd3$^{-/-}$ blastocysts, Kaji et al. (2006) generated an ESC line with floxed Mbd3$^{F/-}$ allele. After MBD3 deletion, the mutant ES cells were unable to repress transcription of Pramel6 and Pramel7 – genes highly expressed in preimplantation stages, and Dppa3 which is an early marker of primordial germ cells. When the Mbd3$^{-/-}$ ES cells were subjected to differentiation conditions, they displayed persistent expression of pluripotent markers (Oct4, Nanog, Rex1). In addition, they failed to express differentiation markers for all developmental lineages (endoderm, mesoderm and ectoderm), except for primitive ectoderm marker Fgf5 at day 3 of differentiation. However, the cells were unable to downregulate the Fgf5 expression at later stages of differentiation as compared with control cells. This suggests that ectodermal differentiation can start, but is arrested at early stage (Kaji et al., 2006). Our results demonstrate that PELO protein inactivation leads to analogous phenotype.

Similarly to Mbd3$^{-/-}$, Pelo$^{\Delta/-}$ ES cells stay pluripotent in differentiation conditions, what was confirmed by alkaline phosphatase staining and sustained Oct4 expression. Analysis of differentiation markers shows that Pelo$^{\Delta/-}$ and Mbd3$^{-/-}$ ES cells subjected to embryoid body formation exhibit a differentiation arrest in either all developmental lineages (Mbd3$^{-/-}$) or mesoderm and endoderm (Pelo$^{\Delta/-}$). Interestingly, both mutant cell lines seem to display primitive cell fate shift to differentiation into one germ layer: ectoderm (Mbd3$^{-/-}$) or mesoderm (Pelo$^{\Delta/-}$). However, the increased mRNA levels of early differentiation markers and decreased transcript levels of late differentiation markers lead us to the assumption that further formation of ectoderm (Mbd3$^{-/-}$) and mesoderm (Pelo$^{\Delta/-}$) is arrested at an early stage of differentiation. This convergent phenotypes suggest that the defect of differentiation capacities of Pelo$^{\Delta/-}$ ES cells may result from malfunction of NuRD complex in methylation of Oct4 promoter, which in these cells is constantly active under differentiation conditions.

DISSCUSSION

This hypothesis is supported by the fact, that pelota was found to interact with CDK2AP1 protein (unpublished data), which is also required for epigenetic silencing of the Oct4 gene during ESC differentiation (Deshpande et al., 2008). In addition, the protein was identified as a core component of MBD2/NuRD and MBD3/NuRD complexes (Le Guezennec et al., 2006). Deletion of Cdk2AP1 results in early embryonic lethality and sustained expression of Nanog and Oct4. As these findings are convergent with the Mbd3-deficiency phenotype, it was assumed that CDK2AP1/MBD3/NuRD complex is responsible for silencing of genes of pluripotent markers during the differentiation process (Deshpande et al., 2008). Due to the fact that PELO protein is localized in the cytoplasm and not in the nucleus, the interaction between CDK2AP1 and PELO may have a regulatory impact on signalling pathways related to promotion of differentiation, like the transforming growth factor β (TGF-β) pathway.

4.3. Signal transduction in differentiation and pluripotency

The development and homeostasis of most mouse tissues are controlled by the TGFβ signal transduction network, which involves distinct receptor families and mediator proteins activating target gene transcription in association with DNA-binding proteins (Massague, 1998). The TGF-β family consists of polypeptide growth factors, which regulate various developmental processes, such as cell proliferation, lineage determination, differentiation and cell death. The TGF-β is also an important antiproliferative factor during early stages of oncogenesis (Hill et al., 2009).

The TGF-β1 is a member of the TGF-β family. It is a cytokine, which exerts suppressive effects on epithelial, endothelial and hematopoietic cells by promoting synthesis of cyclin-dependent kinase inhibitory proteins (Massague, 1990; Hannon and Beach, 1994; Alexandrow and Moses, 1995; Polyak, 1996). Hu et al. (2004) demonstrated that this growth factor leads to induction of CDK2AP1 transcription and in consequence to increased CDK2AP1 association with CDK2. The interaction results in negative regulation of CDK2 activity, i.e. proliferation inhibition. This TGF-β-mediated growth suppression is affected by CDK2AP1 depletion. From these data we can assume that CDK2AP1 protein, a core component of MBD3/NuRD complex, is activated by TGF-β. As it is doubtful that PELO participates directly in the NuRD complex formation, we suppose that disruption of Oct4 promoter methylation in Pelo-deficient ES cells is an effect of upstream deregulation of TGF-β signalling pathway, which controls pluripotent gene expression by epigenetic

DISSCUSSION

silencing and hence differentiation of mouse ES cells. It is probable that PELO/CDK2AP1 interaction plays a role in TGF-β promotion (*Fig.49*).

An alternative pathway, which may be deregulated in pelota-deleted Pelo$^{\Delta/-}$CreERT ES cells is the LIF signalling pathway. LIF signalling inhibits mesoderm and endoderm formation, whereas ectoderm formation in ESCs is blocked by bone morphogenetic protein 4 (BMP4) signalling (Ying et al., 2003). Due to the fact that ectoderm differentiation upon pelota inactivation is unaffected, we assume that BMP4 pathway is not influenced by PELO protein. In normal ES cells, LIF application leads to phosphorylation of distinct factors, including STAT3, a signal transducer and activator of transcription 3 (Boeuf et al., 1997), what leads to maintenance of pluripotent state. Inactivation of STAT3 was reported to induce spontanous differentiation (Paling et al., 2004). The studies concerning STAT3 expression revealed that this factor, activated under differentiation conditions, is capable of sustaining self-renewal of ESCs without addition of LIF (Matsuda et al., 1999). The STAT3-dependent pathway is poorly understood, but it is known that c-myc and Eed genes (cell proliferation propagators) are direct targets of STAT3 (Cartwright et al., 2005; Ura et al., 2008). Recently, 58 genes were identified as target genes of STAT3 (Bourillot et al., 2009). Some of them, like Smad7 or c-myc, are negative regulators of TGF-β signalling (Hayashi et al., 1997; Imamura et al., 1997; Nakao et al., 1997; Feng et al., 2002).

STAT3 pathway sustains pluripotent character of ES cells by inhibiting mesodermal and endodermal differentiation processes activated by TGF- β signals. Pelota function may be associated with downregulation of STAT3 signalling. In Pelo$^{\Delta/-}$CreERT cells subjected to differentiation conditions, mesoderm and endoderm are not formed, as it is shown on the transcript levels of lineage-specific markers (*Fig. 39, 40*). It might be connected with uncontrolled upregulation of STAT3, which is able to maintain pluripotency in the absence of LIF. However, the studies in *Xenopus* embryos have shown that STAT3 can also promote mesoderm formation (Ohkawara et al., 2004). In different conditions, namely various sorts and doses of signals, STAT3 can become also up- or downregulated by BMP2, a TGF-β family member, what in consequence leads to apoptosis or differentiation (Kawamura et al., 2000; Rajasingh et al., 2007). TGF-β and STAT3 signalling pathways form a dynamically balanced network which decides about the fate of the cell depending from incoming signals. Therefore, a putative function of PELO in negative regulation of STAT3 must be well adjusted to the signal influx.

The TGF-β is also a regulator of immune response. It was reported to induce CD8 expression in CD4$^-$CD8$^-$ double negative thymocyte precursors during T cell differentiation

DISSCUSSION

process (Suda and Zlotnik, 1991; 1992; Inge et al., 1992; Plum et al., 1995). The maturation of B cells is also controlled by TGF-β, which positively and negatively regulates the expression of cell surface markers in B cell precursors and mature B cells (Stavnezer, 1996). In activated B cells, TGF-β inhibits cell proliferation and may induce apoptosis (Lomo et al., 1995). However, in epithelial malignancies the cells may become insensitive to TGF-β inhibitory effects what leads to an increase of the cell number and tumor progression (Berg and Lynch, 1991; Tada et al., 1991; Kadin et al., 1994; DeCoteau et al, 1997). Among its numerous functions, the TGF-β blocks also activated lymphocyte proliferation and has been thus suggested to serve as a negative feedback mechanism to reverse the inflammatory response (Wahl et al., 1988). It was also demonstrated that the TGF-β1 deletion leads to autoimmune disease. It indicates a substantial role of TGF-β in self-tolerance of the immune system. It is likely to contribute in negative selection of T cells in thymus. Deletion of TGF-β leads to imbalanced production of CD4$^+$CD8$^+$ double positive cells due to defective apoptosis of differentiating T cells (Letterio and Roberts, 1998).

Lymphocytes composing the immune system develop from mesodermal hematopoietic cells. Our preliminary data demonstrate that Pelo$^{\Delta/-}$CreERT ES cells fail to differentiate into mesoderm. In parallel, the phenotype of Pelo$^{\Delta/-}$CreERT mice indicates an immune system disorder, in which the number of mature B and T cells is highly diminished due to arrest in T cell differentiation in the thymus, and immature thymocytes are increased in number. In case of B cells, it is neccessary to evaluate the number of B cell precursors in a cell population of bone marrow, where the differentiation starts, to confirm that proliferation is not affected. However, the immune system functionality is impaired and inflammation observed in different organs of the mutant mice seems to be the consequence of the immune system malfunction. In accordance with our hypothesis, that pelota is functionally correlated with TGF-β signalling and mesoderm formation. The mouse phenotype, observed upon Pelo inactivation, is prominent in the immune system due to the constant differentiation process occuring in hematopoietic cells. However, the bone marrow is not the only source of pluripotent cells in the adult mouse. The cell fate shift from pluripotency to differentiation happens also in gonads.
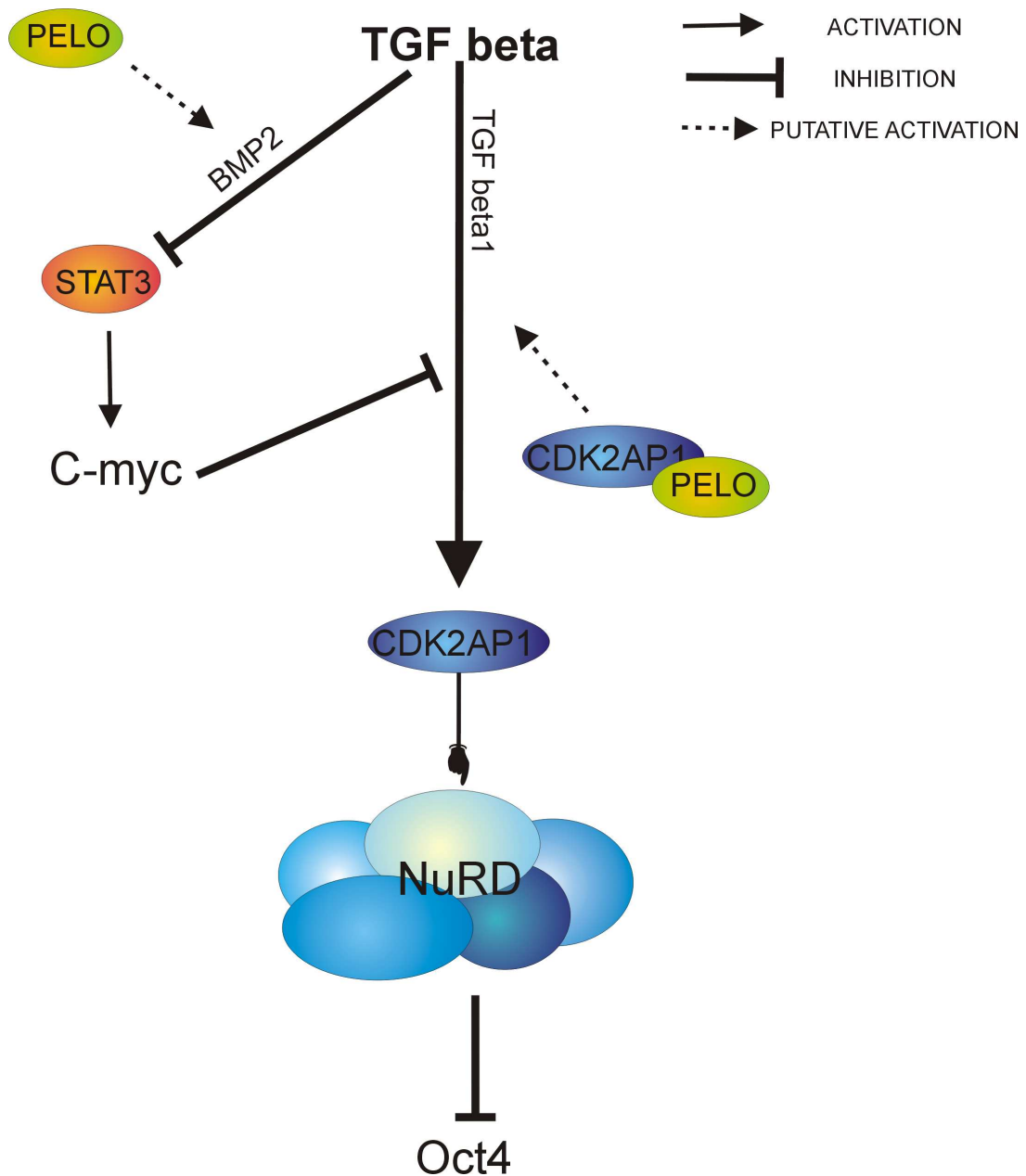
DISSCUSSION

Figure 48. The scheme presenting putative PELO involvment in TGF-β signalling during differentiation process.
TGF beta 1 activates CDK2AP1 expression. CDK2AP1 joins the NuRD complex, which is responsible for Oct4 promoter methylation and in consequence its inactivation. BMP2, a TGF-β family member, inhibits STAT3 pathway, which participates in pluripotency maintenance. In undifferentiated ES cells STAT3 activates c-myc, a proliferation propagator, which inhibits TGF-β pathway. PELO/CDK2AP1 may play as a positive feedback regulator in TGF-β signalling. According to an alternative hypothesis, PELO positively regulates BMP2- mediated STAT3 inhibition.

DISSCUSSION

4.4. Pelota in germ cell differentiation

The testis-specific Pelota knockout mouse (chapter 3.1.6.) demonstrated that spermatogenesis is arrested at the spermatocyte stage during its first wave. Deletion of floxed Pelo region occurs in accordance with Stra8 promoter which derives Cre recombinase expression. As it was reported (Menke et al., 2003; Baltus et al., 2006; Zhou et al., 2008), Stra8 gene is active in premeiotic stages of germ cells either in male or female. However, the highest protein level is present with onset of meiosis in gonads (*Fig. 49*).
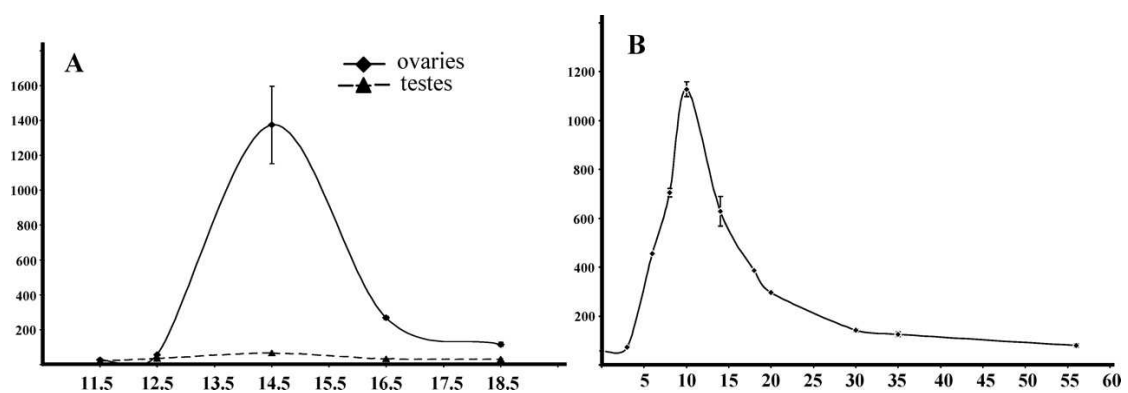

Figure 49. Stra8 expression in developing ovaries and testes (adopted from Zhou et al, 2008)
Constant line represents ovaries and doted line – testes mRNA expression during embryogenesis (A). Raw signal values are shown on the y axis, days postcoitum – on the x axis (A); postnatal Stra8 mRNA expression is presented in B. Raw signal values are shown on the y axis, days postpartum – on the x axis (B).

In ovaries, meiosis commences at prenatal stage E14.5, whereas in males it occurs at day 10 of postnatal development. The highest level of Stra8 expression coincides with the onset of meiosis. The Stra8 expression is thereafter undetectable in ovary, and in testis it decreases to a low level, which is comparable to the state of postnatal day 5, when only premeiotic germ cells are present in the testis (Zhou et al., 2008). It is worth noting that this extreme increase of Stra8 protein happens only during the first wave of spermatogenesis (*Fig. 49*). It indicates that a Stra8-Cre is expressed in the same pattern and the most efficient pelota recombination coincides with this event at day 10 only in the first wave of sperm differentiation. It would explain the phenomenon of fertile Pelo[F/-]Stra8-Cre mice. Namely, Stra8 protein was demonstrated in different types of germ cells – type A and B spermatogonia, preleptotene and early leptotene spermatocytes (Zhou et al., 2008), what

DISSCUSSION

suggests that the Stra8 promoter is activated later than in germ stem cells (GSCs). It means that in all next generations of spermatogonia, the recombination of floxed region will occur *de novo* and due to low expression of Stra8-Cre recombinase, Pelo is excised less sufficiently. Therefore, some amount of sperm is successfully produced and mice stay fertile (*Table 3., chapter 3.1.6.5.*). Moreover, Zhou et al. (2008) demonstrated that retinoic acid (RA) is critical for Stra8 expression (Koubova et al., 2006) what let us speculate that Stra8-Cre recombination is variable and RA-dependent. Nonetheless, one can conclude that PELO plays a role in meiosis progression, what is convergent with experiments performed in yeast and *Drosophila* (Eberhart and Wasserman, 1995; Davis and Engebrecht, 1998).

The quantitative analysis of premeiotic markers revealed that expression of Stra8, Dazl and Ddx4 in 10-day-old testes is similar – all three markers exhibit a drastic increase of transcript level at that time in the control, but in mutant testes we could observe twofold reduction (*Fig. 25, 26, chapter 3.1.6.4.*). In case of Plzf, Sox3 and c-Kit, there is no dramatic discrepancy between the control and the mutant, despite the slight reduction at day 5. It indicates that there is no clear effect of Pelo depletion at the stage of either undifferentiated (Plzf and Sox3) or differentiated (c-Kit) spermatogonia. It suggests that the phenotype appears with the onset of spermatogonial differentiation, that is with entry into meiotic division.

However, the question arises whether pelota has any impact on mitotic divisions, i.e. GSC self-renewal, as it was reported in *Drosophila* (Xi et al., 2005). The Stra8-Cre line is insufficient model to shed light on this issue. Therefore, we used CreERT-mediated Pelota deletion. Tamoxifen-induced recombination occurs independently from developmental stage of cells, what makes possible to affect GSCs and all their derivatives during ever-lasting spermatogenesis – not only its first wave.

15-day-old males were treated with tamoxifen. Histological analysis of their testes was performed 2 months later. During this period, first wave of spermatogenesis is finished and following waves take place. We found complete lack of germ cells, only Sertoli cells could be observed in seminiferous tubules of mutant testes (*Fig. 33, chapter 3.1.7.2.*). The phenotype resembles W/W^V mutant testes, where no germ cells are present, but some spermatogonia could be found. The fact worth mentioning is that W/W^V mutant spermatogonia are capable of proliferating, but their differentiation abilities are defective (Ohta et al., 2003). Our findings suggests that Pelota has also an impact on GSC differentiation and mitotic division is not affected. The phenotype of mutant testis confirms our hypothesis concerning an involvment of pelota in the cell fate shift. As far as TGF-β

DISSCUSSION

pathway is concerned, it was demonstrated that Smad proteins, which are mediators in TGF-β signalling, are upregulated in meiotic germ cells of the rat testis. It was suggested that TGF-β may play a putative role in maturation of the first wave of spermatogenesis (Xu et al., 2003).

4.5. miRNA in pluripotent stem cells during differentiation

MicroRNA is a family of small (~22 nucleotides) non-coding RNAs, which are involved in regulation of gene expression by either degradation of target mRNA transcripts or by disruption of mRNA translation (Kloosterman et Plasterk, 2006). However, it is known that there is a group of miRNAs, the members of miR-290 cluster, which are abundant in embryonic stem cells, but they become silenced upon the onset of differentiation (Houbaviy et al., 2003, 2005). Zovoilis et al. (2009) showed that miR-290 cluster inhibits ES cell differentiation process towards mesoderm through negative regulation of Wnt pathway. In Pelo$^{\Delta/-}$CreERT cells, which fail to form mesoderm, we observed upregulation of the miR-290 cluster, what is consistent with the results published by Zovoilis et al. (2009). However, after repeating the experiment, we did not obtain any increase in miR-290 expression (data not shown). Our data require further investigation to evaluate the putative miR-290 upregulation in our system. The question arises, whether this upregulation effect is directly related to PELO function or it is rather convergent result of balance impairment in the complex signalling network responsible for mesoderm formation in the cell.

4.6. Future perspectives

The aim of this work was to analyze pelota function in self-renewal/differentiation processes. The generated conditional knockout system allowed us to reach the goal. We demonstrated that pelota is involved in cell fate shift to mesoderm formation from pluripotent cells. However, the collected data do not give detailed answers about molecular function of PELO protein. Therefore, it would be of great value to analyze mutant ES cells, which are subjected to mesoderm formation conditions and to study the STAT3 level as well as TGF-β signalling in NuRD complex activation. To estimate the approximal stage in mesodermal pathway which is disrupted upon PELO depletion, it is important to analyze the mRNA levels of lineage-specific markers in embryoid bodies of different age. Further

DISSCUSSION

investigation is also neccessary for analysis of hematopoietic cells to confirm the differentiation failure and unaffected proliferation in pelota mutant mice.

To further investigate the differentiation potential of these cells, control and mutant ES cell lines were injected into blastocysts and transferred to pseudopregnant mice. The generated chimeras will help us to verify the contribution of mutant ES cells in embryonic development. Tissues of chimeras, derived from all three germ layers, will be genotyped.

An alternative way to confirm the potential of $Pelo^{\Delta/-}CreERT$ ES cells to differentiate, is generation of teratoma in immune-deficient (SCID) mice. Histological analysis of teratoma will help us to determine abilities of mutant cells to differentiate into different germ layers in advanced teratomas.

SUMMARY

In this work we analyzed the role of pelota in the conditional knockout mouse model. We shed light on its function during development and report the defects resulting from Pelota depletion. We demonstrated that recombination of floxed Pelo allele was complete in ESC system and sufficiently efficient to study PELO depletion in mouse.

We successfully generated a $Pelo^{\Delta/-}CreERT$ ES cell line. It did not exhibit any proliferation disorder, but the cells were defective in differentiation capacities. They sustained Oct4 expression, and miR-290 cluster specific for pluripotent cells seemed to be upregulated under differentiation conditions. The ectoderm formation was not affected, but analysis of early and late markers, specific for mesoderm and endoderm revealed that both lineages are not formed in the mutant cells. To confirm the hypothesis, we studied differentiation capacities of adult stem cells, i.e. hematopoietic stem cells and spermatogonial stem cells.

Analysis of spermatogenesis revealed that all developmental stages of germ cells are absent. For more comprehensive studies, we generated testis-specific $Pelo^{\Delta/-}Stra8-Cre$ mice, which let us follow the effect of PELO deletion on spermatogenesis progression. The analysis of the testes showed arrest in spermatogenic progression during the onset of meiotic division (day 15). In 10-day-old testes we detected a decrease in expression of Stra8, Dazl and Ddx4, which are markers for premeiotic stages of germ cells. However, we could not find any PELO deletion effect on the level of either undifferentiated (Plzf and Sox3 markers) or differentiated (c-Kit marker) spermatogonia. This suggests that pelota exerts the effect on entry into meiosis, that is the beginning of germ cell differentiation. Unexpectedly, we also found mosaic mice with partially deleted Pelo allele ($Pelo^{F/\Delta/-}Stra8-Cre$) in different somatic tissues, including kidney, liver, heart, spleen, lungs, what indicates Stra8 expression in early embryogenesis.

The studies of mature B and T cells isolated from spleen and thymus of mutant mice revealed the reduction in cell number. Additionally, we detected strong increase of double negative cells ($CD4^-CD8^-$), which are developmental precursors of T cells. Simultanously, we observed a dramatic decrease in the level of all later developmental stages of T cells. All these data confirm the failure in differentiation abilities of mutant cells.

Adham et al. (2003) studied pelota function in the Pelo knockout mouse. The phenotype of homozygous mutants ($Pelo^{-/-}$) was lethal during early stages of

SUMMARY

embryogenesis. To confirm that this phenotype results from pelota inactivation, we crossed Pelo$^{+/-}$ mice with transgenic Pelo^T mice, which rescued the lethal phenotype. This clearly demonstrates the direct relation between lethality and Pelo depletion.

The transgenic mice overexpressiong PELO in testis-specific manner did not show any phenotype. The mice were fertile and histological analysis demonstrated that spermatogenesis is not disrupted.

REFERENCES

REFERENCES

Adham I.M., Sallam M.A., Steding G., Korabiowska M., Brinck U., Hoyer-Fender S., Oh C. and Engel W. (2003) Disruption of the pelota gene causes early embryonic lethality and defects in cell cycle progression. *Mol Cell Biol.* **23**: 1470-1476.

Alexandrow M.G. and Moses H.L. (1995) Transforming growth factor beta and cell cycle regulation. *Cancer Res.* **55**, 1452-1457.

Ausubel FM, Brent R, Kingston RE, Moore DD, Seidman JG, Smith JA, Struhl K. 1994. *Current Protocols in Molecular Biology*, (John Wiley & Sons Inc., USA).

Avilion A.A., Nicolis S.K., Pevny L.H., Perez L., Vivian N. and Lovell-Badge R. (2003) Multipotent cell lineages in early mouse development depend on SOX2 function. *Genes Dev.* **17**, 126-140.

Baltus A.E., Menke D.B., Hu Y-C., Goodheart M.L., Carpenter A.E., de Rooij D.G. and Page D.C. 2006. In germ cells of mouse embryonic ovaries, the decision to enter meiosis precedes premeiotic DNA replication. *Nat. Genet.* **12**, vol. 38, 1430-1434.

Berg D.J. and Lynch R.G. (1991) Immune dysfunction in mice with plasmacytomas. I. Evidence that transforming growth factor beta contributes to the altered expression of activation receptors on host B lymphocytes. *J. Immunol.* **146**, 2865–72.

Birnboim HC, Doly J. 1979. A rapid alkaline extraction procedure for screening recombinant plasmid DNA. *Nucleic Acids Res*. **7**:1513-23.

Boeuf H., Hauss C., De Graeve F., Baran N. and Kedinger C. (1997) Leukemia inhibitory factor-dependent transcriptional activation in embryonic stem cells. *J. Cell. Biol.* **138**, 1207-1217.

Bourillot P.Y., Aksoy I., Schreiber V., Wianny F., Schulz H., Hummel O., Hubner N. and Savatier P. (2009) Novel STAT3 target genes exert distinct roles in the inhibition of mesoderm and endoderm differentiation in cooperation with Nanog. *Stem Cells* **27**, 1760-1771.

Boyer L.A., Plath K., Zeitlinger J., Brambrink T., Medeiros L.A., Lee T.I., Levine S.S., Werning M., Tajonar A., Ray M.K., Bell G.W., Otte A.P., Vidal M., Gifford D.K., Young R.A. and Jaenisch R. (2006) Polycomb complexes repress developmental regulators in murine embryonic stem cells. *Nature* **441**, 349-353.

Bradford M.M. (1976) A rapid and sensitive method for the quantitation of microgram quantities of protein utilizing the principle of protein-dye binding. *Anal Biochem.* **7**, 248-254.

Bult C.J., White O., Olsen G.J., Zhou L., Fleischmann R.D., Sutton G.G., Blake J.A., FitzGerald L.M., Clayton R.A., Gocayne J.D., Kerlavage A.R., Dougherty B.A., Tomb J.F., Adams M.D., Reich C.I., Overbeek R., Kirkness E.F., Weinstock K.G., Merrick J.M., Glodek A., Scott J.L., Geoghagen N.S., Venter J.C. (1996) Complete genome sequence of the methanogenic archaeon, Methanococcus jannaschii. *Science*. **23**:1058-73.

REFERENCES

Busch S.J. and Sassone-Corsi P. (1990) Dimers, leuzine zippers and DNA-binding domains. *Trends Genet*. **6**, 36-40.

Cartwright P., McLean C., Sheppard A., Rivett D., Jones K. and Dalton S.(2005) LIF/STAT3 controls ES cell self-renewal and pluripotency by a Myc-dependent mechanism. *Development* **132(5)**, 885-896.

Castrillon D.H., Gonczy P., Alexander S., Rawson R., Eberhart C.G., Viswanathan S., DiNardo S. and Wasserman S.A. (1993) Toward a molecular genetic analysis of spermatogenesis in Drosophila melanogaster: characterization of male-sterile mutants generated by single P element mutagenesis. *Genetics* **135**, 489-505.

Clark J.M. (1988) Novel non-templated nucleotide addition reactions catalyzed by procaryotic and eucaryotic DNA polymerases. *Nucleic Acids Res*. **16**, 9677-86.

Crook J.M., Dunn N.R. and Colman A. (2006) Repressed by NuRD. *Nature Cell Biol*. **8**, 212-214.

Davis L. and Engebrecht J. (1998) Yeast dom34 mutants are defective in multiple developmental pathways and exhibit decreased levels of polyribosomes. *Genetics* **149**: 45-56.

Deb-Rinker P., Ly D., Jezierski A., Sikorska M. and Walker P.R. (2005) Sequential DNA Methylation of the Nanog and Oct-4 Upstream Regions in Human NT2 Cells during Neuronal Differentiation. *J. Biol. Chem.* **280**, 6257-6260.

DeCoteau J.F., Knaus P.I., Yankelev H., Reis M.D., Lowsky R., Lodish H.F. and Kadin M.E. (1997) Loss of functional cell surface transforming growth factor beta (TGF-β) type 1 receptor correlates with insensitivity to TGF-β in chronic lymphocytic leukemia. *Proc. Natl. Acad. Sci. USA* **94**, 5877–81.

Denhardt D.T. (1966) A membrane-filter technique for the detection of complementary DNA. *Biochem Biophys Res Commun*. **13,** 641-646.

Deshpande A.M., Dai Y., Kim Y., Kim J., Kimlin L., Gao K., Hendrich B. and Wong D.T. (2008) CDK2AP1 is required for epigenetic silencing of Oct4 during murine embryonic stem cell differentiation. *J. Biol. Chem.* **284**, 6043-6047.

Doma M.K. and Parker R. (2006) Endonucleolytic cleavage of eukaryotic mRNAs with stalls in translation elongation. *Nature* **440**, 561-564.

Dooley T.P., Miranda M., Jones N.C. and DePamphilis M.L. (1989) Transactivation of the adenovirus ElA protein is restricted to mouse oocytes and preimplantation embryos. *Development* **107**, 945-956.

Dressel R., Elsner L., Quentin T., Walter L. and Günther E. (2000) Heat shock protein 70 is able to prevent heat shock-induced resistance of target cells to CTL. *J. Immunol* **164**, 2362–2371.

REFERENCES

Duncan S.A., Nagy A. and Chan W. (1997) Murine gastrulation requires HNF-4 regulated gene expression in the visceral endoderm: tetraploid rescue of Hnf-4 (-/-) embryos. *Development* **124**, 279-287.

Ebenhart C.G. and Wasserman S.A. (1995) The pelota locus uncodes a protein required for meiotic cell division: an analysis of G2/M arrest in Drosophila spermatogenesis. *Development* **121,** 3477-3486.

Enders G.C. and May J.J. (1994) Developmentally regulated expression of a mouse germ cell nuclear antigen examined from embryonic day 11 to adult in male and female mice. *Dev. Biol.* **163**, 331-340.

Eurwilaichitr L., Graves F.M., Stansfield I. and Tuite M.F. (1999) The C-terminus of eRF1 defines a functionally important domain for translation termination in *Saccharomyces cerevisiae*. *Mol. Microbiol*. **32**, 485-496.

Feinberg A.P. and Vogelstein B. (1984) A technique for radiolabeling DNA restriction endonuclease fragments to high specific activity. *Anal Biochem.* **137**, 266-267.

Feng X.-H., Liang Y.-Y., Liang M., Zhai W. and Lin X. (2002) Direct interaction of c-Myc with Smad2 and Smad3 to inhibit TGF-β-mediated induction of the CDK inhibitor p15^{Ink4B}. *Mol. Cell* **9**, 133-143.

Frolova L., Le Goff X., Rasmussen H.H., Cheperegin S., Drugeon G., Kress M., Arman I., Haenni A-L., Celis J.E., Philippe M., Justesen J. and Kisselev L. (1994) A highly conserved eukaryotic protein family possessing properties of polypeptide chain release factors. *Nature* **372**, 701-703.

Futaki S., Hayashi Y., Emoto T., Weber C.N. and Sekiguchi K. (2004) Sox7 plays crucial roles in parietal endoderm differentiation in F9 embryonal carcinoma cells through regulating Gata-4 and Gata-6 expression. *Mol. Cell. Biol.* **24**, 10492-10503.

Gershoni J.M. and Palade G.E. (1982) Electrophoretic transfer of proteins from sodium dodecyl sulfate-polyacrylamide gels to a positively charged membrane filter. *Anal Biochem.* **124**, 396-405.

Goldrath A.W. and Bevan M.J. (1999) Selecting and maintaining a diverse T-cell repertoire. *Nature* **402,** 255-262.

Graille M., Chaillet M. and van Tilbeurgh H. (2008) Structure of yeast Dom34 – a protein related to translation termination factor eRF1 and involved in No-Go decay. *J. Biol. Chem.* **11**, Vol. 283, 7145-7154.

Hannon G.J. and Beach D. (1994) pl5INK4B is a potential effector of TGF-β-induced cell cycle arrest. *Nature* **371**, 257–61.

Hattori N., Nishino K., Ko Y.G., Hattori N., Ohgane J., Tanaka S. and Shiota K. (2004) Epigenetic control of mouse Oct4 gene expression in embryonic stem cells and trophoblast stem cells. *J. Biol. Chem.* **279**, 17063-17069.

REFERENCES

Hayashi,H., Abdollah S., Qiu Y., Cai J., Xu Y.Y., Grinnell B.W., Richardson M.A., Topper J.N., Gimbrone M.A. Jr., Wrana J.L. and Falb D. (1997) The MAD-related protein Smad7 associates with the TGFb receptor and functions as an antagonist of TGFβ signaling. *Cell* 89, 1165-1173.

Held T., Paprotta I., Khulan J., Hemmerlein B., Binder L., Wolf S., Schubert S., Meinhardt A., Engel W. and Adham I.M. (2006) Hspa4l-deficient mice display increased incidence of male infertility and hydronephrosis development. *Mol. Cell. Biol.* **21**, 8099-8108.

Hendrich B., Guy J., Ramsahoye B., Wilson V.A. and Bird A. (2001) Closely related proteins MBD2 and MBD3 play distinctive but interacting roles in mouse development. *Genes Dev.* **15**, 710-723.

Hill J.J., Tremblay T.L., Cantin C., O'Connor-McCourt M., Kelly J.F. and Lenferink A.E. (2009) Glycoproteomic analysis of two mouse mammary cell lines during transforming growth factor (TGF)-beta induced epithelial mesenchymal transition. *Proteome Sci.* **7:**2, published online doi:10.1186/1477-5956-7-2.

Hodge R. 1994. Preparation of RNA gel blots. *Methods Mol Biol*. **28**, 49-54.

Houbaviy H., Murray M. and Sharp P. (2003) Embryonic stem cell-specific microRNAs. *Dev. Cell* **5**, 351-358.

Houbaviy H., Dennis L., Jaenisch R. and Sharp P.A. (2005) Characterization of a highly variable eutherian microRNA gene. *RNA* **11**, 1245-1257.

Hu G. (1993) DNA polymerase-catalyzed addition of nontemplated extra nucleotides to the 3' end of a DNA fragment. *DNA Cell Biol*. **12**, 763-770.

Hu M., Hu G.-F., Kim Y., Tsuji T., McBride J., Hinds P. and Wong D.T.W. (2004) Role of p12$^{CDK2-AP1}$ in transforming growth factor-β1-mediated growth suppression. *Cancer Research* **64**, 490-499.

Imamura T., Takase M., Nishihara A., Oeda E., Hanai J., Kawabata M. and Miyazono K. (1997) Smad6 inhibits signalling by the TGF-β superfamily. *Nature* **389,** 622–626.

Inge T.H., McCoy K.M., Susskind B.M., Barrett S.K., Zhao G., Bear H.D. (1992) Immunomodulatory effects of transforming growth factor-beta on T lymphocytes. Induction of CD8 expression in the CTLL-2 cell line and in normal thymocytes. *J. Immunol.* **148**, 3847–56.

Izumi N., Era T., Akimaru H., Yasunaga M. and Nishikawa S. (2007) Dissecting the molecular hierarchy for mesendoderm differentiation through a combination of embryonic stem cell culture and RNA interference. *Stem Cells* **25**, 1664-1674.

Kadin M.E., Cavaille-Coll M.W., Gertz R., Massague J., Cheifetz S. and George D. (1994) Loss of receptors for transforming growth factor beta in human T-cell malignancies. *Proc. Natl. Acad. Sci. USA* **91**, 6002–6.

REFERENCES

Kaji K., Caballero I.M., MacLeod R., Nichols J., Wilson V.A. and Hendrich B. (2006) The NuRD component Mbd3 is required for pluripotency of embryonic stem cells. *Nature Cell Biol.* **8**, 285-292.

Kanwar N., Fayyazi A., Backofen B., Nitsche M., Dressel R. and Fisher von Mollard G. (2008) Thymic alteration in mice deficient for the SNARE protein VAMP8/endobrevin. *Cell Tissue Res* **334**, 227-242.

Kawamura C., Kizaki M., Yamato K., Uchida H., Fukuchi Y., Hattori Y., Koseki T., Nishihara T. and Ikeda Y. (2000) Bone morphogenetic protein-2 induces apoptosis in human myeloma cells with modulation of STAT3. *Blood* **96**, 2005-2011.

Kawasaki H., Mizuseki K., Nishikawa S., Kaneko S., Kuwana Y., Nakanishi S., Nishikawa S.-I. and Sasai Y. (2000) Induction of midbrain dopaminergic neurotechnique neurons from ES cells by stromal cell-derived inducing activity. *Neuron* **28**, 31-40.

Kloosterman W.P. and Plasterk R.H. (2006) The diverse functions of microRNAs in animal development and disease. *Dev. Cell* **11**, 441-450.

Koubova J., Menke D.B., Zhou Q., Capel B., Griswold M.D. and Page D.C. (2006) Retinoic acid regulates sex-specific timing of meiotic initiation in mice. *Proc. Natl. Acad. Sci. USA* **103**, 2474-2479.

Laird PW, Zijderveld A, Linders K, Rudnicki MA, Jaenisch R, Berns A. 1991. Simplified mammalian DNA isolation procedure. *Nucleic Acids Res*. **19,** 4293.

Lakso M., Sauer B., Mosinger Jr. B., Lee E.J., Manning R.W., Yu S.H., Mulder K.L. and Westphal H. (1992) Targeted oncogene activation by site-specific recombination in transgenic mice. *Proc. Natl. Acad. Sci. USA* **89**, 6232-6236.

Lakso M., Pichel J.G., Gorman J.R., Sauer B., Okamoto Y., Lee E., Alt F.W. and Westphal H. (1996) Efficient *in vivo* manipulation of mause genomic sequences at the zygote stage. *Proc. Natl. Acad. Sci. USA* **93**, 5860-5865.

Lalo D., Stettler S., Mariotte S., Gendreau E., Thuriaux P. (1994) Organization of the centromeric region of chromosome XIV in *Saccharomyces cerevisiae*. *Yeast* **10**, 523-533.

Lan Z.-J., Chung A.C., Xu X., DeMayo F.J. and Cooney A.J. (2002) The embryonic function of germ cell nuclear factor is dependent on the DNA binding domain. *J. Biol. Chem.* **277**, 50660-50667.

Le Guezennec X., Vermeulen M., Brinkman A.B., Hoeijmakers W.A.M., Cohen A., Lasonder E. and Stunnenberg H.G. (2006) MBD2/NuRD and MBD3/NuRD, two dinstinct complexes with different biochemical and functional properties. *Mol. Cell. Biol.* **26**, 843-851.

Lee T.I., Jenner R.G., Boyer L.A., Guenther M.G., Levine S.S., Kumar R.M., Chevalier B., Johnstone S.E., Cole M.F., Isono K., Koseki H., Fuchikami T., Abe K., Murray H.L., Zucker J.P., Yuan B., Bell G.W., Herbolsheimer E., Hannett N.M., Sun K., Odom D.T., Otte A.P., Volkert T.L., Bartel D.P., Melton D.A., Gifford D.K., Jaenisch R. and Young R.A. (2006)

REFERENCES

Control of developmental regulators by Polycomb in human embryonic stem cells. *Cell* **125**, 301-313.

Lee H.H., Kim Y.-S., Kim K.H., Heo I., Kim S.K., Kim O., Kim H.K., Yoon J.Y., Kim H.S., Kim D.J., Lee S.J., Yoon H.J., Kim S.J., Lee B.G., Song H.K., Kim V.N., Park C.-M. and Suh S.W. (2007) Structural and functional insights into Dom34, a key component of No-Go decay. *Mol Cell* **27**, 938-950.

Letterio J.J. and Roberts A.B. (1998) Regulation of immune responses by TGF-β. *Annu. Rev. Immunol.* **16**, 137-161.

Lomo J., Blomhoff H.K., Beiske K., Stokke T. and Smeland E.B. (1995) TGF-β1 and cyclic AMP promote apoptosis in resting human B lymphocytes. *J. Immunol.* **154**, 1634–43.

Massague J. (1990) Transforming growth factor-α. A model for mrmbrane-anchored growth factors. *J. Biol. Chem.* **265(35)**, 21393-21396.

Massague J. (1998) TGF-β signal transduction. *Annu. Rev. Biochem.* **67**, 753-791.

Matsuda T., Nakamura T., Nakao K., Arai T., Katsuki M., Heike T. and Yokota T. (1999) STAT3 activation is sufficient to maintain an undifferentiated state of mouse embryonic stem cells. *EMBO J.* **18**, 4261-4269.

Menke D.B., Koubova J. and Page D.C. (2003) Sexual differentiation of germ cells in XX mouse gonads occurs in an anterior-to-posterior wave. *Dev. Biol.* **262**, 303-312.

Miller J.F.A.P. (2002) The discovery of thymus function and of thymus-derived lymphocytes. *Immunol. Rev.* **185**, 7-14.

Mitsui K., Tokuzawa Y., Itoh H., Segawa K., Murakami M., Takahashi K., Maruyama M., Maeda M. and Yamanaka S. (2003) The homeoprotein Nanog is required for maintenance of pluripotency in mouse epiblast and ES cells. *Cell* **113**, 631-642.

Nakao A., Afrakhte M., Moren A., Nakayama T., Christian J.L., Heuchel R., Itoh S., Kawabata M., Heldin N.E., Heldin C.H. and ten Dijke P. (1997) Identifcation of Smad7, a TGFβ-inducible antagonist of TGF-β signalling. *Nature* **389,** 631–635.

Ng H.H., Zhang Y., Hendrich B., Johnson C.A., Turner B.M., Erdjument-Bromage H., Tempst P., Reinberg D. and Bird A. (1999) MBD2 is a transcriptional repressor belonging to the MeCP1 histone deacetylase complex. *Nat. Genet.* **23**, 58-61.

Nichols J., Zevnik B., Anastassiadis K., Niwa H., Klewe-Nebenius D., Chambers I., Scholer H. and Smith A. (1998) Formation of pluripotent stem cells in the mammalian embryo depends on the POU transcription factor Oct4. *Cell* **95**, 379-391.

Niwa H., Miyazaki J. and Smith A.G. (2000) Quantitative expression of Oct3/4 defines differentiation, dedifferentiation or self-renewal of ES cells. *Nat. Genet.* **24**, 372-376.

Nomi M., Oishi I., Kani S., Suzuki H., Matsuda T., Yoda A., Kitamura M., Itoh K., Takeuchi S., Takeda K., Akira S., Ikeya M., Takada S. and Minami Y. (2001) Loss of

REFERENCES

mRor1 enhances the heart and skeletal abnormalities in mRor2-deficient mice: redundant and pleiotropic functions of mRor1 and mRor2 receptor tyrosine kinases. *Mol. Cell. Biol.*, **December 2001**, 8329-8335.

Ohkawara B., Shirakabe K., Hyodo-Miura J., Matsuo R., Ueno N., Matsumoto K. and Shibuya H. (2004) Role of the TAK1-NLK-STAT3 pathway in TGF-β-mediated mesoderm induction. *Genes Dev.* **18**, 381-386.

Ohlstein B. and McKearin D. (1997) Ectopic expression of the *Drosophila* Bam protein eliminates oogenic germline stem cells. *Development* **124**, 3651-3662.

Ohta H., Tohda A. and Nishimune Y. (2003) Proliferation and differentiation of spermatogonial stem cells in the W/W^v mutant mouse testis. *Biol. Reprod.* **69**, 1815-1821.

Ormerod M.G., Collins M.K.L., Rodriguez-Tarduchy G. and Robertson D. (1992) Apoptosis in interleukin-3-dependent haemopoietic cells. Quantification by two flow cytometric methods. *J. Immunol Meth.* **153**, 57-65.

Oulad-Abdelghani M., Bouillet P., Decimo D., Gansmuller A., Heyberger S., Dolle P., Bronner S., Lutz Y. And Chambon P. (1996) Characterization of premeiotic germ cell-specific cytoplasmic protein encoded by Stra8, a novel retinoic acid-responsive gene. *J. Cell Biol.* **135**, 469-477.

Paling N.R., Wheadon H., Bone H.K. and Welham M.J. (2004) Regulation of embryonic stem cell self-renewal by phosphoinositide 3-kinase-dependent signalling. *J. Biol. Chem.* **279**, 48063-48070.

Passos D.O., Doma M.K., Shoemaker C.J., Muhlrad D., Green R., Weissman J., Hollien J. and Parker R. (2009) Analysis of Dom34 and its function in No-Go Decay. *Mol. Biol. Cell.* **20**, 3025-3032.

Pichel J.G., Lakso M. and Westphal H. (1993) Timing of SV40 oncogene activation by site-specific recombination determines subsequent tumor progression during murine lens development. *Oncogene* **12**, 3333-3342.

Plum J., De Smedt M., Leclercq G. and Vandekerckhove B. (1995) Influence of TGF-β on murine thymocyte development in fetal thymus organ culture. *J. Immunol.* **154**, 5789–98.

Polyak K. (1996) Negative regulation of cell growthh by TGF beta. *Biochim Biophys. Acta* **1242(3)**, 185-199.

Ragan M.A., Logsdon J.M. Jr, Sensen C.W., Charlebois R.L., Doolittle W.F. (1996) An archaebacterial homolog of pelota, a meiotic cell division protein in eukaryotes. *FEMS Microbiol Lett*. **144**, 151-5.

Rajasingh J., Bord E., Hamada H., Lambers E., Qin G., Losordo D.W. and Kishore R. (2007) STAT3-dependent mouse embryonic stem cell differentiation into cardiomyocytes: analysis of molecular signaling and therapeutic efficacy of cardiomyocyte precommitted mES transplantation in a mouse model of myocardial infarction. *Circ. Res.* **101**, 910-918.

REFERENCES

Raverot G., Weiss J., Park S.Y., Hurley L. and Jameson J.L. (2005) Sox3 expression in undifferentiated spermatogonia is required for the progression of spermatogenesis. *Dev. Biol.* **283**, 215-225.

Rius C. and Aller P. (1992) Vimentin expression as a late event in the *in vitro* differentiation of human promonocytic cells. *J. Cell Sci.* **101**, 395-401.

Ruggiu M., Speed R., Taggart M., McKay S.J., Kilanowski F., Saunders P., Dorin J. and Cooke H.J (1997) The mouse Dazla gene encodes a cytoplasmic protein essential for gametogenesis. *Nature* **389,** 73-77.

Salas-Marco J. and Bedwell D.M. (2004) GTP hydrolysis by eRF3 facilitates stop codon decoding during eukaryotic translation termination. *Mol. Cell. Biol.* **24**, 7769-7778.

Sambrook J, Fritsch EF, Maniatis T. (1989) Molecular cloning: a laboratory manual (2nd edition). *Cold Spring Habour*, New York, USA.

Sanger F., Nicklen S. and Coulson A.R. (1977) DNA sequencing with chain-terminating inhibitors. *Proc Natl Acad Sci U S A.* **74**, 5463-5467.

Schrans-Stassen B.H., van de Kant H.J.G., de Rooij D.G. and van Pelt A.M.M. (1999) Differential expression of c-Kit in mause undifferentiated and differentiating type A spermatogonia. *Endocrinology* **140**, 12: 5894-5900.

Shamsadin R., Adham I.M., von Beust G. and Engel W. (2000) Molecular cloning, expression and chromosome location of the human pelota gene PELO. *Cytogenet Cell Genet* **90**, 75-78.

Shamsadin R., Adham I.M. and Engel W. (2002) Mouse pelota gene (Pelo): cDNA cloning, genomic structure and chromosomal localization. *Cytogenet Genome Res.* **97**, 95-99.

Song H., Mugnier P., Das A.K., Webb H.M., Evans D.R., Tuite M.F., Hemmings B.A. and Barford D. (2000) The crystal structure of human eukaryotic release factor eRF1 – mechanism of stop codon recognition and peptidyl-tRNA hydrolysis. *Cell* **100**, 311-321.

Southern EM. 1975. Detection of specific sequences among DNA fragments separated by gel electrophoresis. *J Mol Biol.* **98**, 503-17.

Starr T.K., Jameson S.C. and Hogquist K.A. (2003) Positive and negative selection of T cells. *Annu Rev Immunol* **21**, 139–176.

Stavnezer J. 1996. Transforming growth factor beta. In *Cytokine Regulation of Humoral Immunity: Basic and Clinical Aspects*, ed.CMSnapper, pp. 289–324. New York: Wiley.

Suda T. and Zlotnik A. (1991) IL-7 maintains the T cell precursor potential of CD3⁻CD4⁻CD8⁻ thymocytes. *J. Immunol.* **146**, 3068-3073.

Suda T. and Zlotnik A. (1992) *In vitro* induction of CD8 expression on thymic pre-T cells. II. Characterization of

REFERENCES

CD3⁻CD4⁻CD8 alpha + cells generated *in vitro* by culturing CD25⁺CD3⁻CD4⁻CD8⁻ thymocytes with T cell growth factor-beta and tumor necrosis factor-alpha. *J. Immunol.* **149**, 71–76.

Tada T., Ohzeki S., Utsumi K., Takiuchi H., Muramatsu M., Li X.F., Shimizu J., Fujiwara H. and Hamaoka T. (1991) Transforming growth factor-beta-induced inhibition of T cell function. Susceptibility difference in T cells of various phenotypes and functions and its relevance to immunosuppression in the tumor-bearing state. *J. Immunol.* **146**, 1077–82.

Toyooka Y., Tsunekawa N., Takahashi Y., Matsui Y., Satoh M. and Noce T. (2000) Expression and intracellular localization of mouse Vasa-homologue protein during germ cell development. *Mech. Dev.* **93**, 139-149.

Tritschler F., Eulalio A., Truffault V., Hartmann M.D., Helms S., Schmidt S., Coles M., Izurralde E. and Weichenrieder O. (2007) A divergent Sm fold in EDC3 proteins mediates DCP1 binding and P-body targeting.
Mol. Cel. Biol. **27**, 8600-8611.

Ura H., Usuda M., Kinoshita K., Sun C., Morl K., Akagl T., Matsuda T., Kolde H. and Yokota T. (2008) STAT3 and Oct-3/4 control histone modification through induction of Eed in embryonic stem cells. *J. Biol. Chem.* **283**, 9713-9723.

Wade P.A., Gegonne A., Jones P.L., Ballestar E., Aubry F. and Wolffe A.P. (1999) Mi-2 complex couples DNA methylation to chromatin remodelling and histone deacetylation. Nat Genet 23, 62-66.

Wahl S.M., Hunt D.A., Wong H.L., Dougherty S., McCartney-Francis N., Wahl L.M., Ellingsworth L., Schmidt J.A., Hall G., Roberts A.B. and Sporn M.B. (1988) Transforming growth factor-beta is a potent immunosuppressive agent that inhibits IL-1-dependent lymphocyte proliferation. *J. Immunol.* **140(9)**, 3026-3032.

Williams-Simons L. and Westphal H. (1999) EIIaCre – utility of a general deleter strain. *Transgenic Research* **8**, 253-254.

Wilusz C.J. amd Wilusz J. (2005) Eukaryotic Lsm proteins: lessons from bacteria. *Nat. Struct. Mol. Biol.* **12**, 1031-1036.

Xi R., Doan C., Liu D. and Xie T. (2005) Pelota controls self-renewal of germline stem cells by repressing a Bam-independent differentiation pathway. *Development* **132**, 5365-74.

Xu J., Beyer A.R., Walker W.H. and McGee E.A. (2003) Developmental and stage-specific expression of Smad2 and Smad3 in rat testis. *J. Androl.* **24(2)**, 192-200.

Xue Y., Wong J., Moreno G.T., Young M.K., Cote J. and Wang W. (1998) NuRD, a novel complex with both ATP-dependant chromatin-remodeling and histone deacetylase activities. Mol Cell 2, 851-861.

Yeom, Y.I., Fuhrmann, G., Ovitt, C.E. *et al.* (1996) Germline regulatory element of Oct-4 specific for the totipotent cycle of embryonal cells. *Development* **122,** 881–894.

REFERENCES

Ying Q.L., Nichols J., Ccambers I. and Smith A. (2003) BMP induction of Id proteins suppresses differentiation and sustains embryonic stem cell self-renewal in collaboration with STAT3. *Cell* **115**, 281-292.

Yoshimizu T, Sugiyama N, De Felice M, Yeom YI, Ohbo K, Masuko K, Obinata M, Abe K, Scholer HR, Matsui Y. (1999) Germline-specific expression of the Oct-4/green fluorescent protein (GFP) transgene in mice. *Dev Growth Differ* **41**, 675–684.

Zhang Y., Ng H.H., Erdjument-Bromage H., Tempst P., Bird A. and Reinberg D. (1999) Analysis of the NuRD subunits reveals a histone deacetylase core complex and a connection with DNA methylation. *Genes Dev.* **13**, 1924-1935.

Zhou Q., Tam W.L., Tong G.Q., Wu Q., Chan H.Y., Soh B.S., Lou Y., Yang Y., Ma Y., Chai L., Ng H.H., Lufkin T., Robson P. and Lim B. (2006) Sall4 modulates embryonic stem cell pluripotency and early embryonic development by the transcriptional regulation of Pou5f1. *Nat. Cell Biol.* **8**, 1114-1123.

Zhou Q., Nie R., Li Y., friel P., Mitchell D., Hess R.A., Small C. and Griswold M.D. (2008) Expression of stimulated by retinoic acid gene 8 (Stra8) in spermatogenic cells induced by retinoic acid: an *in vivo* study in vitamin A-sufficient postnatal murine testes. *Biol. Reprod.* **79**, 35-42.

Zovoilis A., Smorag L., Pantazi A. and Engel W. (2009) Members of the miR-290 cluster modulate *in vitro* differentiation of mouse embryonic stem cells. *Differentiation* **78**, 69-78.

<u>*Acknowledgements*</u>

Curriculum vitae

Personal details:

FIRST NAME: Aleksandra

LAST NAME: Kata

ADDRESS   Rosenbachweg 4/406
37075 Goettingen, Germany

DATE OF BIRTH: 8th December 1982

PLACE OF BIRTH: Łódź, Poland

NATIONALITY/SEX: Polish/female

PHONE No.   **+48 603053353**
+49 17665578847

EMAIL: **akata82@gmail.com**

Education:

2006 – 2010   PhD studies, Institute of Human genetics, Georg_August University in Goettingen, Germany
Title of the thesis: **On putative role of Pelota in stem cell differentiation**
Graduation date: January 2010

2003 – 2006   Master of Science thesis, Experimental work in The Laboratory of Molecular Genetics, The Institute of General and Molecular Biology at Nicolas Copernicus University in Torun, Poland
Title of the thesis: **The influence of temperature on catalase gene expression pattern during regeneration in embryogenic and non-embryogenic calli of *Triticum aestivum* and *Vicia faba ssp. minor*.**

Graduation date: 7th June 2006

2001 – 2006   Biology Studies at the Faculty of Biology

and Earth Sciences at the Nicolas Copernicus University in Torun, Poland

2001   High School Diploma

1989 - 2001   Primary and Secondary School (Profile: *Biology & Chemistry*), Łódź, Poland

Laboratory experience:

2006 – 2010   Experimental work in the laboratory of Institute of Human genetics in Goettingen, Germany

                                    Scientific supervision: PD Dr I. Adham

2003 –2006   Experimental work in The Laboratory of Molecular Genetics, The Institute of General and Molecular Biology at Nicolas Copernicus University in Torun, Poland

                                    Scientific supervision: PD Dr A. Goc

January – June 2004   Institute of Cancer Genetics, Saint Joseph St. 53/59, 87-100 Torun, Poland

Occupation   Proffesional Practice : Laboratory Assistant (Diagnostics of hereditary cancer)